Improved calibration of a groundwater model using atmospheric tracers and particle tracking analysis, Pilbara WA

By

Zlatko Eterovic

Thesis
Submitted to Flinders University
for the degree of

Master of Science (Groundwater Hydrology)

College of Science and Engineering
29th of November 2021

TABLE OF CONTENTS

ABSTRACT

Elevated concentrations of chlorofluorocarbon (CFC)-12 have been measured from dewatering bores in the vicinity of a large open pit mine in the Pilbara, WA, indicating the presence of younger groundwater attributed to localised recharge processes from an adjacent creek. The calibration of a groundwater model with the assistance of atmospheric tracers has re-affirmed that creek recharge is contributing to the dewatering network within the surrounds of the mine. In this study, a pre-existing transient numerical groundwater model was calibrated using simulated equivalents of atmospheric CFC-12 concentrations via particle tracking methods. Particles were distributed uniformly along the screens/open intervals of the dewatering bores and simulated by reverse tracking back in time to areas of recharge. Particle tracking simulations were firstly undertaken on the pre-existing model and then calibrated by applying creek recharge to produce a closer match between simulated and measured CFC-12 concentrations. Both models were ultimately compared to assess calibration quality. Results from the simulations showed that applying a creek recharge rate equivalent to 0.009 m/d into the groundwater model improved calibration performance. Results proved to be spatially variable as some areas produced a closer match between simulated and measured concentrations over time in comparison to others. A sensitivity analysis was also undertaken using different rates of recharge to address sensitivities and uncertainty in recharge parameterisation. The root mean square error (RMSE) indicated that a recharge rate equivalent to 0.009 m/d (74 pg/kg) produced a closer match between simulated and measured concentrations in comparison to 0.006 m/d (81 pg/kg) or 0.012 m/d (76 pg/kg). However, all scenarios produced the same temporal trends indicating minor sensitivities in recharge were not enough to significantly alter results.

DECLARATION

I certify that this thesis does not incorporate without acknowledgment any material previously submitted for a degree or diploma in any university; and that to the best of my knowledge and belief it does not contain any material previously published or written by another person except where due reference is made in the text.

Signed

ACKNOWLEDGEMENTS

LIST OF FIGURES

LIST OF TABLES

1. INTRODUCTION

Role of tracers in groundwater models

The measurement of environmental tracers in groundwater can be used to estimate groundwater age (or residence time) and help characterise groundwater flow processes and aquifer recharge (Cook and Bohlke, 2000). When used in conjunction with other hydraulic data, they can be valuable tools in the evaluation and improvement of conceptual hydrogeological models. Additionally, environmental tracers can be used as targets in the calibration of numerical groundwater models, providing an alternate means to more traditional calibration targets. Traditional targets typically include hydraulic head (i.e. groundwater level) and stream flow data and focus on achieving the best statistical match between observed and simulated hydraulic head or stream water levels.

Calibration targets obtained from environmental tracers that have been used in previous studies include age and travel time (Izbicki et al. 2004; Tiedeman et al. 2003; Chesnaux et al. 2013; Clark et al. 2008), solute dispersion (Starn, Bagtzoglou & Robbins, 2010) or a combination of these targets (Sanford et al. 2004). The success of these studies is largely attributed to the use of post-processing particle tracking codes such as MODPATH (Pollock, 2012) and mod-PATH3DU (Papadopolous, 1994) which produce simulated equivalents to observations for model calibration by calculating the path a "particle" of water would follow through a simulated groundwater system along with its distance, velocity and travel time along its path. The comparison of simulated and measured measurements of various tracers provides independent information for refining model calibration beyond matching simulated and observed hydraulic heads. They can help constrain groundwater model parameters, and assist in the delineation of various hydrogeological processes, such as groundwater recharge zones (Crandall et al. 2008; Lindgren et al. 2011). Additionally, environmental tracers can help reduce the uncertainty surrounding groundwater models and minimise model non-uniqueness.[1]

Tracers such as Chlorofluorocarbons (CFCs) are particularly useful as they can help determine the presence of younger or modern water (Wilske, et al. 2019; Hinkle and Snyder, 1997). CFCs are synthetic organic compounds that have been produced since the 1930s for a range of domestic and industrial purposes, including refrigerants, solvents and aerosol sprays. CFC-11 ($CFCl_3$), CFC-12 (CF_2CL_2) and CFC-113 ($C_2F_3CL_3$) have relatively long residence times in the atmosphere (between 50 and 180 years depending on the tracer) and undergo equilibrium partitioning into surface waters (that is in contact with the atmosphere) as a function of temperature. Atmospheric concentrations of the respective tracers increased after the 1950s to peak in concentrations between 1994 and 2002 and have since decreased between 3 and 13 % (Cook et

---

[1] Model non-uniqueness is the basis that numerous combinations of model parameters can produce the same match to field measured data (i.e. hydraulic heads)

al. 2017, p. 41) (Figure 1). Comparisons of concentrations of CFCs in groundwater with atmospheric concentrations can indicate the time at which a groundwater sample was last in contact with the atmosphere and therefore the groundwater age (Busenberg & Plummer, 1992; Cook & Solomon, 1997; cited in Cook and Dogramaci, 2019, p. 5469). CFCs with higher measured concentrations are typically indicative of younger groundwater and localised recharge processes given that peak concentrations were only reached in the last 20 years (Hinkle and Snyder, 1997; Cook et al. 2017).

Image removed due to copyright restriction.

Figure 1 Atmospheric CFC concentrations in the southern hemisphere (Cook et al. 2017)[2]

Background

Changes in tracer concentrations in groundwater over time can be indicative of changes in a groundwater system (e.g. flow behaviours, variations in groundwater inflow to outflow). This is particularly evident in groundwater systems encircling large open pit mines. When a mine extends below the regional water table, groundwater will inevitably infiltrate mine workings due to gravity. To prevent this, open pit mines require large scale dewatering to maintain groundwater levels below mining operations. The design and implementation of a mine dewatering borefield is dependent on several factors, including the size of the mine pits themselves, the hydraulic characteristics of the groundwater system (i.e. porosity and permeability of the aquifer) and the requirement of water for mining operations (e.g. dust suppression, general operations). Mass dewatering at an open pit mine often produces significant groundwater drawdown (i.e. reduction in groundwater levels due to pumping) which inevitably leads to changes in

---

[2] CFC-12 concentrations are based on measured atmospheric concentrations at Cape Grimm (Tasmania) and a solubility of 24 °C and recharge elevation of 600 m AHD

groundwater flow behaviours. These changes are dependent on the level of stress applied to the system and to the degree the flow field has changed (Cook et al. 2017, p. 40).

The Hope Downs 1 (HD1) iron ore mine, located in the Pilbara region in Western Australia, is a prime example. Since onset of mining in 2007, dewatering has averaged 110 ML/d (megalitres per day) producing significant groundwater drawdown which has consequently reversed the regional hydraulic gradient. Temporal sampling of various environmental tracers (CFCs, Carbon-13, tritium) by Cook et al. (2017) from the dewatering bores at HD1 has identified the water to contain a mix of younger and older groundwater likely attributed to transient changes in the groundwater flow system. Recent sampling undertaken in 2017 identified elevated concentrations of CFCs, namely CFC-12, in comparison to previous sampling rounds (Figure 2). The study found that localised recharge from an adjacent ephemeral creek, specifically Weeli Wolli Creek, was now forming a larger proportion of the pumped groundwater at HD1, indicating that significant groundwater recharge was occurring underneath the creek during high flow events.
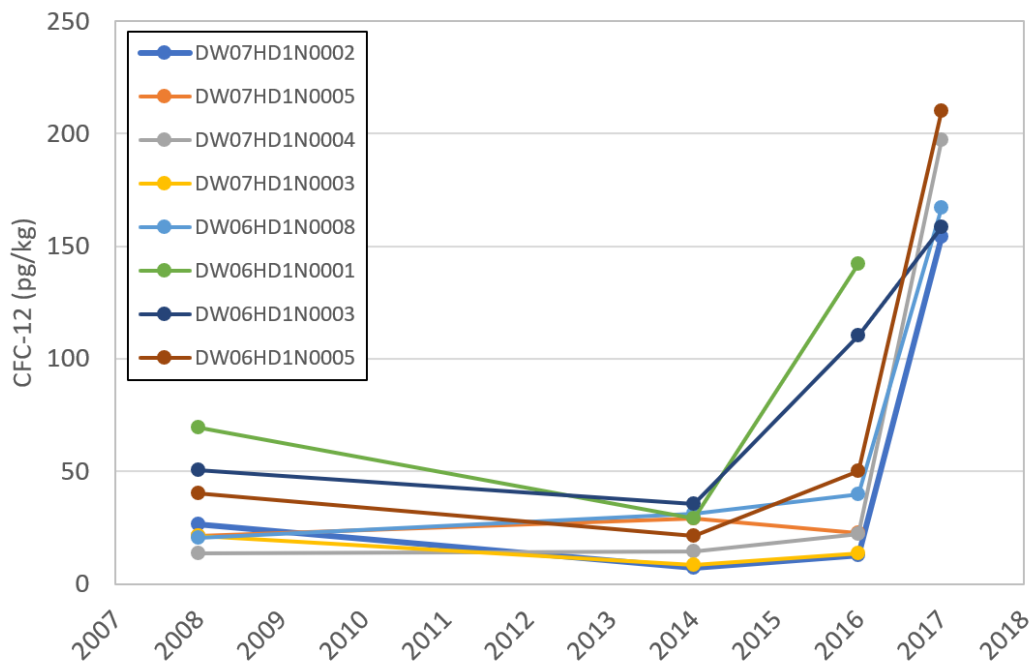
Figure 2 Measured CFC-12 concentrations within the dewatering bores at HD1

The work undertaken by Cook et al. (2017) recommended a series of additional studies to confirm these findings and more clearly define recharge rates and flow systems at HD1. One of these recommendations highlighted the need for simulating groundwater age distributions in a groundwater model domain that will assist in further development of the regional hydrogeological conceptualisation (Cook et al. 2017. p. 51). Numerical groundwater modelling of the regional aquifer at HD1 has been ongoing for the better part of 20 years to refine dewatering predictions during mining and assess groundwater management options at closure (RTIO, 2018).

Scope and objectives

The objective of this study is to determine if concentrations of atmospheric CFCs, specifically CFC-12, can help calibrate a pre-existing transient groundwater model at HD1 and help improve estimates of groundwater recharge from creek infiltration. The study utilises a backward particle tracking approach by placing particles along the screens or open intervals of individual bores and tracking to their points of origin (i.e. recharge areas). For each particle endpoint, the date of recharge is calculated by subtracting the travel time from date of sampling then assigning a concentration to the particle equal to the concentration in equilibrium with the atmosphere for the simulated recharge date. The arithmetic mean of the aged derived concentrations are then used to generate the simulated equivalent concentrations for comparison to measured concentrations to assess calibration quality.

The simulation of particle tracking is first undertaken on the pre-existing groundwater model at HD1 (RTIO, 2018) and adjusted as needs to constrain model parameters. This involves the application of recharge along Weeli Wolli Creek as evidenced by the increase in CFC-12 concentrations in the dewatering bores at HD1. Particle tracking is undertaken on the model with creek recharge applied in addition to the pre-existing calibrated RTIO model and compared to assess fit. A sensitivity analysis on the amount of creek recharge applied is also undertaken to determine sensitivities and potential uncertainties.

Particle tracking is simulated using the post-processing particle tracking software mod-PATH3DU version 2.0 (Papadopolous, 1994) via the MODFLOW-USG (Panday et al, 2013) groundwater flow simulating code operating under the Groundwater Vistas graphical interface Version 7 (ESI, 2020).

The full methodology undertaken is described in detail in following sections and can be summarised as a five-stage approach:

1. Reverse particle tracking on the pre-existing groundwater model (RTIO, 2018)
2. Estimation of Weeli Wolli Creek recharge using the Water Table Fluctuation (WTF) method
3. Reverse particle tracking simulations on model with creek recharge applied
4. Sensitivity analysis of creek recharge in simulations
5. Assess calibration quality of all scenarios

Thesis structure

The thesis structure is summarised as follows:

1. Literature review (Chapter 2)
2. Site description (Chapter 3)
   - Setting, climate, geology, hydrogeological conceptualisation

3. Pre-existing model (Chapter 4)

- Model construction details of the pre-existing HD1 transient groundwater model (model discretisation, aquifer parameterisation, boundary conditions, temporal variability, system stresses)

4. Methodology (Chapter 5)

- Particle tracking set up
- Water Table Fluctuation (WTF) method for estimating for creek recharge
- Model refinements and parameter adjustments to pre-existing model

5. Results (Chapter 6)

- Creek recharge estimation results
- Model calibration performance with application of creek recharge and comparison to pre-existing model
- Particle tracking results and comparison of all simulations (pre-existing model, creek recharge applied model and sensitivity scenarios)

6. Discussion (Chapter 7)

7. Conclusion (Chapter 8)

2. LITERATURE REVIEW

The environmental tracer calibration approach to numerical groundwater models can be split into two methodologies (Zuber et al. 2011; Gusyev et al: 2013). One approach is by using lumped parameter models (LPMs) to ascertain groundwater ages from measured concentrations (Maloszewski & Zuber 1998; Weissman et al: 2002). The other method is by calibrating distributed parameter models (DPMs) directly from measured concentrations (Gusyev et al. 2013; Starn, Bagtzoglou and Robbins, 2010). In this method, steady-state or transient groundwater models are firstly calibrated to observed hydraulic heads by adjusting model parameters (groundwater recharge, hydraulic conductivity, etc). Results from transport modelling are then matched to age concentrations to constrain model parameters and make additional adjustments to the previously calibrated model parameters as needs. Tracers are required in both approaches because calibrated numerical groundwater models with known transmissivity or volumetric flow rates can often under or overestimate the flow velocity/age of water, which is fundamentally the main transport parameter (Zuber et al. 2011).

Calibration of flow and transport models involving environmental tracer data typically use inferred groundwater age or measured concentrations. In the case of groundwater age, calculated age values from measured environmental tracer concentrations are compared to a simulated age. One of the more common ways to numerically simulate groundwater age is via particle tracking methods that simulate advective transport using various post-processing codes (Chesnaux, et al. 2011; Hinkle and Snyder, 1997; Doyle et al. 2015). For example, Weissman et al. (2002) used particle tracking simulations to model CFC groundwater ages within several monitoring wells using cumulative frequency curves. Several studies have used age dates from measured sulfur hexafluoride (SF_6) and tritium in the calibration of groundwater flow and advective transport models near water supply bores (Crandall et al. 2008; Lindgren et al; 2011). Equally, concentrations of environmental tracers can also be used in model calibration and can assist in constraining conceptual models similarly to groundwater age. Starn et al. (2014) combined age distributions obtained from particle tracking and tracer recharge time series by matching measured concentrations to simulated concentrations to calibrate a transient flow model. Thiros, Gardner, and Kuhlman (2021) utilised a pilot point calibration procedure by a subset of data, including liquid pressures, as well as the concentrations and groundwater apparent ages of tritium, CFCs and SF6. In their research they discovered that calibration to observations of environmental tracer concentrations as opposed to apparent groundwater ages resulted in lower pilot point permeability uncertainties in the model.

This study utilises the second approach outlined above by Zuber et al. (2011), to calibrate a pre-existing model using atmospheric CFC-12 concentrations coupled with particle tracking to improve estimates of recharge. The benefit of this methodology lies in its effective simplicity. The simulated equivalents (i.e atmospheric concentrations) are obtained by reverse tracking particles from an observation location (bore)

to the source location (creek). The travel time associated with each particle is then compared with known atmospheric concentrations of CFC-12 at time of recharge. The arithmetic mean of all aged derived concentrations at the source location are then used to generate the simulated equivalent concentrations for comparison to measured concentrations. The success of this methodology hinges on carefully constructing source-type observations to accurately represent the relation between the source types and flow paths. These are controlled by the aquifer properties/boundary conditions in the numerical groundwater model that are being estimated during calibration (Hanson et al. 2013). Namely, uncertainties in the calibration methodology mostly pertain to groundwater flow and transport model structure as opposed to the specific environmental tracer being used.

Recharge delineation with particle tracking has been used in several studies to improve model calibration. Clark et al. (2008) assessed the contributing recharge areas to public supply wells utilising a particle tracking approach and comparing measured age tracer and chemical data with simulated values. Crandall et al. (2008) adopted a similar methodology in their assessment of area contributing recharge to water supply wells near Tampa, Florida. Most notably, Sanford et al (2004) were able to delineate recharge rates using an array of hydrochemical data in the Middle Rio Grande Basin, New Mexico. Their work superseded previous models of the basin which had greatly overestimated groundwater recharge on account of a lack of data to constrain the rates.

This study aims to calibrate a flow model and constrain groundwater recharge in a transient groundwater system that has experienced significant change in groundwater flow a relatively short span of time (as a result of drawdown induced by mine dewatering). Many of the studies outlined above apply to steady-state models or transient flow systems that have not seen significant change in groundwater level or flow behaviours over time (Gusyev et al. 2014; Ackerman, et al. 2004). Thus, it is important to recognise the uncertainties pertaining to poor calibration results brought on from structural errors in model construction or particle tracking performance. For example, particle placement in advective transport models can have several implications as small errors in particle positioning can lead to misleading model results, particularly for models that are simulating large changes in the groundwater system. This can be alleviated by performing several trial runs or distributing the particles in such a way to minimise errors in the simulations (i.e. circular or linear distributions as opposed to single point placements). Hinkle and Snyder (1997) demonstrated this when using CFCs to calibrate a regional flow model in the Portland Basin. The researchers conducted a sensitivity test to determine optimum particle distributions per model cell and found that the highest particle numbers and greater densities provided a better estimate of minimum groundwater travel times to individual wells. Similarly, Lindgren et al. (2011) utilised a comparative assessment of particle distributions in their delineation of recharge areas to public supply wells in San Antonio, Texas.

A problem inherent in almost every combined tracer and particle tracking approach to model calibration is the inability of particle paths to be simulated across the vadose (i.e unsaturated) zone, something that is also relevant to this research. In studies involving unconfined aquifers with shallow water tables, this is usually not a detriment nor is it in the delineation of historic recharge zones in steady state models where ages often exceed thousands of years (Izbicki et al. 2004; Kunianksy, Fahlquist and Ardis, 2001). However, deeper water tables with slow infiltration rates can often to lead to misinterpretations in simulated results as groundwater ages or concentrations can be greatly underestimated. Advective transport can be used in tandem with software designed to model solute transport within the unsaturated zone, such as SEEP/W (Siracusa et al. (2007) or analytical solutions.

Spatial variability in hydraulic conductivity and aquifer heterogeneity can also have a profound impact on model calibration and potentially produce different simulated ages and concentrations (Sanford, 2011). From an advective transport perspective, this can lead to considerably convoluted and erratic particle pathlines as found by Anderman and Hill (2001). In the case of recharge delineation, many studies assess the effect of spatially varying hydraulic conductivity (Kunstmann and Kastens, 2006; Frind, Molson and Rudolph, 2006) however, they do not address the uncertainties caused by parameter values estimates. Starn, Bagtzoglou and Robbins (2010) addressed uncertainties in recharge contributing areas by using a Monte Carlo approach by deriving parameters sets from a model sensitivity analysis.

A significant limitation to particle tracking is that it only simulates advection along a pathline. Most of the studies discussed only simulate advection and ignore the effects of hydrodynamic dispersion and other solute transport processes. In fact, there is still some uncertainty as to how to accommodate the effects of hydrodynamic dispersion, retardation, adsorption, diffusion, and other factors common to conditions in the field that cause sub-surface transport to vary from flow represented by conventional particle tracking. One approach is by incorporating reactive transport models such as MT3DMS (Bedekar et al. 2016) which models the effects of dispersion, diffusion and dual porosity in conjunction with traditional advective particle tracking schemes. Gusyev et al. (2014) utilised this approach by comparing particle tracking and solute transport methods for simulation of tritium concentrations and transit times in river water. They found that simulated concentrations and travel times derived from traditional advective modelling via MODPATH (Pollock, 2012) were typically in agreeance with concentrations derived from MT3DMS. Particle tracking results using advection are only an approximation of the actual transport processes taking place, but nevertheless provide a good representation of average travel times and is suitable for this study.

3. SITE DESCRIPTION

Overview

Setting

The study area occurs within the surrounds of the Hope Downs 1 (HD1) iron ore mine, located approximately 75 km north-west of Newman within the southern half of the Weeli Wolli Creek catchment (Figure 3). HD1 is an unincorporated Joint Venture between Hope Downs Iron Ore Pty Ltd (a member of the Hancock Prospect Group) and Hammersley WA Pty Ltd (a member of the Rio Tinto Group) and is situated on active mining lease AM70/00282 section M282SA (RTIO, 2018a).

Weeli Wolli Creek and its tributary systems converge roughly 2 km downstream of HD1 and drain towards Weeli Wolli Spring in the north-east, located approximately 7.5 km up-gradient. The spring is home to a thriving groundwater dependent ecosystem comprising stygofauna habitat and a riparian vegetation area, made up of River Red Gum, Silver Cadjeput trees and various other species (Environmental Protection Authority, 2018).

Open pit mining at HD1 commenced in 2007. Approximately 60% of the mineable reserve was found to lie beneath the regional water table, requiring the need for large scale dewatering in the order of 100 to 110 ML/d (megalitres per day) throughout the life of mine. Mining at HD1 is split into two distinct pits, specifically Hope Downs 1 North (HD1N) and Hope Downs 1 South (HD1S) each with respective borefields designed to maintain groundwater levels beneath the base of the pits over the mining period. The dewatering borefields for HD1N and HD1S became operational in 2007 and 2011, respectively.

It was discovered though the initial Environmental Impact Assessment (EIA) that, without proper mitigating measures, dewatering would have severe implications on spring health. To counteract the potential effects from a decline in groundwater levels due to mine dewatering, approximately 30 % or close to 20 ML/d of surplus mine water is discharged via 13 off-take spurs which irrigate the riparian vegetation and help maintain spring flow at pre-mining levels. The remaining 70 % of surplus water is discharged further downstream of Weeli Wolli Spring at a gabion discharge point.

Climate

Temperatures in the study area are characteristic of an arid to semi-arid climate. Average daily summer maximum temperatures typically range from 37 to 39 °C, while average daily winter temperatures range from 22 to 25 °C (1965 – 1997, BOM 2021). Mean annual rainfall at Newman is 318 mm (1965 - 2003, BOM 2021) with most rainfall occurring during the summer months (December to February). Summer rainfall in the region is often associated with tropical cyclones moving in from the north-west which regularly generate heavy surface flows in Weeli Wolli Creek and neighbouring ephemeral streams.
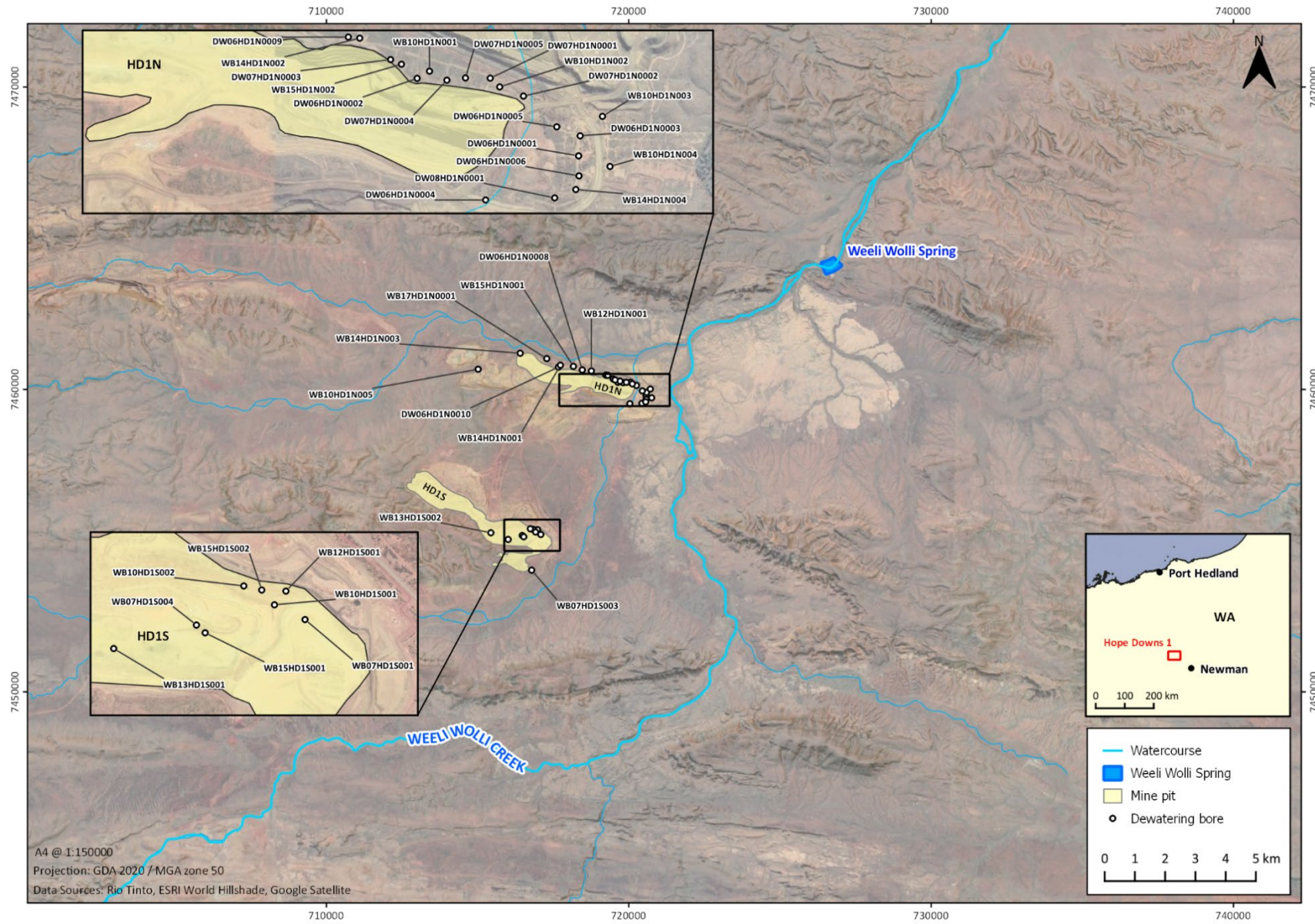
Figure 3 Study area

Geology

The HD1 area is situated at the south-eastern corner of the Pilbara craton. The cratonic basement is comprised of Archaean granite and greenstone and is overlain by a depositional basin of Archaean-Proterozoic sedimentary rocks (Hammersley Basin). These sedimentary rocks are divided into three major stratigraphic groups, specifically the Fortescue, Hammersley and Turee Creek Groups, with the Hammersley Group forming the outcrop at HD1. The Hammersley Group lies conformably over the Fortescue Group and is made up of sequences of various metasedimentary rocks, including banded iron formations (BIF), interbedded with shale, dolomite, minor felsic volcanics and intruded by doleritic dykes (Johnson and Wright, 2001, p. 4).

The sedimentary sequences of the Hammersley Group are comprised of the Wittenoom and Marra Mamba Formations, with the latter (along with the Brockman Formation) hosting most of the known iron ore deposits in the Pilbara. At HD1, the orebodies occur in the core of the Weeli Wolli Anticline where the Marra Mamba Formation is exposed. Thickness of the orebody ranges from approximately 20 to 270 m deep and has a strike length of over 7 km (Cook et al. 2017, p. 42). Extensive weathering of the less resistant Wittenoom Formation has eroded the flanks of the anticline to form characteristic east-west trending valleys, also known as the North and South Flank Valleys (RTIO, 2018). Additionally, weathering of the Wittenoom Formation has resulted in considerable bedrock relief allowing for the accumulation of a variety of Tertiary to Quaternary aged sediments along the drainage channels and low-lying areas. These sediments include alluvial and colluvial clays, silts and sands (detritals), calcrete and chemical precipitates of limonite. The stratigraphy (from youngest to oldest) relevant to HD1 is summarised in Table 1.

Table 1 Stratigraphic summary at HD1 from youngest to oldest (Johnson and Wright, 2001)

Age	Group	Formation	Member	Dominant lithology
Quaternary				Alluvium, colluvium
Tertiary				Calcrete, Pisollitic limonite
Early Proterozoic - Archaean	Hammersley Group	Wittenoom Formation	Bee Gorge Member	Calcareous shale and dolomite
			Paraburdoo Member	Karstic dolomite
			West Angela Member	Magnesium-rich shale with minor BIF and chert bands

		Marra Mambra Iron Formation	Mt Newman Member	BIF with thin shale bands
			MacLeod Member	BIF with extensive interbedded shales
			Nammuldi Member	BIF with chert and shale bands

Hydrogeological setting

Hydrology

Weeli Wolli Creek and its tributary systems converge roughly 2 km downstream of HD1 and drain towards Weeli Wolli Spring in the north-east, located approximately 7.5 km up-gradient. Weeli Wolli Creek is ephemeral in nature, flowing only after high rainfall events. Between 1985 and 2006, the creek flowed for approximately 25% of the time, with a maximum flow duration of 387 days (Cook et al. 2017 p. 43). Peak flows of up to 62 GL/day were recorded at Tarina gauging station, located approximately 6 km north of Weeli Wolli Spring (Environmental Protection Authority, 2018). Since mining began in 2007, excess mine water has been discharged into Weeli Wolli Creek approximately 7.5 km north-east of the HD1 north pit. The creek has seen continuous flow for 24 – 27 km north of Weeli Wolli Sping (Dogramaci et al. 2015, cited in Cook et al. 2016, p. 43) with the Tarina gauging station averaging a stream discharge in excess of 100 ML/d since 2007.

Aquifer geometry and properties

The groundwater system at HD1 consists of one unconfined aquifer unit which is comprised of the mineralised Marra Mamba Formation, weathered Wittenoom Formation, and Tertiary detrials. The aquifer extent covers an area of 206 km^2 and is bounded by dolerite dykes to the south and south-west and geological units which act as hydraulic barriers (Figure 4). The base of the aquifer sits at approximately 400 m AHD in the vicinity of HD1N and 450 m AHD at HD1S. Aquifer thickness ranges from over 180 m within the surrounds of HD1N to only 7 m along Weeli Wolli Creek in the north-east where it pinches out to form Weeli Wolli Spring, as shown in Figure 5.

The composition of the aquifer underlying Weeli Wolli Creek consists of sedimentary detrials, alluvium and weathered detrials belonging to the Paraburdoo Member of the Wittenoom Formation. Groundwater level monitoring data in both stratigraphic units exhibit similar trends, suggesting a strong hydraulic connection. The bottom of the aquifer is primarily bounded by the fresh Wittenoom Formation but also the unmineralised Brockman Iron Formation.

Most installed dewatering bores at HD1 have been subjected to aquifer tests to determine hydraulic parameters of the aquifer and assess bore efficiency. The hydraulic conductivity of the aquifer underlying Weeli Wolli Creek is much higher (=>100 m/d) in comparison to the remaining domain to maintain continuity in flow (RTIO, 2018a). This is evidenced by groundwater monitoring data in the area with an almost immediate groundwater level decline observed in BH15 (located approximately 2.5 km downstream of HD1N) shortly after the commencement of dewatering in 2007 (Figure 6). Regionally, the specific yield of the aquifer has been estimated to be 8% by RTIO (2018a) based on the volume of groundwater removed from 10 years of dewatering (2007 – 2017) versus the volume of material dewatered.

Groundwater throughflow

Prior to mass dewatering, the potentiometric surface of the surficial aquifer generally followed the elevation of the land surface and flowed towards Weeli Wolli Spring in the north-east (Figure 4). The pre-mining groundwater levels typically ranged from 574 m AHD in the vicinity of HD1S to approximately 556 m AHD at Weeli Wolli Spring (RTIO, 2018a). Since the onset of mining, mass dewatering has reversed the hydraulic gradient north of HD1N whereby groundwater throughflow is now directed towards the pits.

Two potential groundwater throughflow boundaries made of saturated detritals along drainage lines overly the hydraulic barriers associated with the North and South Flank Valleys (RTIO, 2018a). Pre-mining throughflow estimates have been estimated at a shared 4.6 ML/d between the two valleys (RTIO, 2018a) This rate has likely reduced considerably however, due to the propagation of drawdown through the entire aquifer.
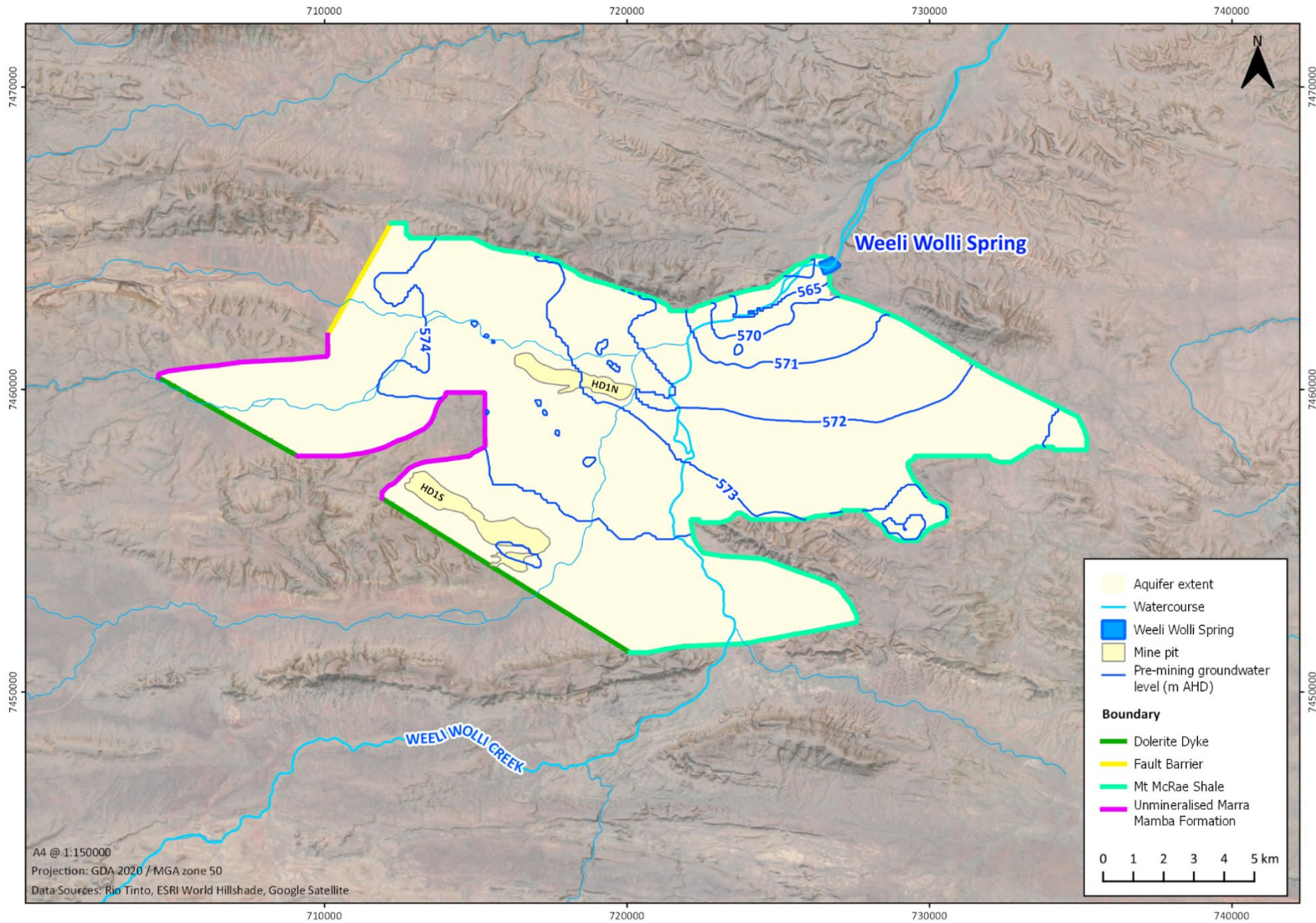
Figure 4 Aquifer extent and pre-mining groundwater levels (after RTIO, 2018)
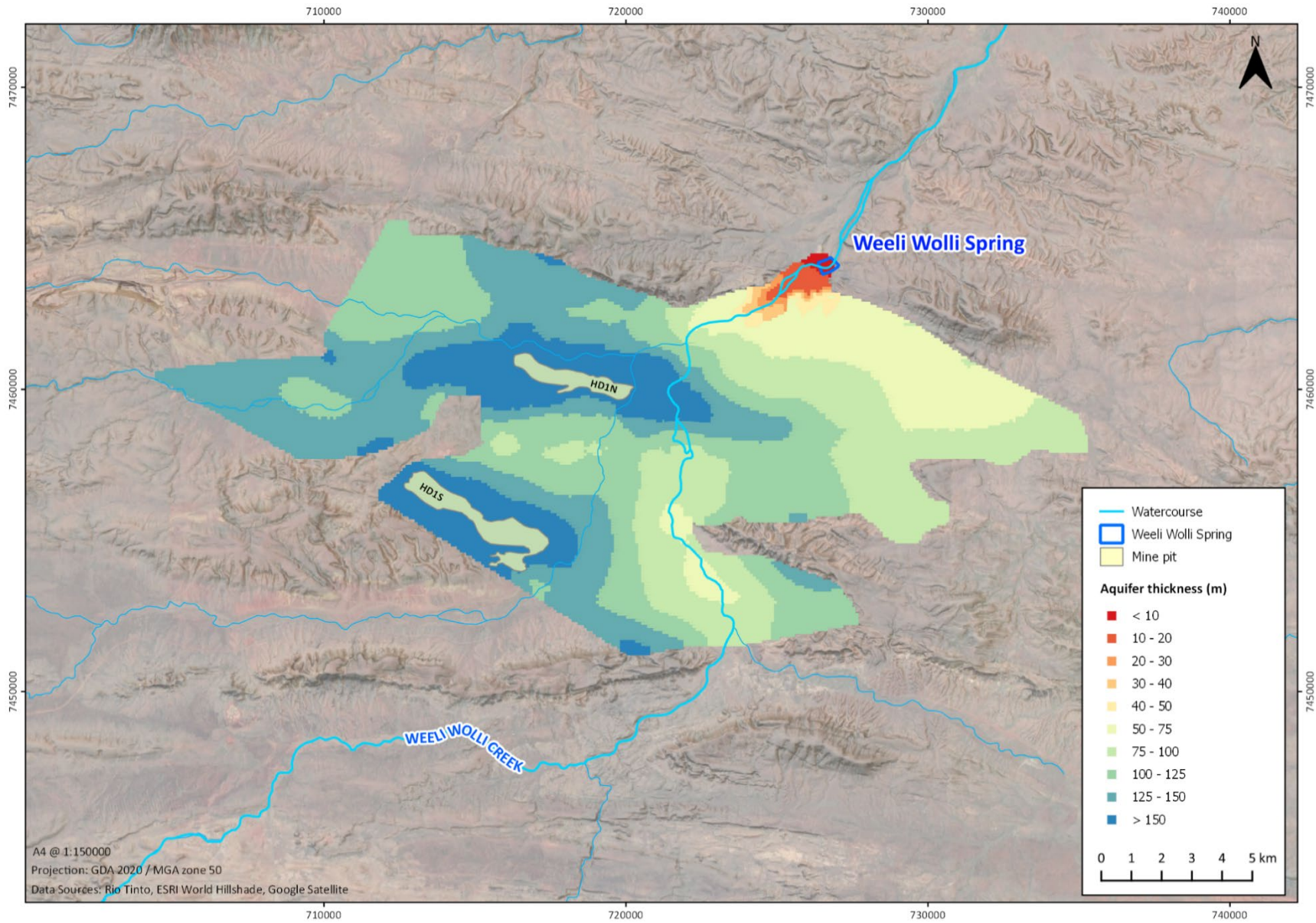
Figure 5 Aquifer thickness

Groundwater recharge

Groundwater recharge in the study area primarily occurs through diffuse rainfall recharge and leakage underneath Weeli Wolli Creek and other ephemeral streams. The diffuse recharge rate based on chloride mass balance has been estimated to be in the order of 5.8 mm/year (Cook et al. 2016 p. 51). Recharge from creek infiltration downstream of Weeli Wolli Spring (near the confluence of Marillana Creek and towards Fortescue Valley) has been previously estimated by Dogramaci et al. (2016) to be in the order of 0.1 to 8.4 $m^3/d/m$ using water balance and water table fluctuation (WTF) methods (Healy and Cook, 2002). Creek recharge at HD1 is evidenced by groundwater level monitoring data across the site, namely at BH15 which has seen groundwater level increases of up to 5 m during periods of heavy rainfall (Figure 6). Temporal sampling of environmental tracers within the dewatering bores shows an increase in CFC-12 concentrations, further verifying that younger groundwater is being recharged via creek infiltration.

Groundwater discharge

Groundwater primarily discharges out of the aquifer towards the north-east at Weeli Wolli Spring. The spring is formed by the absence of the weathered Wittenoom Formation where groundwater is forced to the surface as the aquifer pinches out. Baseflow underneath the spring is approximately 5 ML/d (RTIO, 2018a) and has not changed since mining began at HD1 largely due to it being thin coupled with spur irrigation discharge in the area.

Surplus groundwater from dewatering has been discharged to Weeli Wolli Spring and the adjacent phreatophytic vegetation along Weeli Wolli Creek since onset of mining in 2007. Discharge occurs through a series of 13 off-take spurs along a 4 to 5 km stretch of Weeli Wolli Creek located roughly 5 km north-east of HD1N. Approximately 30 % (20 ML/d) of surplus mine water irrigates the spring while the remaining 70 % of excess water is discharged further downstream of Weeli Wolli Spring at a gabion discharge point. Aquifer recycling rates from spur irrigation are estimated to be 9 – 12 ML/d which is approximately 50 % of irrigated mine water (RTIO, 2018a). Groundwater levels in the vicinity of the spring have remained at pre-mining water levels, with only minor drawdown of 1 – 2 m observed immediately upstream of the spring. This is further verified by groundwater level monitoring data at BH17d (Figure 6). Groundwater levels have remained at approximately 556 m AHD at BH17d since onset of mining.

Groundwater abstraction

Dewatering associated with mining operations has developed an extensive cone of depression in the area, lowering the water table by over 100 m in the immediate vicinity of HD1N with drawdown propagating to ~ 7 km away from the mine. Dewatering rates vary across the HD1 due to variations in aquifer heterogeneity, depth of the ore body, and differences in hydraulic conductivity between the aquifer and ore bodies in the area. In total, dewatering abstraction at HD1 has consistently averaged above 100 ML/d since 2012 (RTIO,

2018). All production bores are situated along the perimeters of the pits (Figure 3) with utilisation remaining consistently high throughout the mining period.

Evapotranspiration

Using a mathematical stochastic approach, loss of groundwater via evapotranspiration has been estimated to be in the order of 2 to 6 ML/d (RTIO, 2018a). Evapotranspiration rates have likely increased in recent years due to the constant discharge of mine water into Weeli Wolli Creek. This has caused a substantial amount of Melaleuca trees to establish along the creek line and in the spring which have more than likely increased transpiration rates since commencement of mining (RTIO, 2018).

Groundwater quality

Regionally, total dissolved solids (TDS) content in the groundwater is less than 700 mg/L, which is considered fresh. Major ion concentrations show no dominant species type, but samples are hard to very hard. This is likely attributed to the dissolution of dolomite and other calcium bearing sequences within the aquifer (RTIO, 2018a).

Groundwater level response

Time series hydrographs of various groundwater level monitoring bores in the study area are presented in Figure 6 with their locations shown in Figure 7. Groundwater levels in the immediate vicinity of HD1N show a decline of 90 m between 2007 and 2017. In comparison, the drawdown observed at HD1S is markedly less, having seen a groundwater level decline of only 30 m for the corresponding time period. It should be noted, the initial drawdown observed at HD1S is attributed to the dewatering at HD1N given the southern borefield only became operational in 2011. Furthermore, the quantity of bores at HD1S undergoing dewatering is far fewer in comparison to HD1N.

Apart from BH17d, all monitoring bores show evidence of drawdown decline associated with HD1 dewatering. Groundwater levels at BH13 (located approximately 5 km west of HD1N) show a drawdown of almost 50 m between 2007 and 2017. BH15 is also characterised by fluctuations in groundwater levels which are brought on by periods of weather induced recharge events. The rainfall event of late 2013/early 2014 shows groundwater levels rising by over 5 m, which indicates a significant portion of rainwater is recharged to the underlying aquifer. Weather attributed fluctuations are also observed in BH19, although not as prominently as observed at BH15, suggesting recharge from creek infiltration is occurring along ephemeral drainage lines in the alluvial plain east of Weeli Wolli Creek. Despite its proximity to Weeli Wolli Creek, BH20d does not show the same weather influenced fluctuations in groundwater levels which indicates that creek recharge is substantially less in the southern part of the aquifer. This is potentially attributed to a difference in the lithological composition of the creek bed, a reduced vertical hydraulic conductivity or that more water is being lost to evapotranspiration processes.
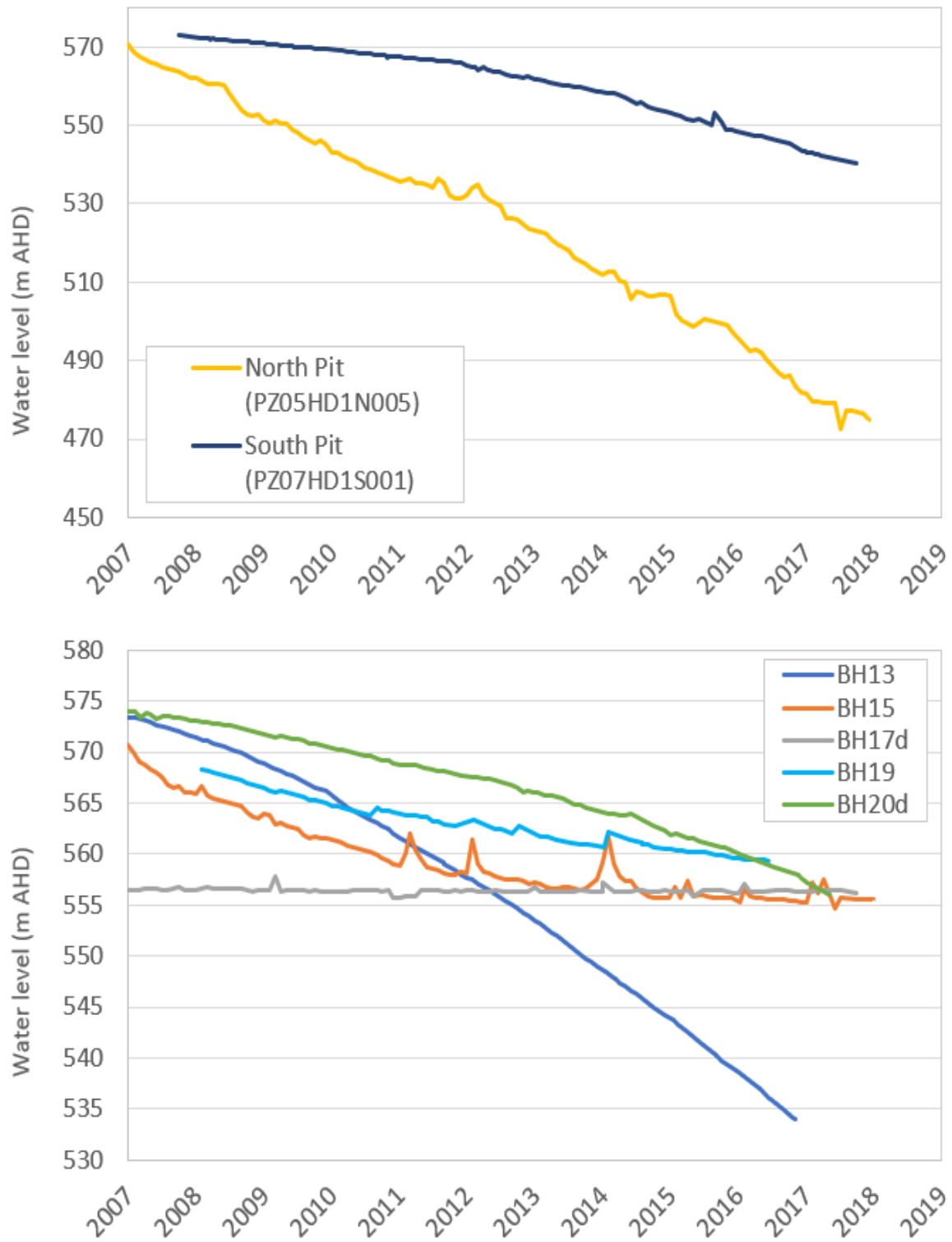
Figure 6 Groundwater level monitoring at HD1 (locations in Figure 7)
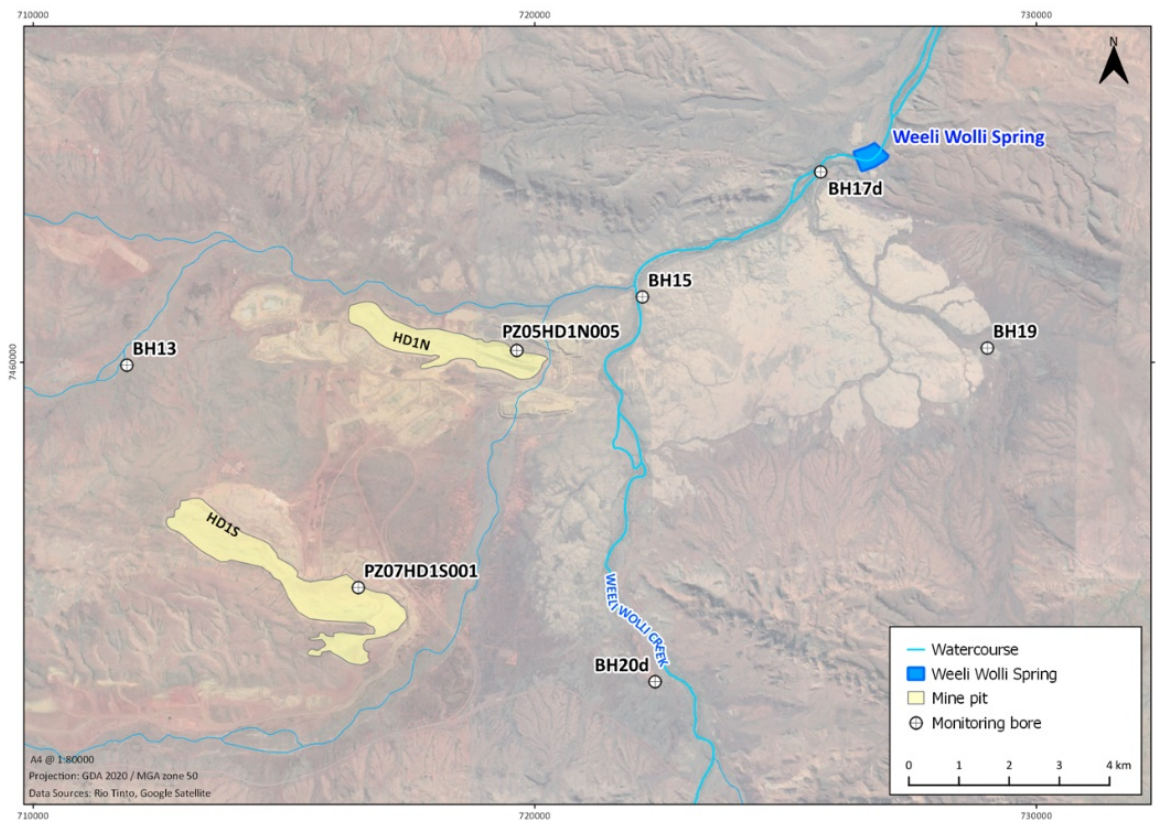
Figure 7 Monitoring bore locations

Summary

The key hydrogeological processes/properties relevant to HD1 are presented in Figure 8 and can be summarised as follows:

1. **Pre mining groundwater water levels**
    - Prior to mining, groundwater levels ranged from 574 m AHD in the immediate vicinity of HD1S to 556 m RL near Weeli Wolli Spring, with flow directed towards the north-east

2. **Groundwater drawdown**
    - Change in water table depth due to mass dewatering
    - Groundwater level monitoring data at HD1N and HD1S shows groundwater levels of 475 and 540 m AHD at the end of 2017, respectively

3. **Diffuse rainfall recharge**
    - Diffuse rainfall recharge using chloride mass balance is estimated to be in the order of 5.8 mm/year (Cook et al. 2016)

4. **Creek recharge**
    - Recharge via creek infiltration occurs during periods of flow brought on by heavy rainfall, as evidenced by groundwater level monitoring data at BH15 and BH19
    - Temporal sampling of dewatering bores shows a recent increase in CFC-12 concentrations, indicating that younger groundwater is recharging the aquifer though creek infiltration

19

5. **Spur irrigation recharge**

   - 30 % of excess mine water is discharged via 13 off-take spurs into Weeli Wolli Creek to help main baseflow at Weeli Wolli Spring

   - Aquifer recycling rates underneath the creek are estimated to be in the order of 9 – 12 ML/d (RTIO, 2018a)

6. **Evapotranspiration**

   - Evapotranspiration rates near Weeli Wolli Spring range between 2 – 6 ML/d and have likely increased in recent years due to the constant discharge of surplus mine water into Weeli Wolli Creek

7. **Weeli Wolli Spring baseflow**

   - Baseflow underneath Weeli Wolli Spring is approximately 5 ML/d (RITO, 2018a) and has remained relatively unchanged since onset of mining

8. **Surface water outflow via gabion discharge**

   - The remaining 70 % of excess water is discharged further downstream of Weeli Wolli Spring at a gabion discharge point

Figure 8 Conceptual model at HD1 (after RTIO, 2018a)

4. PRE-EXISTING MODEL

Overview

This study utilises a pre-existing MODFLOW (McDonald and Harbaugh, 1988) groundwater numerical model to simulate advective transport with particle tracking, specifically the RTIO (2018) HD1 closure model which was developed in response to the RTIO Order of Magnitude (OoM) HD1 Partial Closure Study.

The study aimed at assessing the appropriate closure options of HD1, by defining water closure strategy options for restoring a self-sustaining Weeli Wolli Spring and Creek ecosystem (RTIO, 2018). This subsequently led to an updated hydrogeological conceptualisation (RTIO, 2018a) and development of a groundwater model designed to assess groundwater recovery timeframes and volumes following mine closure in order to define water management strategies required to meet Ministerial Statement (MS) commitments, specifically MS584 (RTIO, 2018).

Previous work

Numerical groundwater modelling of the regional aquifer at HD1 has been ongoing for the better part of 20 years to refine dewatering predictions during mining and assess groundwater management options at closure (RTIO, 2018). Adjustments have been made over time to several models in response to updated hydrogeological information received. The works completed at HD1 thus far are presented in Table 2, with the OoM closure mode highlighted.

Table 2 Previous modelling work undertaken at HD1

Author	Highlights
Aquaterra (2000)	• First numerical model developed to simulate groundwater recovery at HD1 as part of investigations for the Public Environmental Review (PER)
Aquaterra (2002)	• Adaptation of the initial groundwater model with the acquisition of new long-term monitoring data and short-term pumping test data
Aquaterra (2008)	• Revision of existing groundwater model with updates to aquifer geometry and hydraulic properties • Incorporation of operational pumping data from 2007
RPS (2011)	• Updated aquifer geometry

	• Improved model performance with an updated calibration spanning January 2007 to March 2011
RPS (2015)	• Updates to closure scenarios
RTIO (2018a) RTIO (2018)	• Updated hydrogeological conceptualisation • Development of RTIO HD1 OoM closure model
Golder (2019)	• RTIO HD1 closure model used to assess predictive dewatering and predictive closure scenarios • Volume and rates of water required to recover groundwater levels to pre-mining within a 20-year timeframe post mine-closure

Model design

Numerical code

The model utilises the MODFLOW-USG (Panday et al, 2013) code to simulate groundwater flow in the HD1 surficial aquifer, operating under the Groundwater Vistas graphical interface Version 7 (ESI, 2020). The initial model as developed by RTIO (2018) utilised the MODFLOW-SURFACT code (Hydrogeologic Version 4.0). MODFLOW-USG provides several advantages as it allows a wide variety of structured and unstructured grid types, including nested grids, rectangles and other cell shapes. Unstructured gridding offers greater flexibility in grid design and can be used to focus resolution along areas of importance (i.e. bores, rivers). The relevance of unstructured gridding to this study is discussed further in the following chapter (Chapter 5).

Model domain and extent

The model extent and grid offset coordinates of the lower left-hand corner at set at 704000 E and 74151000 N (GDA 94, MGA zone 50). The model is discretised and arranged into one layer comprising of 20,622 active cell nodes with a uniform grid size of 100 x 100 m (Figure 9). A single layer represents the surficial aquifer at HD1 (as per the conceptualisation, see Chapter 3) and is bounded by dyke barriers and geological units with negligible hydraulic connection (i.e. Mt McRae Shale and unmineralised Marra Mamba Formation). The top of the layer is defined by the regional topography (50K mapsheet) and ranges from approximately 560 m nearby to Weeli Wolli Spring to 650 m along the southern flank. The bottom of the layer is defined as per the conceptualisation undertaken by RTIO (2018a) and ranges from 410 m in the immediate vicinity of HD1N to approximately 550 m near Weeli Wolli Spring. The aquifer thickness is also shown in Figure 5.

Boundary conditions

All lateral boundaries into and out of the groundwater model are represented as no flow boundaries, apart from a single set of drain cells in the north-east which represent groundwater outflow from Weeli Wolli Spring (Figure 9). Drain cells are represented using the MODFLOW Drain Package. The cells are assigned with a stage height of 556 m AHD and a very high conductance (5000 m^2/d). The package assumes the water level stays constant throughout the simulation and allows the flux through the drain to increase or decrease down to zero but not reverse (i.e. add water into the groundwater model).

Temporal variation

The HD1 closure model (RTIO, 2018) is a transient model, and therefore simulates changes in groundwater levels and fluxes over time. The temporal model spans from 2007 (onset of mining) to the beginning of 2018 (development date of model). The model utilises quarterly stress periods (approximately 90 days), which amounts to 45 stress periods between Q1 2007 and Q1 2018 in total.

Pre-mining water levels

Pre-mining water levels represent the initial conditions in the model. The pre-mining water level contours from RTIO (2018a) were converted to a surface and subsequently imported into the model via a matrix file to define the initial water levels in the calibration simulation (RTIO, 2018). The pre mining water levels range from 572 m AHD at HD1N and HD1S to 556 m AHD at Weeli Wolli Spring (see Figure 4).

System stresses

Groundwater recharge

Recharge in the HD1 model is represented using the MODFLOW Recharge Package. Diffuse recharge is applied uniformly over the entire model domain at a uniform rate of 1.6 x 10^{-5} m/d (equivalent to approximately 3 ML/d as consistent with the conceptualisation and chloride mass balance). Historical spur irrigation rates have been applied evenly over the assigned spur area with historical rates ranging from 0.002 to 0.065 m/d (equivalent to 1 to 34 ML/d over the assigned surface area) throughout the transient period with an average rate of approximately 20 ML/d. The groundwater recharge zonation applied to the model is presented in Figure 10.

The Groundwater inflow zones along the northern and southern flank valleys (as conceptualised, see section 3) are not represented in the model. The respective zones were left out of the initial calibration undertaken by RTIO (2018) and only used for the closure scenarios on account of desaturation of the alluvium/detritals (brought on by propagated drawdown from mass dewatering). This study utilises the calibrated model developed by RTIO (2018), thus regional inflow is not incorporated.

Groundwater abstraction

Groundwater abstraction in the model is represented using the MODFLOW Continuous Linear Network (CLN) Package. The initial model utilised the multi-node well (MNW) package for MODFLOW (Halford and Hanson, 2002) which is not compatible with MODFLOW-USG run models, notwithstanding the CLN package provides many of the same functionalities as the MNW Package. A total of 38 dewatering bores are used to simulate the withdrawal of groundwater from the HD1N and HD1S ex-pit dewatering borefields. Historical dewatering rates range from 5 to 110 ML/d. The locations of the bores relative to the pits are presented in Figure 3.

Evapotranspiration

Evapotranspiration in the numerical model is represented with the MODFLOW Evapotranspiration Package to a line of cells in the confines of Weeli Wolli Creek (Figure 11). Evapotranspiration ranges from 2 – 6 ML/d as per the conceptualisation. A nominal extinction depth of 0.5 m is applied to ensure the aquifer remains fully saturated underneath the creek

Hydraulic parameters

Hydraulic parameters differ substantially between the northern and southern pits on account of the disproportionate amount of drawdown observed between the two pits (see section 3, Figure 6). Furthermore, the hydraulic conductivity underlying Weeli Wolli Creek is conceptualised to be very high due to thinning of the aquifer and no change in throughflow. Table 3 summarises the calibrated hydraulic parameters adopted in the RTIO model in relation to their respective zones. Hydraulic zoning of the parameters in the model is based on the conceptualisation as undertaken by RTIO (2018a). The different zones of hydraulic conductivity are presented in Figure 12.

Table 3 Summary of hydraulic parameters adopted in the numerical model (RTIO, 2018)

Zone	Area (km^2)	Kh (m/d)	Kz (m/d)	Specific yield (-)	Specific storage (-)	Porosity (%)
North Pit	15.64	20	20	0.1	1 x 10^{-5}	0.15
South Pit	13.91	3	3	0.08	1 x 10^{-5}	0.15
Weeli Wolli Creek	0.61	100	100	0.35	1 x 10^{-5}	0.50
Remaining domain	175.84	2	2	0.05	1 x 10^{-5}	0.15
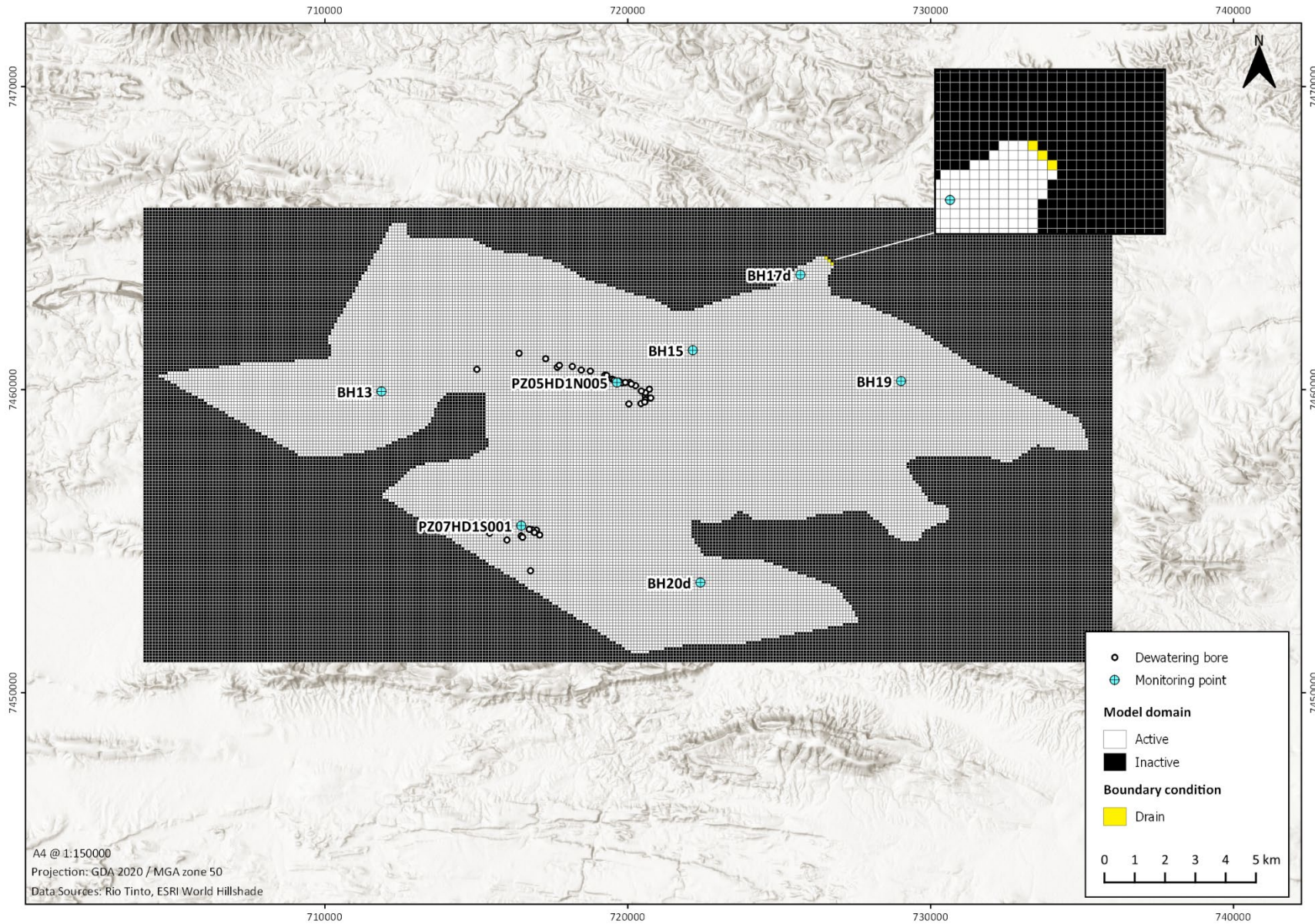
Figure 9 Model domain and boundary conditions
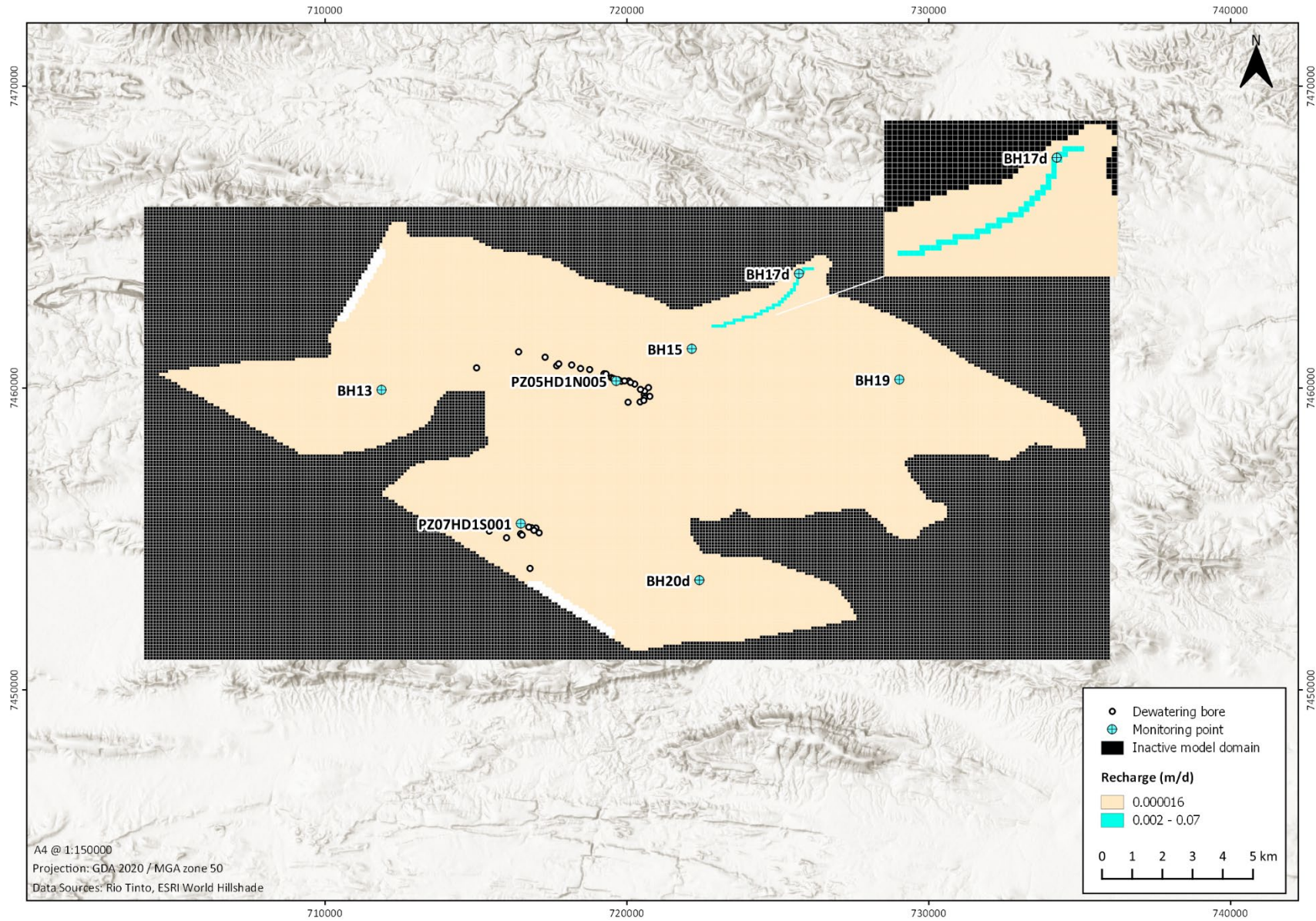
Figure 10 Recharge zonation
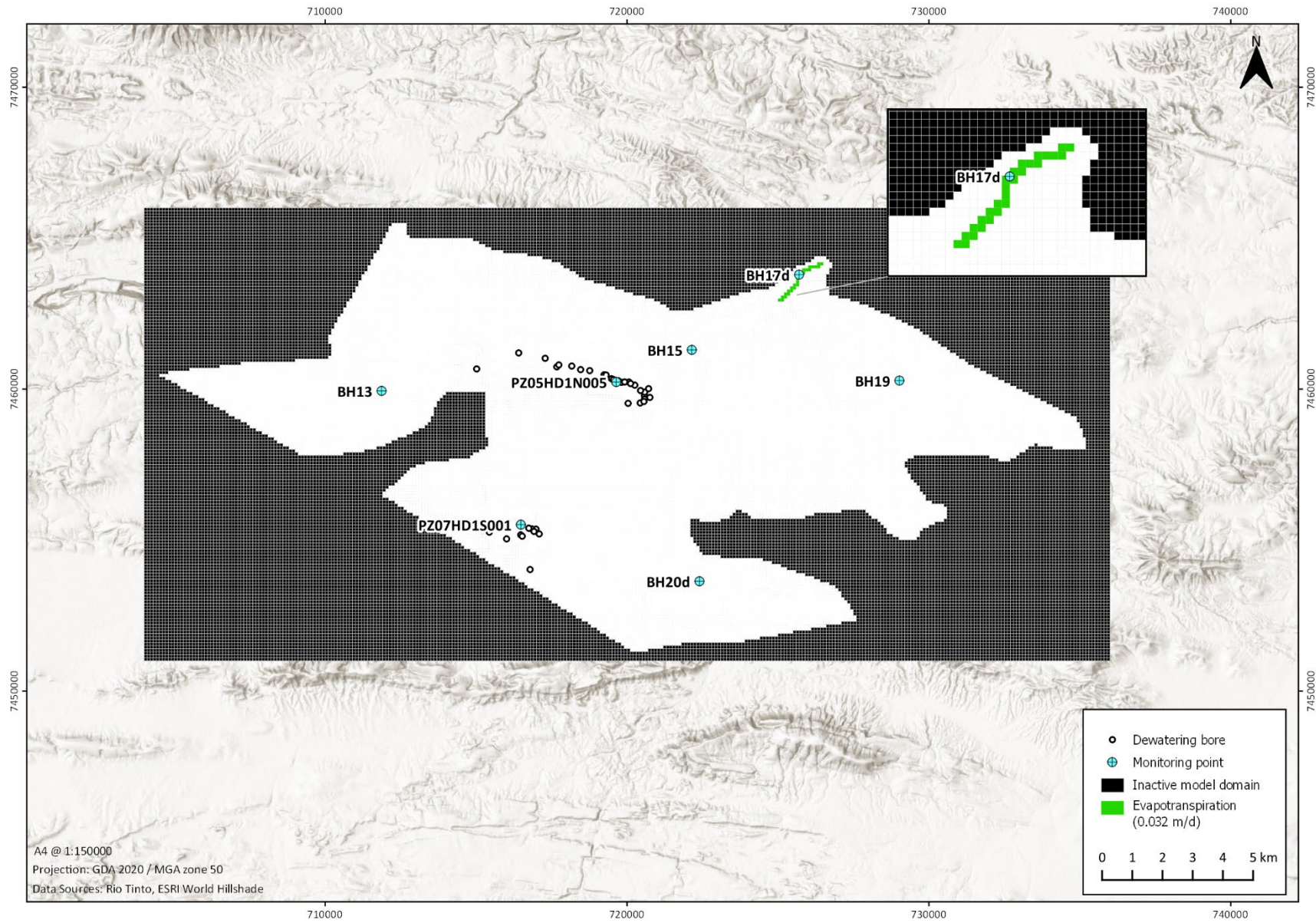
Figure 11 Evapotranspiration zonation
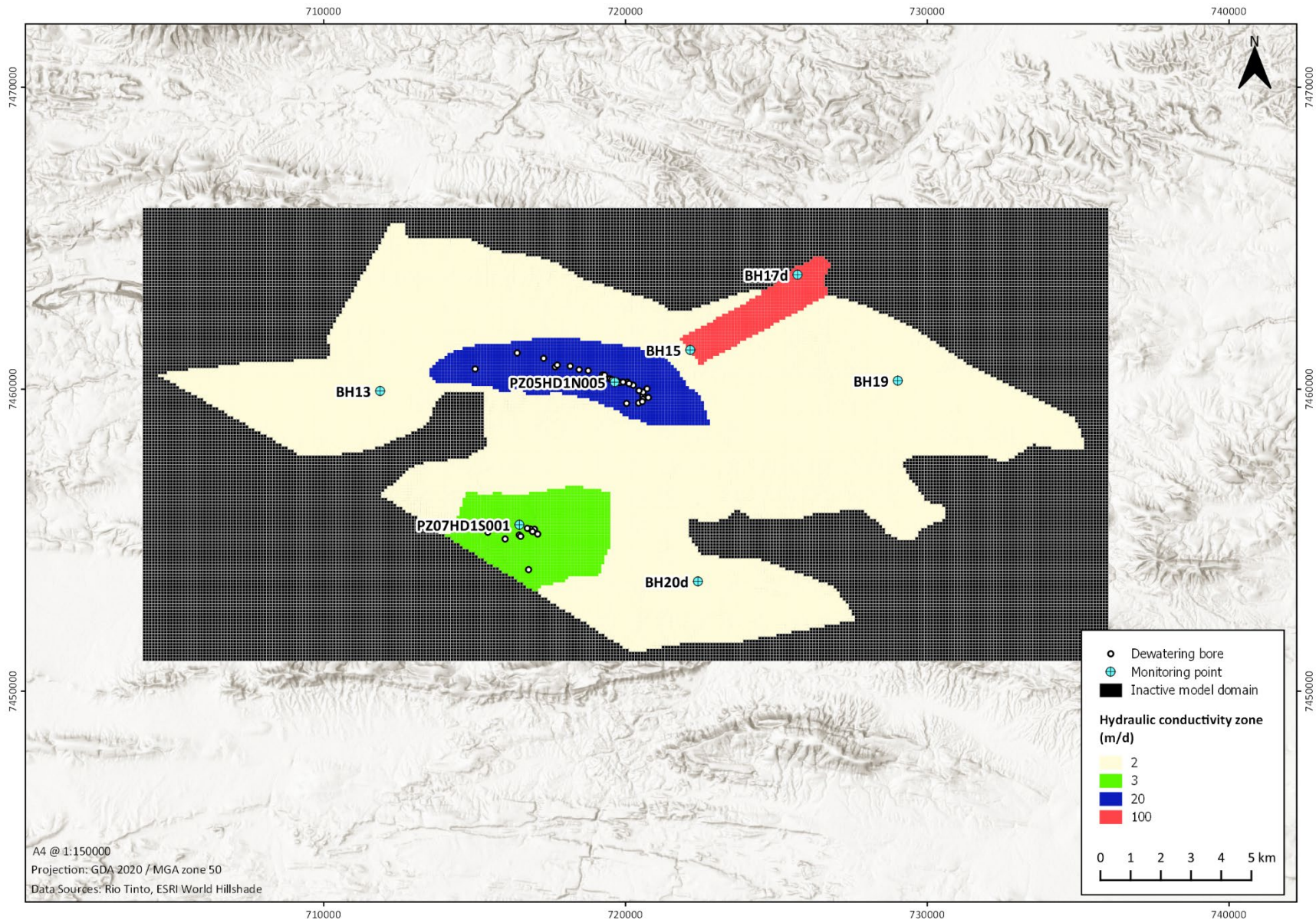
Figure 12 Hydraulic conductivity zoning

Initial model calibration

The calibration methodology as undertaken by RTIO (2018) focused on achieving a representative cone of depression at the end of 2017 which broadly matched observed levels with historical abstraction rates from 10 years of dewatering (2007 – 2017). This was achieved by the visual matching of drawdown and observation data at key locations via automatic and manual adjustment of hydraulic parameters. Final calibrated hydraulic parameters are shown in Table 3.

PZ05HD1N0005 and PZ07HD1N0001 were the two primary bores used to track model performance with time. This is largely due to their proximity to their respective borefields and availability of drawdown observation data throughout the historical period. Additionally, simulated water levels were also tracked against monitoring data at BH15 and BH17d to ensure hydraulic parameters underlying Weeli Wolli Spring were sufficiently represented. The monitoring locations utilised in the model are shown in the preceding figures (Figure 9, Figure 10, Figure 11, Figure 12). Regionally, the hydrogeology is less understood and there are large areas which lack significant observation data; thus emphasis was not placed on monitoring bores located on the fringes of the model domain during model calibration (BH13, BH19, BH20d). Figure 13 shows the calibration performance modelled water levels against the observed water levels (RTIO, 2018).

Image removed due to copyright restriction.

Figure 13 Model calibration performance (RTIO, 2018)

5. METHODOLOGY

Particle tracking

Overview

Particle tracking post-processing programs such as MODPATH and mod-PATH3DU provide a valuable tool for simulating the performance of advective transport within a numerical groundwater model. The programs use model outputs from steady-state or transient MODFLOW simulations to compute paths for imaginary particles of water moving through a simulated groundwater system. In addition to providing computed particle paths, they are capable of computing travel times for particles moving through a groundwater system and can delineate areas of recharge (i.e. locations where particles enter a simulated groundwater domain).

In this study, a backward particle tracking approach is utilised to compute flow paths and determine advective travel times by placing particles along the well screens of individual dewatering bores and tracking back to their points of origin (i.e. recharge areas). The final travel times are compared with known atmospheric concentrations of CFC-12 at time recharge and averaged to obtain an average CFC-12 concentration within each bore. The resulting calculated concentrations are ultimately compared with measured (i.e. sampled) concentrations of CFC-12 to:

> (1) determine how tracer concentrations can help constrain and calibrate a groundwater model, and

> (2) improve estimates of model parameters, specifically groundwater recharge.

Software

Particle tracking is undertaken using mod-PATH3DU version 2.0 (Papadopolous, 1994). This particle tracking software is chosen for its compatibility with MODFLOW-USG run models, unstructured grid types and transient groundwater models in general. When using MODPATH with transient models, particles are only tracked for the length of the simulation. Using mod-PATH3DU, particles continue to migrate beyond the total simulation time by using the groundwater flow field from the last time step of the simulation, or in the case of reverse tracking (as utilised in this study), using the flow field from the first time step. This is particularly important in the delineation of recharge areas as particles may continue to flow beyond the total simulation time. Currently, MODPATH and MODPATH6 (Pollock, 2012) are not compatible with MODFLOW-USG run models and can only support groundwater flow simulations for structured grids based on MODFLOW. The relevance of the unstructured grid format to this study is discussed further below.

The main difference between MODPATH and mod-PATH3DU is attributed to the particle tracking schemes utilised in both programs. Currently, two distinct tracking schemes are carried out in mod-PATH3DU, namely the Pollock and SSP&A methods. MODPATH solely uses the Pollock method, which linearly interpolates groundwater velocities within each finite-difference grid to evaluate velocity fields (Pollock, 1989, cited in Muffles, et al. 2014, p. 2). The path of a particle is then computed by moving the particle between adjacent cells until a boundary or termination point is reached. The linear velocity interpolated via the Pollock method is not applicable to grids which are designed to provide greater flexibility and more options in terms of spatial discretisation (i.e. unstructured). Unlike the Pollock method, the SSP&A method computes the velocity flow field based on the distribution of hydraulic head generated by MODFLOW-USG using kriging methods and is grid independent. Kriging is a multi-step process which is often used to interpolate spaced measurement data to unsampled locations. In this context, the groundwater levels calculated by MODFLOW that are used to determine velocity represent the "measured" data while the particle's position is the "unsampled" location (Muffles et al. 2014, p. 9).

Despite it being grid independent, the accuracy of the kriging interpolation method is dictated by grid discretisation, in addition to aquifer heterogeneity and proximity to specific boundaries (Muffles et al. 2014, p. 17). Specifically, the refinement of grid cells (i.e. more cells spaced closer together) provides the model better information by reducing the number of unsampled location points to calculate velocities and represent flow paths in areas of importance. For this reason, grid cells hosting the HD1N dewatering bores are discretised using the quadtree refinement function in MODFLOW-USG. In quadtree refinement, each cell is assigned an integer code between 1 and 7 with each higher number representing an exponential increase in grid cells. For example, a value of 1 indicates that cell will not be divided. A value of 2 means the cell will be divided into 2 columns and 2 rows, 3 indicates a 4 x 4 division, etc. Grid cells hosting and adjacent to the HD1N dewatering bores have been assigned a value of 4, indicating an 8 x 8 split, as shown in Figure 14.
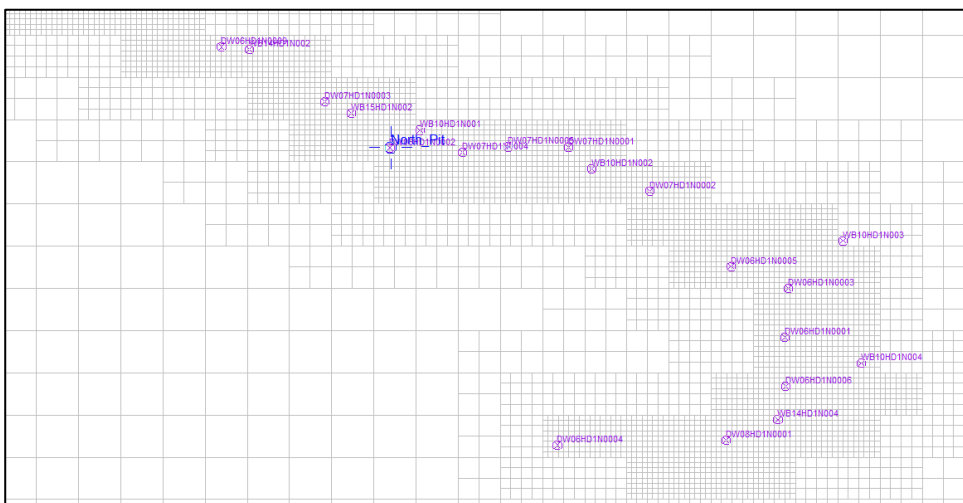
Figure 14 Quadtree grid refinement around HD1N

32

Simulation of particle tracking

To date, four sampling rounds have been undertaken to determine groundwater ages from concentrations of CFCs and other tracers in the groundwater abstracted from the dewatering bores at HD1 (2008, 2014, 2016 and 2017) with a total 17 bores having been sampled at some point thus far (Cook et al. 2017, p. 43). Most of the bores are situated nearby to HD1N, while two bores are close to HD1S. In this study, six of the sampled dewatering bores are used a basis for the particle tracking due to the temporal variability of the sampled data (2008, 2014 and 2017).

Details of the specific bores are presented in Table 4, all of which are in the immediate vicinity of HD1N. Screen lengths vary from 83 m at DW07HD1N0002 to 157 m at DW06HD1N0008. DW06HD1N0003 and DW06HD1N0005 are the eastern-most and closest bores to Weeli Wolli Creek, located approximately 0.8 and 0.95 km from the creek, respectively. DW07HD1N0004 and DW07HD1N0005 are situated immediately north of HD1N while DW06HD1N0008 is the western-most bore and is located roughly 3 km west of Weeli Wolli Creek. Locations of the dewatering bores subject to particle tracking in this study are shown in Figure 15.

Table 4 Details and specifications of bores utilised in particle tracking analysis

Well	Easting	Northing	Elevation (m AHD)	Screen length (m)	Top of screen (m AHD)	Bottom of screen (m AHD)
DW07HD1N0002	720254	7460130	585.8	83	476	393
DW07HD1N0004	719792	7460219	587.4	118	524	406
DW07HD1N0005	719918	7460235	588.0	137	511	374
DW06HD1N0003	720580	7459887	592.5	148	577	429
DW06HD1N0005	720441	7459960	588.6	150	572	422
DW06HD1N0008	718466	7460647	597.4	157	436	593
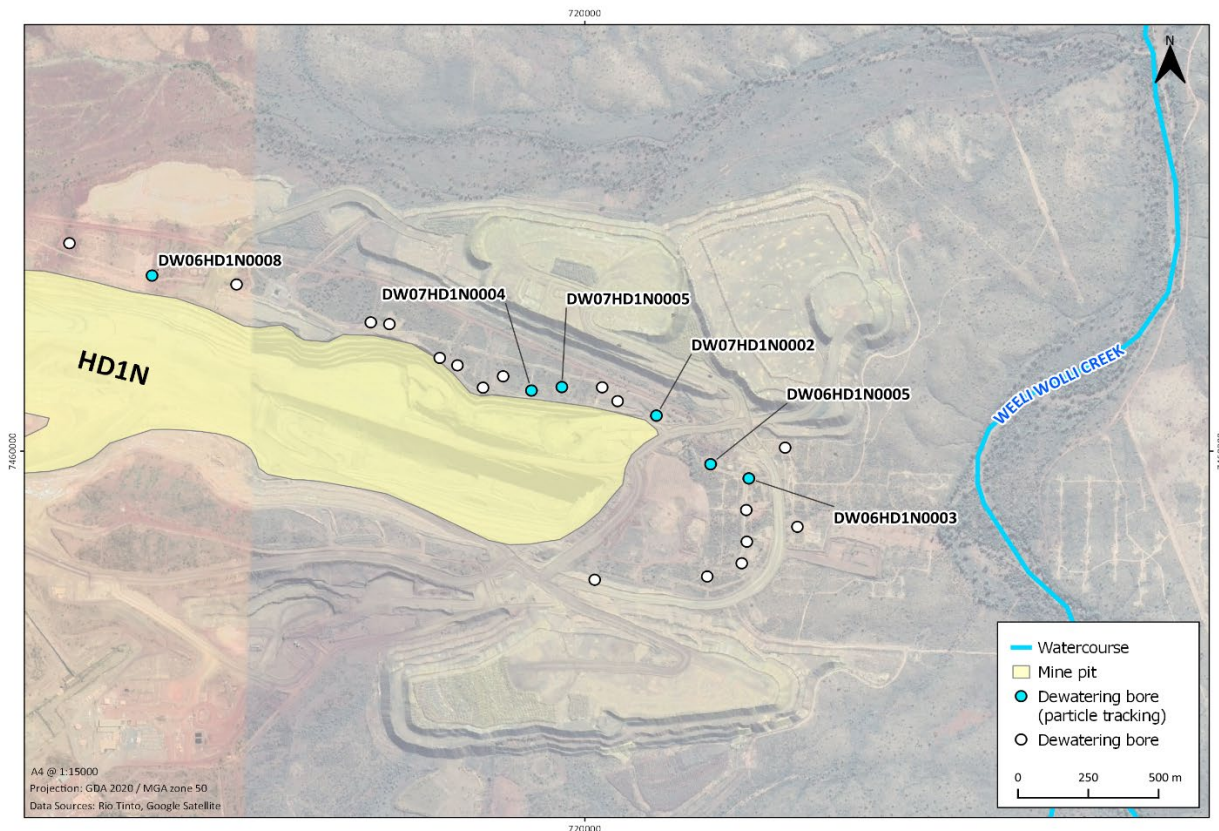
Figure 15 Dewatering bores utilised in particle tracking analysis

For the particle tracking, 100 particles are distributed along the well screens for each bore and tracked backward in time to their points of origin (i.e. areas of recharge). This is achieved by circularly distributing 5 particles along 20 vertical release points across the lengths of the screens for each of the respective bores (amounting to 100 particles for each bore). Particle placement can have severe implications on model results (Pollock, 2012). For example, a particle released from a single point at the centre of a bore will take the preferential path based on the potentiometric surface calculated from the corresponding MODFLOW simulation and may not capture all potential recharge areas. Using a circular distribution of particles reduces this uncertainty and provides a realistic representation of pumping conditions (i.e. a pumping bore is extracting water from all directions).

Each particle is associated with a flow pathline, a travel time along the pathline, and an endpoint which determines the particles final travel time. The endpoint signifies the area in the model where the particle enters the groundwater system. Travel times of particles are dependent on a number of factors, including the amount of recharge in the corresponding grid cell, hydraulic characteristics of the cell (i.e. hydraulic conductivity, porosity) and position/orientation of the water table in the corresponding time step. The influence model parameters have on particle pathlines and travel times are explored further in following sections of this study.

For each dewatering bore, the travel time associated with each particle is compared with atmospheric equilibrium concentrations of CFC-12 at time of recharge. CFC-12 concentrations are based on measured atmospheric concentrations at Cape Grimm in Tasmania (Cunnold et al. 1994; cited in Cook et al. 2017) and converted to equivalent concentrations in water (pg/kg) based on the solubility of the gas and a recharge elevation of 600 m (average surface elevation in the study area). A recharge temperature of 24 °C is assumed which is the mean annual air temperature at Newman, located approximately 75 km south-east of site. Atmospheric equilibrium concentrations of CFC-12 used for the analysis are presented in Appendix A.

Age derived concentrations from the simulations are averaged for each bore and compared with measured concentrations. For example, a particle that terminates 20 years into a simulation (i.e. recharge year of 1997 assuming the simulation begins in 2017) will have a CFC-12 concentration in water of 180 pg/kg, while a particle that terminates 50 years into the same simulation will have a concentration of approximately 23 pg/kg. Hypothetically, if these are the only two particles released from the simulation then the corresponding bore would have an average CFC-12 concentration of 102 pg/kg. Particles that take longer than 85 years to terminate (recharge prior to 1930) are assigned with as having a zero concentration and factored into the calculations accordingly.

The processes described above are undertaken using simulated groundwater levels from four different time periods (2008, 2011, 2014 and 2017) with the goal being to compare changes in simulated concentrations to measured concentrations temporally. Measured concentrations of CFC-12 at HD1 are not available for 2011. However, due to the gap between sampling periods has been simulated. The measured concentrations from the various sampling rounds are presented in Table 5. A time series concentration graph of measured CFC-12 concentrations at HD1 is also shown in Figure 2.

It should be noted, particle tracking via mod-PATH3DU only simulates advective transport. Other transport processes that affect constituent concentrations such as dispersion, adsorption, diffusion, retardation and degradation are not included in the mod-PATH3DU simulation for determining the travel times of groundwater. Thus, particle tracking results are only an approximation of the actual transport processes taking place, but nevertheless provide a good representation of average travel times. It is also important to recognise that MODFLOW is a saturated flow model, meaning that the upper boundary of the model is the water table. Particle travel times through the vadose zone (i.e. unsaturated zone) are not factored into the simulations, as identified in the review of literature. Thus, the model produces particle tracking ages that represent the travel time from the particle release location along the well screens to the top of the water table.

Table 5 Measured CFC-12 concentrations in the groundwater at HD1 in pg/kg

Well	CFC-12 (pg/kg)			
	2008	**2014**	**2016**	**2017**
DW07HD1N0002	26.5	7	12.5	154
DW07HD1N0004	13.5	14.5	22	197
DW07HD1N0005	21.5	29	22.7	144
DW06HD1N0003	50.5	35.5	110.3	159
DW06HD1N0005	40	21.5	50	210
DW06HD1N0008	20.5	20.5	39.7	167

Summary

A conceptualised diagram of the particle tracking methods undertaken in this study is presented in Figure 16 and can be summarised as follows:

1. **Placement of particles along the length of the screens**
   - Release points across the well screens vary depending on the simulation period, specifically the water table elevation in comparison to the top of the well screen
2. **Backward particle tracking toward area of recharge**
   - Travel times of particles are dependent on a number of factors, including the amount of recharge in the corresponding grid cell, hydraulic characteristics of the cell (i.e. hydraulic conductivity, porosity) and position/placement of the water table
   - In a transient model, the water table is a moving boundary hence the particles recharge at different elevations
   - Particles continue to migrate using the water table height in the first time step (for backward tracking) if the area of recharge is not reached before the end of the simulation
   - For each particle endpoint, the date of recharge is calculated by subtracting the travel time from date of sampling then assigning a concentration to the particle equal to the concentration in equilibrium with the atmosphere for the simulated recharge date

3. **Determination of average CFC-12 concentrations**
   - The arithmetic mean of the aged derived concentrations are then used to generate the simulated equivalent concentrations for comparison to measured concentrations to assess calibration quality
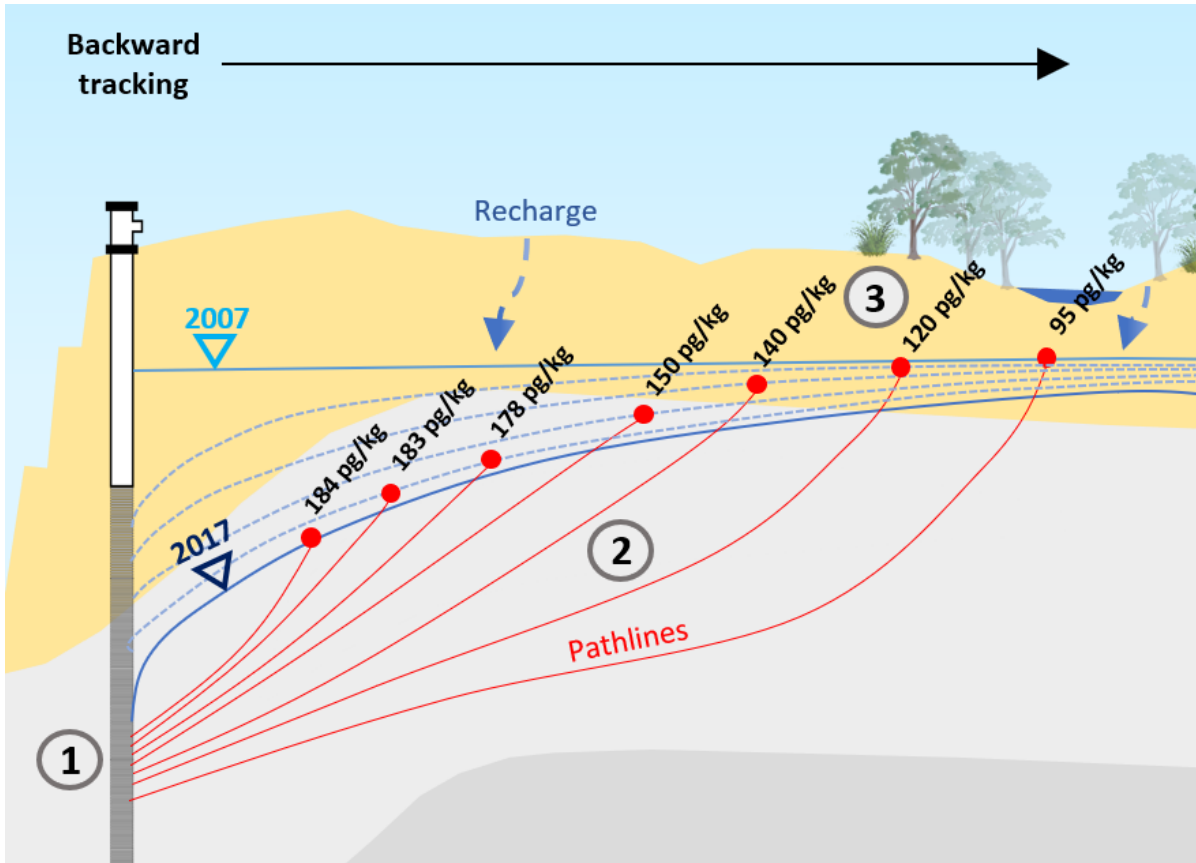
Figure 16 Backward tracking conceptual model

Model refinement

Creek recharge

The environmental tracer calibration approach can be split into several methodologies, as identified earlier (Zuber et al. 2011). One method is by calibrating a steady-state or transient model to observed hydraulic heads by adjusting model parameters (groundwater recharge, hydraulic conductivity, etc) whereby results from particle tracking are then matched to measured concentrations to constrain model parameters. The calibration methodology undertaken in this study utilises this approach, whereby particle tracking is first simulated on the pre-existing HD1 model (RTIO, 2018, see section 4) and adjusted to constrain model parameters as needs.

This involves the application of recharge along Weeli Wolli Creek which is evidenced by the increase in CFC-12 concentrations in the dewatering bores at HD1. Weeli Wolli Creek recharge has been independently

estimated, and not manually adjusted until a viable fit between measured and simulated concentrations is gathered for two reasons:

(1) manually adjusting recharge parameters until an optimum match between measured and simulated concentrations is observed can produce significant bias, whereby excessive/unrealistic quantities of recharge are applied to the domain to obtain a better match;

(2) initial calibration is significantly compromised where groundwater flow patterns and simulated hydraulic heads are not representative of actual conditions.

Thus, the calibration approach aims at adequately representing recharge along Weeli Wolli Creek without compromising the initial calibration as undertaken by RTIO (2018). Nevertheless, the application of additional recharge requires the necessary adjustments of several parameters of which are described in the following section. Ultimately, particle tracking is undertaken on the model with creek recharge applied in addition to the initially calibrated RTIO model and compared to assess fit. A sensitivity analysis on creek recharge is also undertaken to determine sensitivities and potential uncertainty to the creek recharge applied.

Water Table Fluctuation (WTF) method

Recharge along Weeli Wolli Creek has been estimated using the water table fluctuation (WTF) method (Healy and Cook, 2002) which estimates episodic recharge using water table hydrographs. The method is best applied to unconfined aquifers that display sharp rises in groundwater level due to recharge water arriving at the water table. For this reason, the WTF method has been implemented using the hydrograph from BH15 (located adjacent to Weeli Wolli Creek) which has seen groundwater level rises of up to 5 m during periods of heavy rainfall (Figure 17). The WTF method has been utilised in the area previously by Dogramaci et al. (2016) and quantified to be in the order of 0.1 to 8.4 $m^3/d/m$ downstream of Weeli Wolli Spring (near the confluence of Marillana Creek and towards Fortescue Valley).

The basis of the WTF method is that groundwater level rises in unconfined aquifers are due to recharge water arriving at the water table (Healy and Cook, 2002, p. 92). The method is best applied to short-term rises in groundwater levels in response to single storms (Healy and Cook, 2002 p. 93). Groundwater recharge is calculated as:

$$R = S_y \, \Delta h / \Delta t$$

Where S_y is specific yield, h is water table height, and t is time. WTF methods can approximate episodic recharge using water-table hydrographs measured with an appropriate time resolution. A recharge episode is defined as a period during which the recharge rate extends beyond its steady-state condition due to a sizable water input, such as a rainstorm (Nimmo, Horowitz and Mitchell 2011, p. 3). In this study, the

episodic master recession (EMR) method (Nimmo, Horowitz and Mitchell 2011) has been utilised to quantify recharge episodes by partitioning the BH15 hydrograph into discrete time intervals (based on time between measurements). To calculate the total recharge for each time interval, Δh is set equal to the difference between the peak of the rise and low point of the extrapolated recession curve at the time of the peak, as shown in Figure 17. The extrapolated recession curve is the path the groundwater level would have followed without the influence of rainfall derived recharge (Healy and Cook, 2002, p. 92).

Intervallic rates are first added and applied to the corresponding stress periods in the model, then averaged to obtain a uniform rate. WTF calculations for each interval are presented in Appendix B. Transient recharge fluxes are not applied into the model due to limitations in particle tracking post-processing. Particle tracking performed through MODPATH or mod-PATH3DU requires a "reference" time to be specified in order to be successfully simulated. Namely, boundary conditions and system stresses (i.e. recharge) remain the same in a particle tracking simulation and cannot change over time.
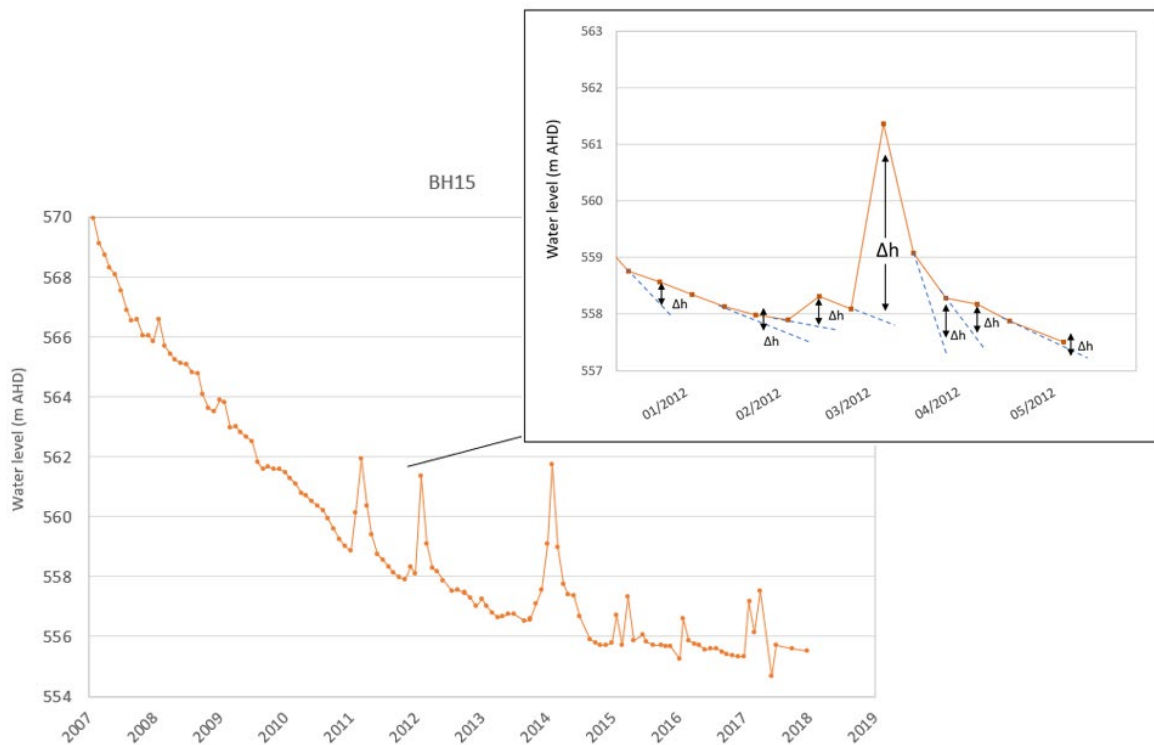
Figure 17 Water table fluctuation (WTF) method for BH15

Parameter adjustments

Spur irrigation recharge in the model has predictably been reduced to prevent a surplus a water from entering the system brought on by the addition of recharge along Weeli Wolli Creek. The model in its previous form assumes a 100% recharge rate from spur irrigation into the system with some periods of recharge exceeding 0.06 m/d. This is unlikely to be a realistic representation of actual conditions, as a large

portion of discharge water from the spurs would not be recharged into the aquifer and would either be lost via evapotranspiration processes or as surface flow downstream of Weeli Wolli Spring. The conceptualisation (see section 3) indicates aquifer recycling rates to be in the order of 9 – 12 ML/d underneath Weeli Wolli Creek, thus the spur irrigation rate has been adjusted to reflect this in the model. Spur irrigation rates in the calibrated model range from 0.001 – 0.04 m/d (equivalent to 0.5 to 20 ML/d over the assigned surface area) throughout the transient period with an average rate of approximately 12 ML/d (60% of the initial spur recharge applied to the model). Diffuse recharge in the system remains at 5.8 mm/year (equivalent to approximately 3 ML/d) as conceptualised and initially parameterised in the model.

Specific yield and hydraulic conductivity underlying Weeli Wolli Creek were necessarily adjusted to avoid a misrepresentation of the already calibrated model. This involved manual and automated adjustment of the parameters until an acceptable match to observed groundwater levels at the relevant monitoring points was found. Automated adjustment was performed using PEST (Doherty, 2018) to determine optimal hydraulic parameters. Revised and previously utilised parameters used in the model are presented in Table 6.

Through manual and automated adjustment, it has been found that a hydraulic conductivity of 180 m/d in the Weeli Wolli Creek zone produces the closest match to observed measurements. The specific yield of the zone underlying Weeli Wolli Creek has been reduced to 0.25 from an initial value of 0.35. Typically, specific yields as high as 0.35 are only observed in materials such as soil or dune sand (Heath, 1983; Morris and Johnson, 1967), therefore has been adjusted to a more suitable value. Similarly, specific yield in the zone surrounding HD1N has also been adjusted to 0.08, as per the conceptualisation which indicates regional specific yield to be approximately 8%. The porosity of detritals and other weathered unconsolidated sediments can range anywhere from 0.1 to 0.5 (Heath, 1983), thus a uniform porosity of 0.25 has also been applied across the entire domain as no clear justification is provided to the porosity parameterised in the initially calibrated model. The hydraulic conductivity of the north pit zone and remaining domain have not been altered.

Table 6 Revised and previously utilised parameters in the models

Parameter	Units	Zone	Pre-existing model	Model with creek recharge
Spur irrigation recharge	m/d	-	0.002 – 0.065	0.0012 – 0.04 (approximately 60% of initial spur irrigation recharge)

Hydraulic conductivity	m/d	Weeli Wolli Creek	100	180
Specific yield	-	Weeli Wolli Creek	0.35	0.25
		North Pit	0.1	0.08
Porosity	%	Weeli Wolli Creek	0.5	0.25
		North Pit	0.15	0.25
		Remaining Domain	0.15	0.25

6. RESULTS

Recharge estimation

By applying the WTF method outlined in section 5, Weeli Wolli Creek recharge has been estimated at an average rate of 0.009 m/d for the simulated time period (2007 – 2018) assuming a specific yield of 0.25. WTF calculations for each interval are presented in Appendix B.

Recharge has been applied along the Weeli Wolli Creek floodplain using the MODFLOW-Recharge Package at a uniform rate of 0.009 m/d. The width of the floodplain typically varies between approximately 50 and 150 m through the study area, thus a generalised width of 100 m has been applied to the cells hosting Weeli Wolli Creek in the groundwater model. Recharge zonation along the creek over the entire domain is shown in Figure 19. Grid cells hosting Weeli Wolli Creek have also been discretised with the quadtree refinement function and assigned an integer value of 4, indicating an 8 x 8 split, as shown in Figure 18. This ensures a uniform 100 m width over the course of the creek and reduces the risk of particles bypassing creek cells.
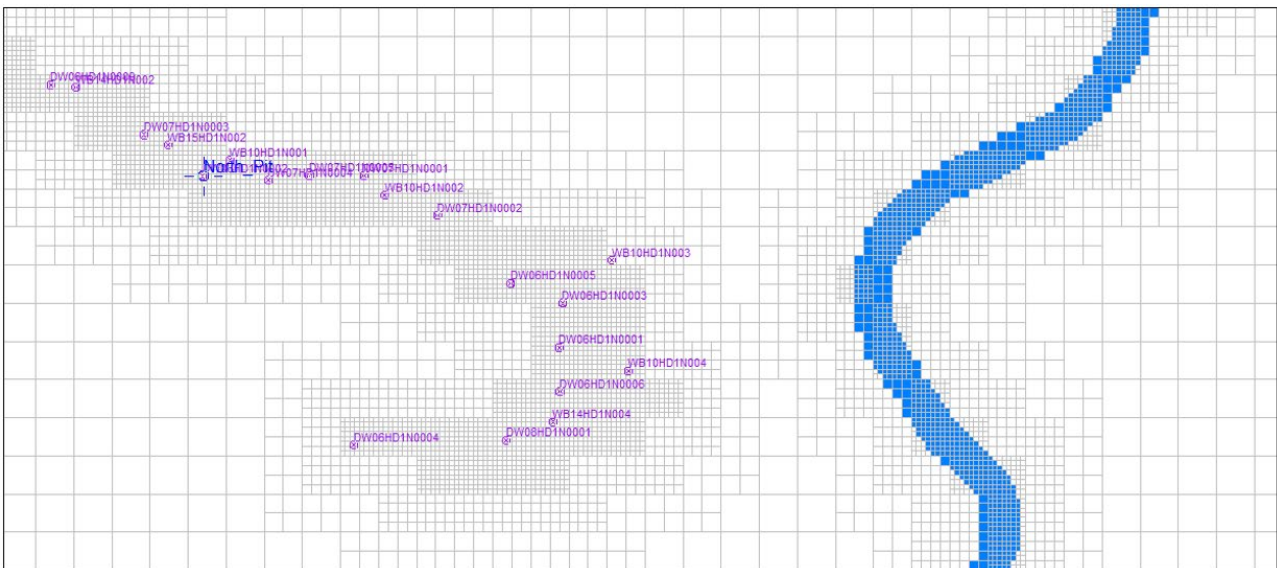
Figure 18 Quadtree grid refinement at Weeli Wolli Creek
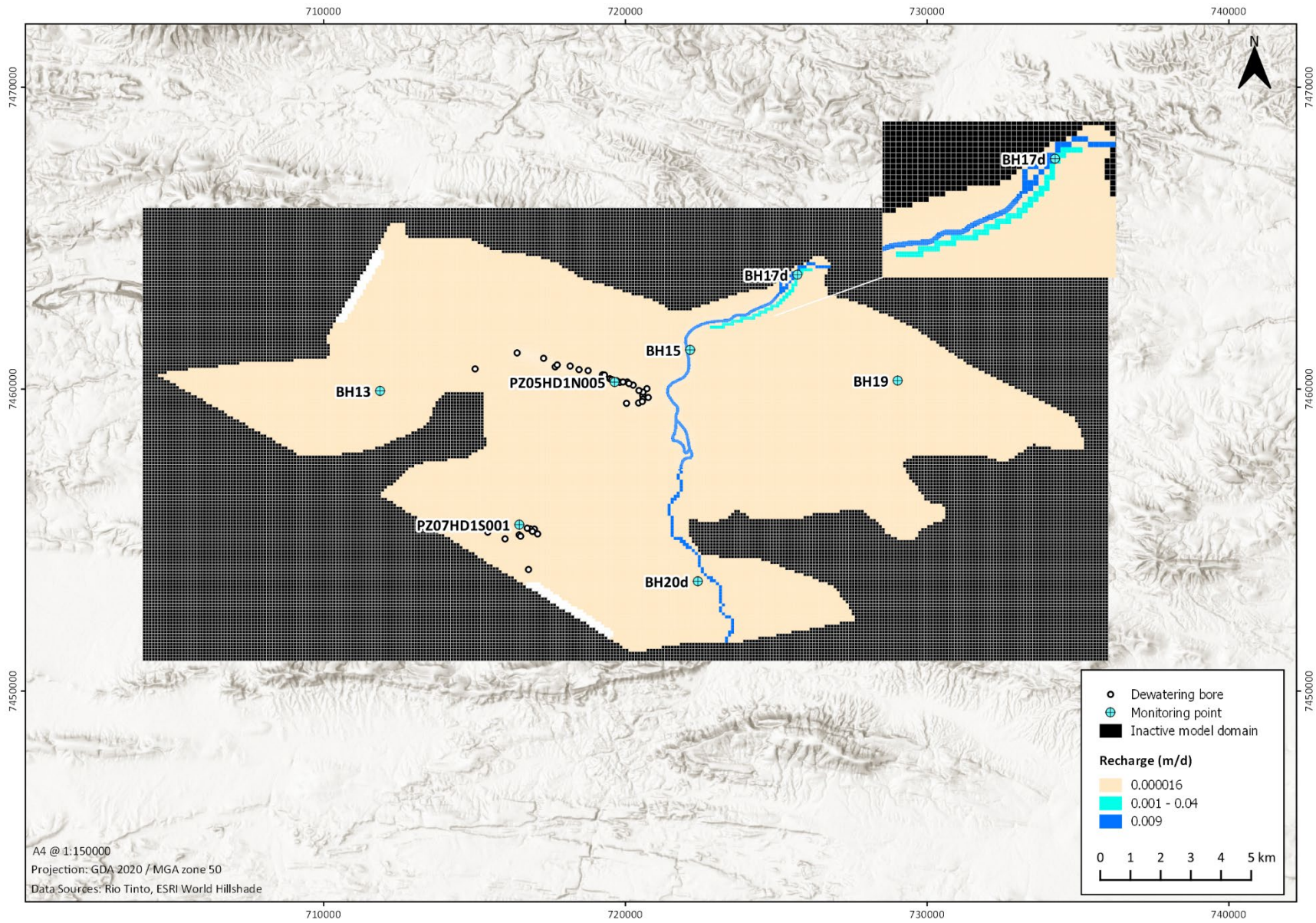
Figure 19 Weeli Wolli Creek recharge zonation

Calibration performance

Results

The simulated and observed hydrographs representing groundwater levels in key monitoring locations in the model show good agreement to the pre-existing RTIO (2018) model (Figure 20). Values of the root mean square error (RMSE) between observed and simulated measurements are 3.8, 8, 10.1 and 3.9 m at BH15, BH17d, H1DN and HD1S, respectively. Comparatively, the RMSE between observed and simulated measurements in the pre-existing model are 4.7, 10.8, 9 and 3.6 m for the same monitoring points. The model with creek recharge applied reduces the mean residual by 0.9 m at BH15 and by 2.8 m at BH17d, indicating a better fit has been achieved to observed measurements in the vicinity of Weeli Wolli Creek and Weeli Wolli Spring.
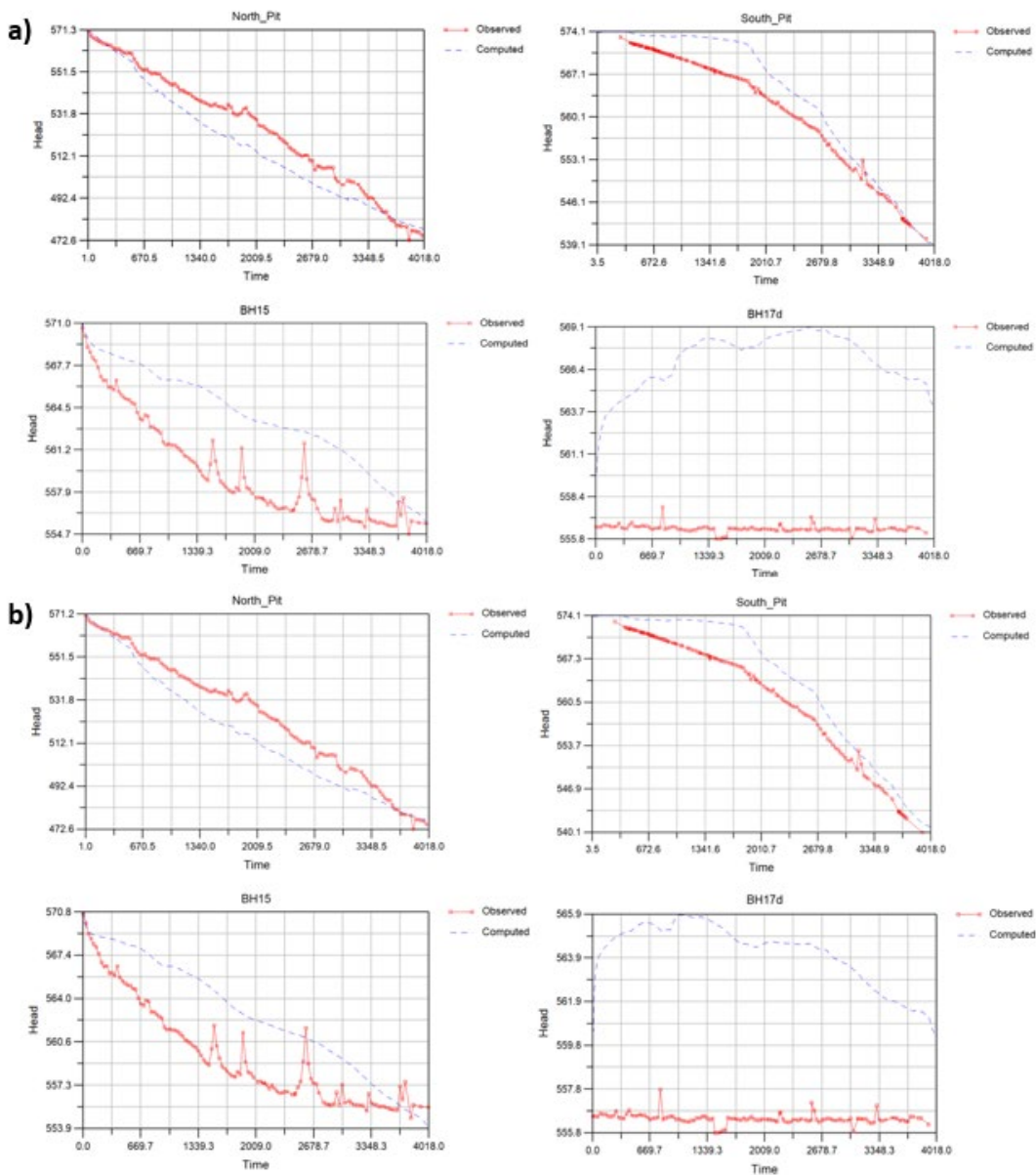
Figure 20 Calibration performance, a) pre-existing RTIO (2018) model and b) model with creek recharge

Water balance

Table 7 shows the individual water balance components for the calibrated model in comparison to the pre-existing model (RTIO, 2018). The mass balance error at completion of the model with creek recharge was 0.00%, confirming an accurate numerical solution was achieved. Overall, the disparity between respective models is not significant as indicated by total inputs and outputs. The total amount of water entering and exiting the system is 430 and 436 GL (less than a 2% differential) for the pre-existing RTIO and creek recharge models, respectively. Recharge via Weeli Wolli Creek accounts for 54% of all groundwater recharge entering the system in the calibrated model with a total volume of 72 GL, equivalent to 18 ML/d. Groundwater baseflow is slightly higher, averaging a rate of 7.7 ML/d in comparison to 6 ML/d simulated in the pre-existing model. This is mostly due to increased hydraulic conductivity in the zone underlying Weeli Wolli Creek coupled with drain conductance not being altered in the calibration. The baseflow rate is slightly higher than conceptualised (~5 ML/d) however still acceptable for the purposes of this model. Groundwater lost through evapotranspiration is slightly lower but still within acceptable bounds as per the conceptualisation (2 – 6 ML/d). Evapotranspiration averages approximately 2 ML/d in comparison to 3.5 ML/d in the pre-existing model. Model outputs and water balance components for both the pre-existing RTIO and creek recharge models are presented in Appendix C and Appendix D, respectively.

Simulated flows and heads

The temporal changes in simulated hydraulic heads for both models are presented from Figure 21 – Figure 28. The figures verify the calibration in that there are no major discrepancies between the cone of depression surrounding HD1N as well as the potentiometric surface along Weeli Wolli Creek and towards the spring in the north-east. However, the application of an additional 0.009 m/d of creek recharge does lead to significant groundwater mounding underneath Weeli Wolli Creek in the southern part of the domain. Groundwater mounding in excess of 20 m is observed in 2017 in comparison to the pre-existing RTIO calibrated model for the corresponding time period. This likely due to a low hydraulic conductivity in the surrounding area (2 m/d) and is far away enough from HD1S not to be impeded by drawdown.

The hydrogeology in the southern part of the study area is not as well understood in comparison to areas in the immediate vicinity of the pits and Weeli Wolli Creek/Spring (RTIO, 2018a). Low priority was placed during the initial calibration undertaken by RTIO (2018) along the fringes of the model domain. Similarly, the calibration undertaken in this study focused on adequately representing drawdown in key areas surrounding HD1N and Weeli Wolli Creek. For the purposes of this study a uniform recharge rate of 0.009 m/d was deemed sufficient. Further work would need to be undertaken to effectively represent the groundwater system along lesser-known parts of the study area.

Table 7 Water balance comparison between pre-existing RTIO calibrated and creek recharge model

| | RTIO (2018) – Pre-existing model | | | | Model with creek recharge (0.009 m/d) | | | |
| | In | | Out | | In | | Out | |
	GL	ML/d	GL	ML/d	GL	ML/d	GL	ML/d
Storage	334	83.3	10	2.6	302	75.2	16	4
Diffuse recharge	13	3.2			13	3.2		
Spur irrigation	83	20.6	83	12.4	49	12.4		
Creek recharge	-	-			72	17.8		
Well abstraction			382	95.1			382	95.1
Groundwater outflow			24	6.0			31	7.7
Evapo-transpiration			14	3.5			7	1.8
Total	**430**	**107**	**430**	**107**	**436**	**108.6**	**436**	**108.6**
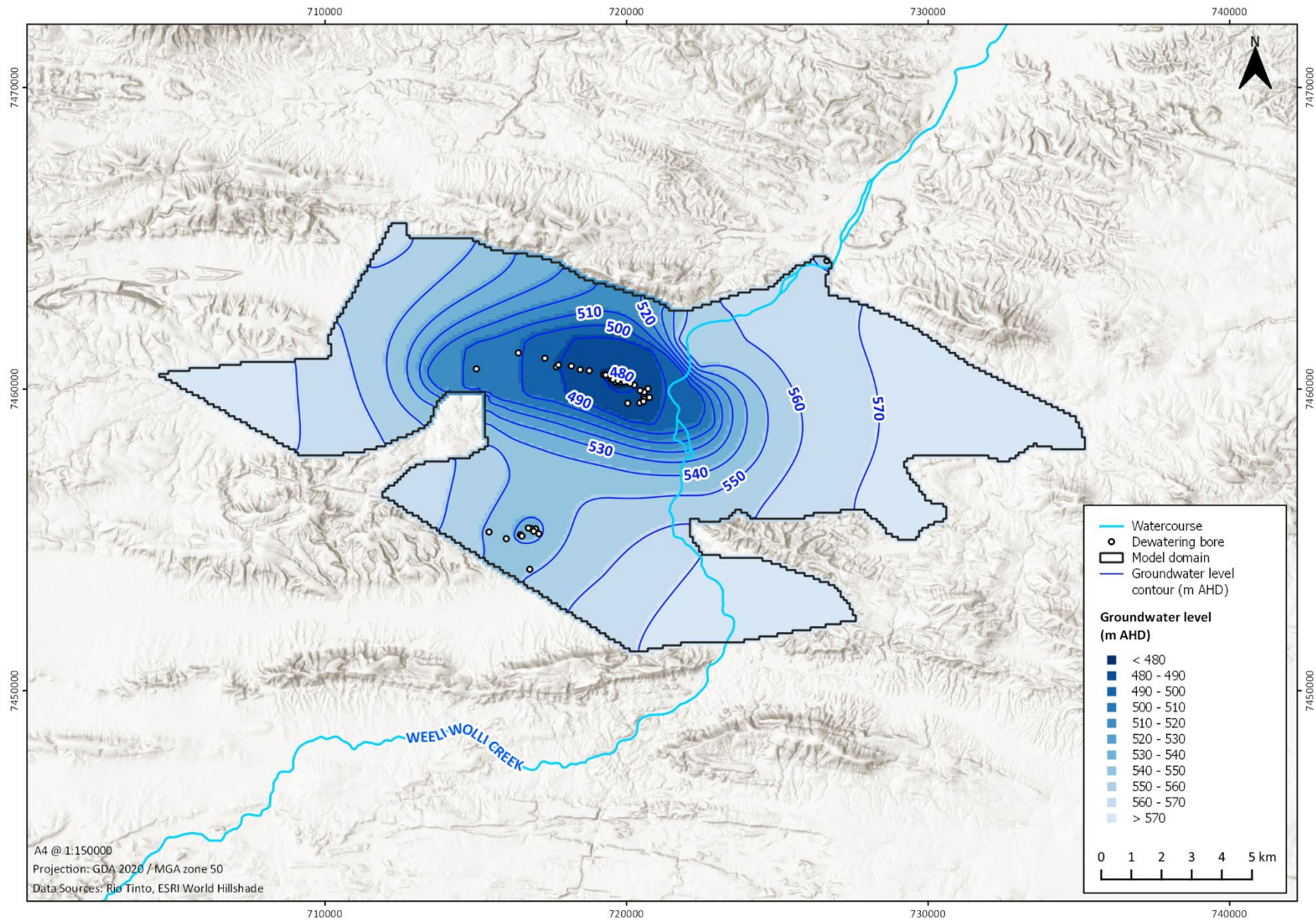
Figure 21 2017 Simulated hydraulic heads for RTIO model
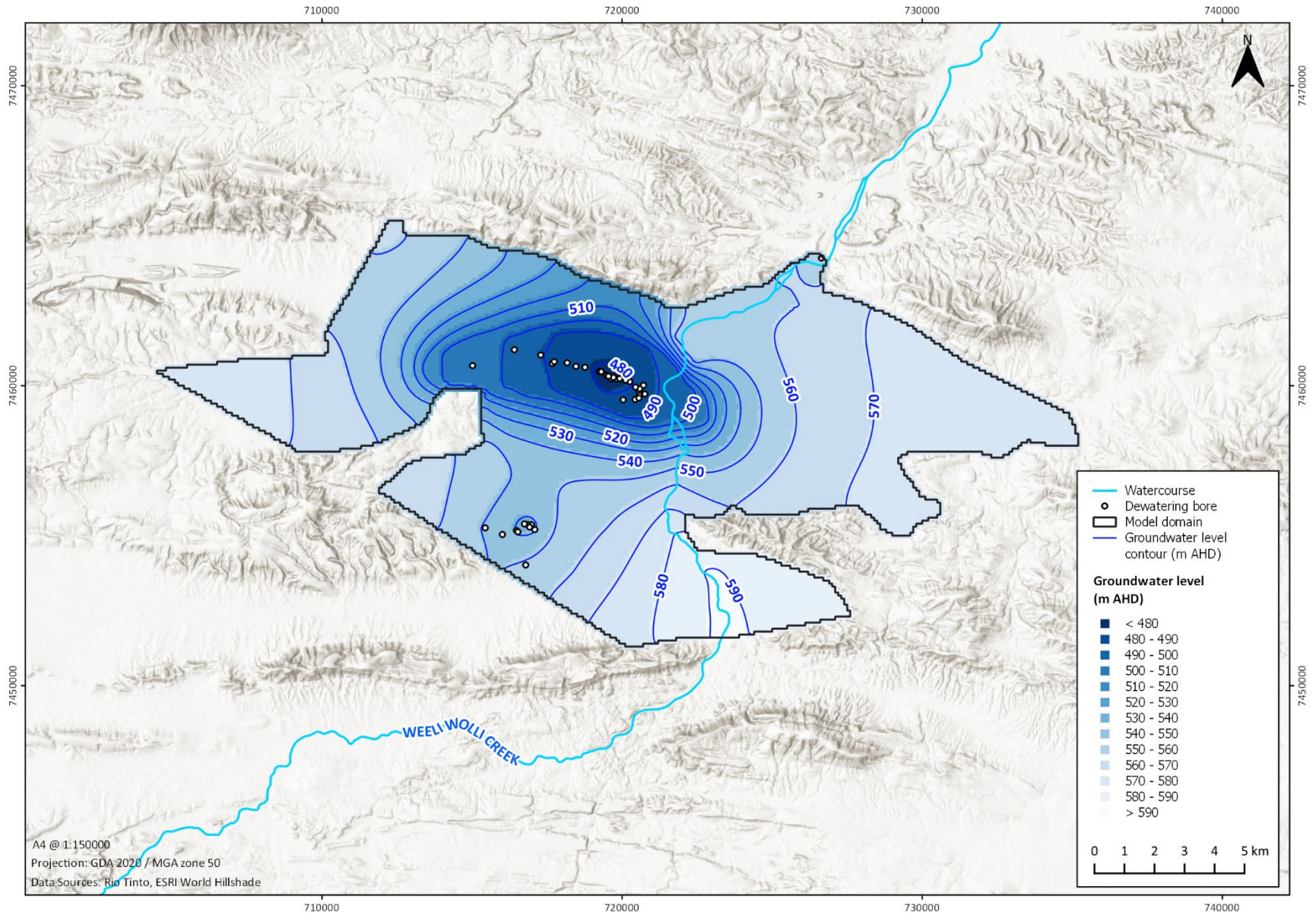
Figure 22 2017 simulated hydraulic heads for model with creek recharge (0.009 m/d)
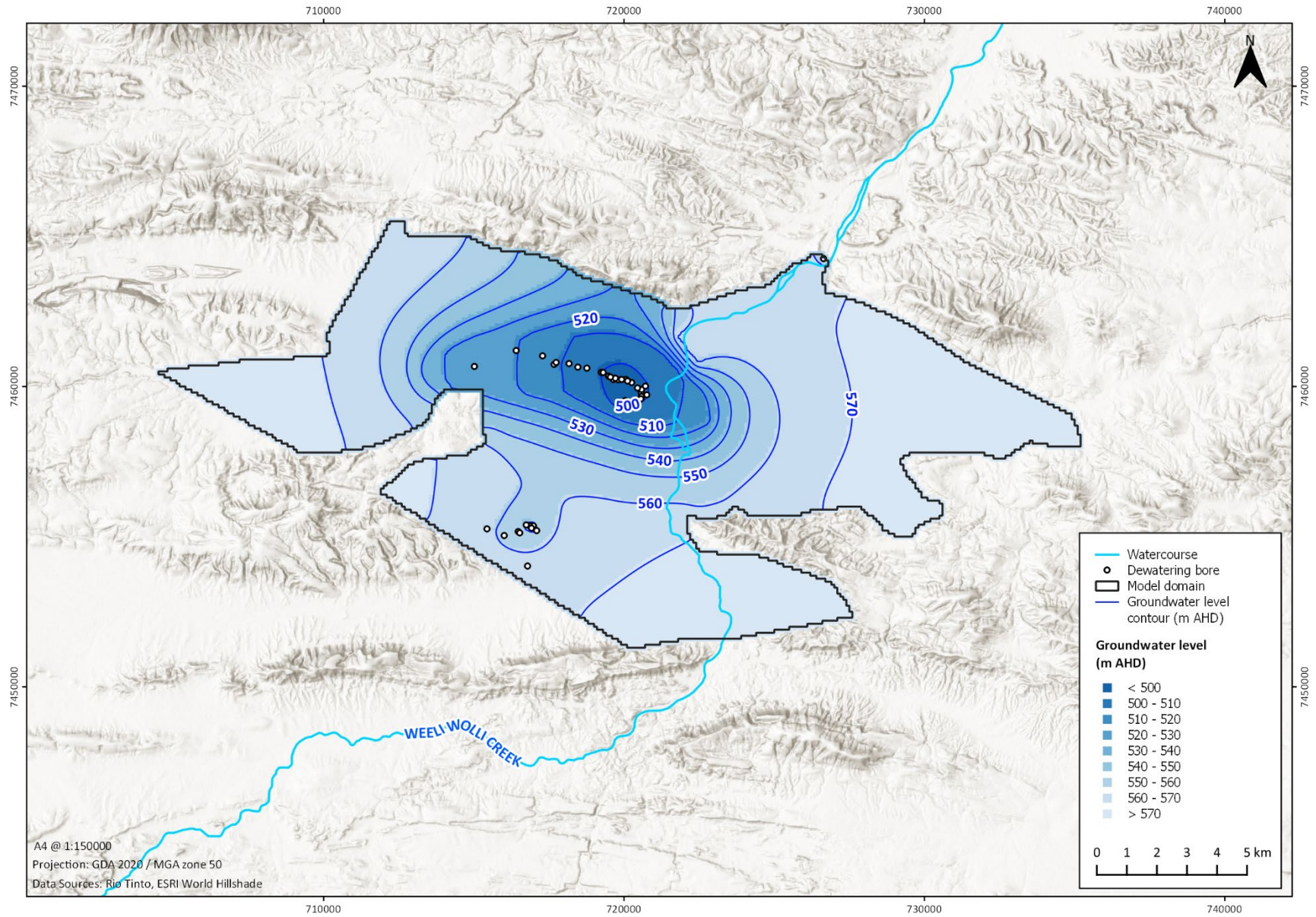
Figure 23 2014 simulated hydraulic heads for RTIO model
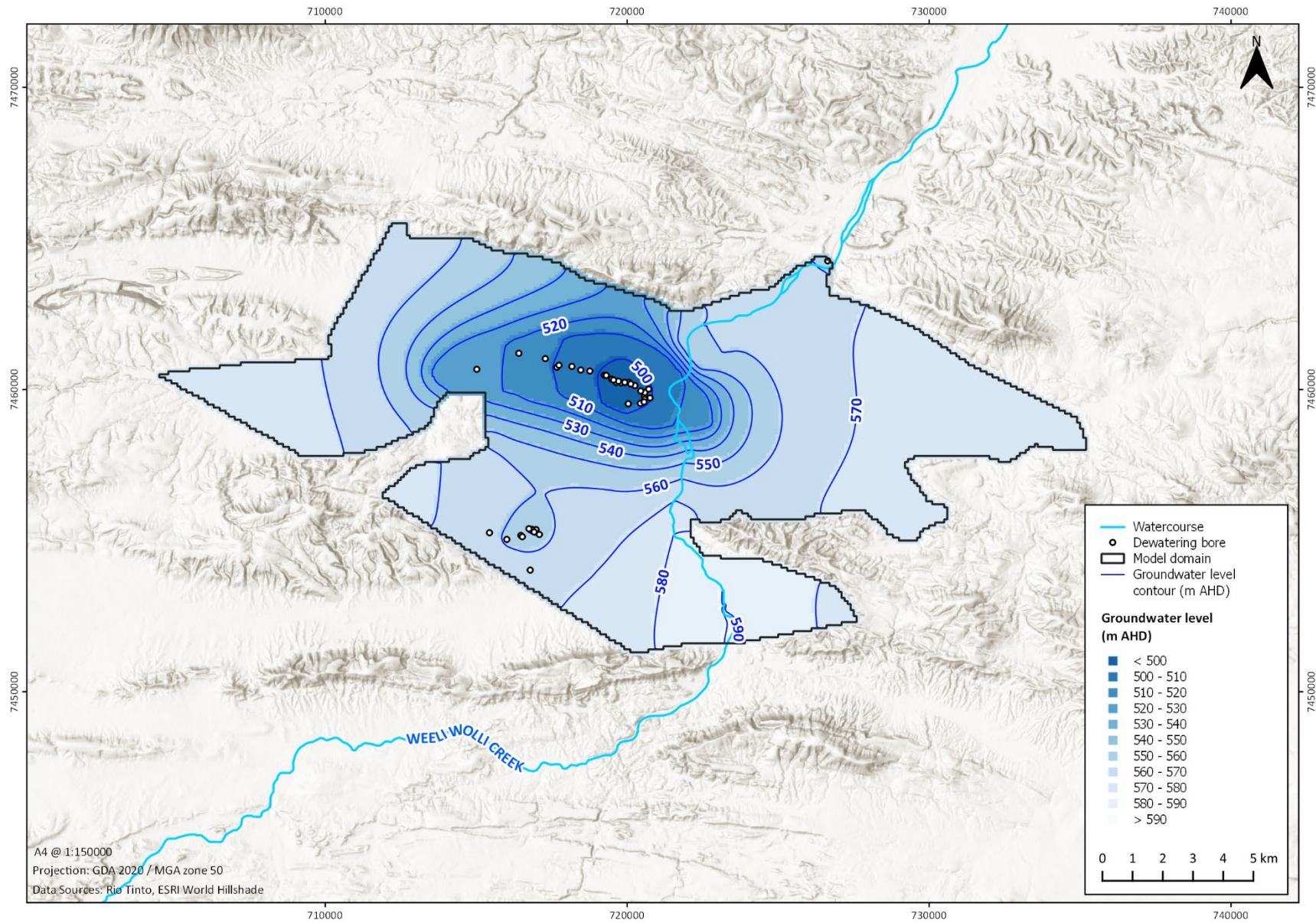
Figure 24 2014 simulated hydraulic heads for model with creek recharge (0.009 m/d)
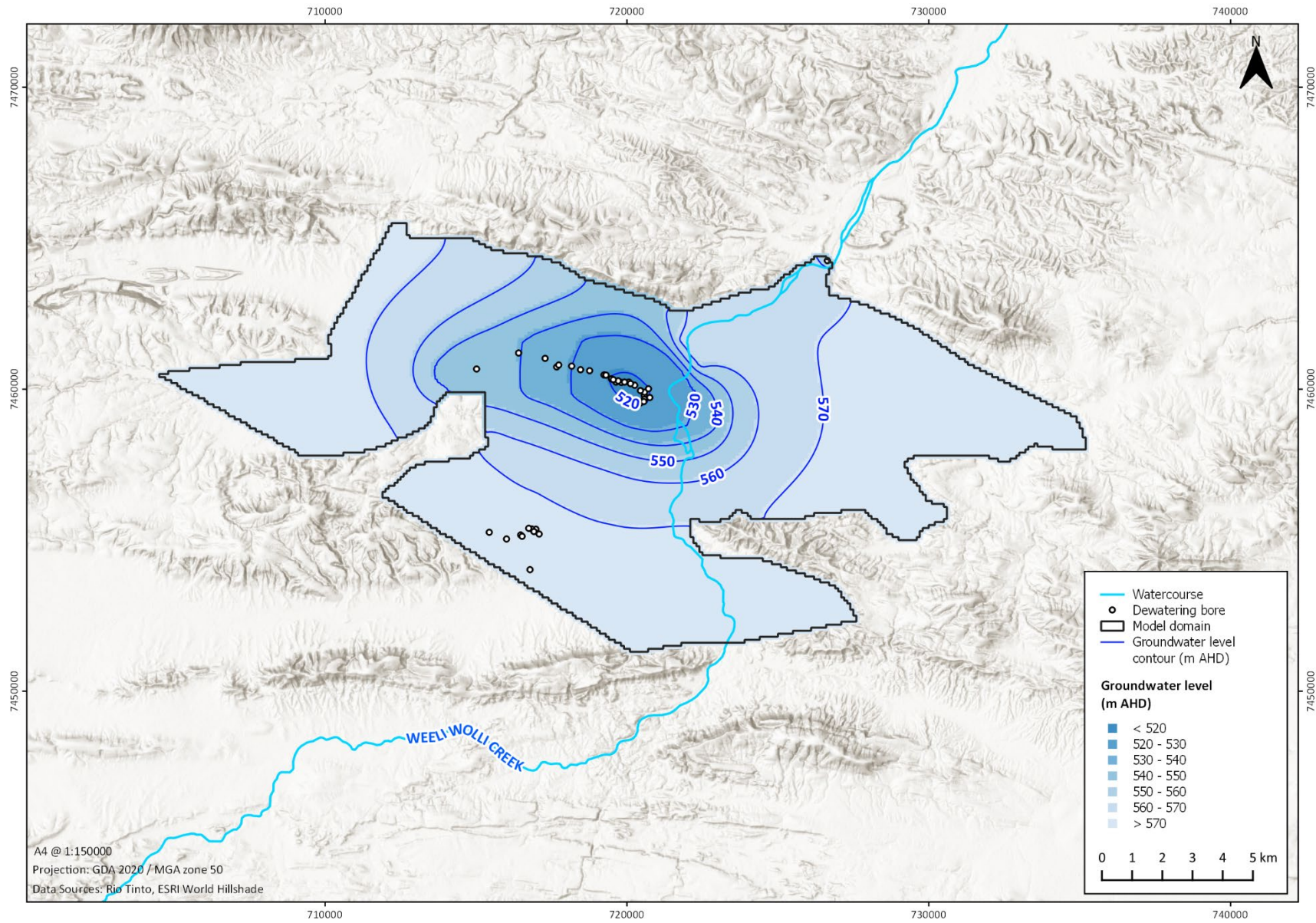
Figure 25 2011 simulated hydraulic heads for RTIO model
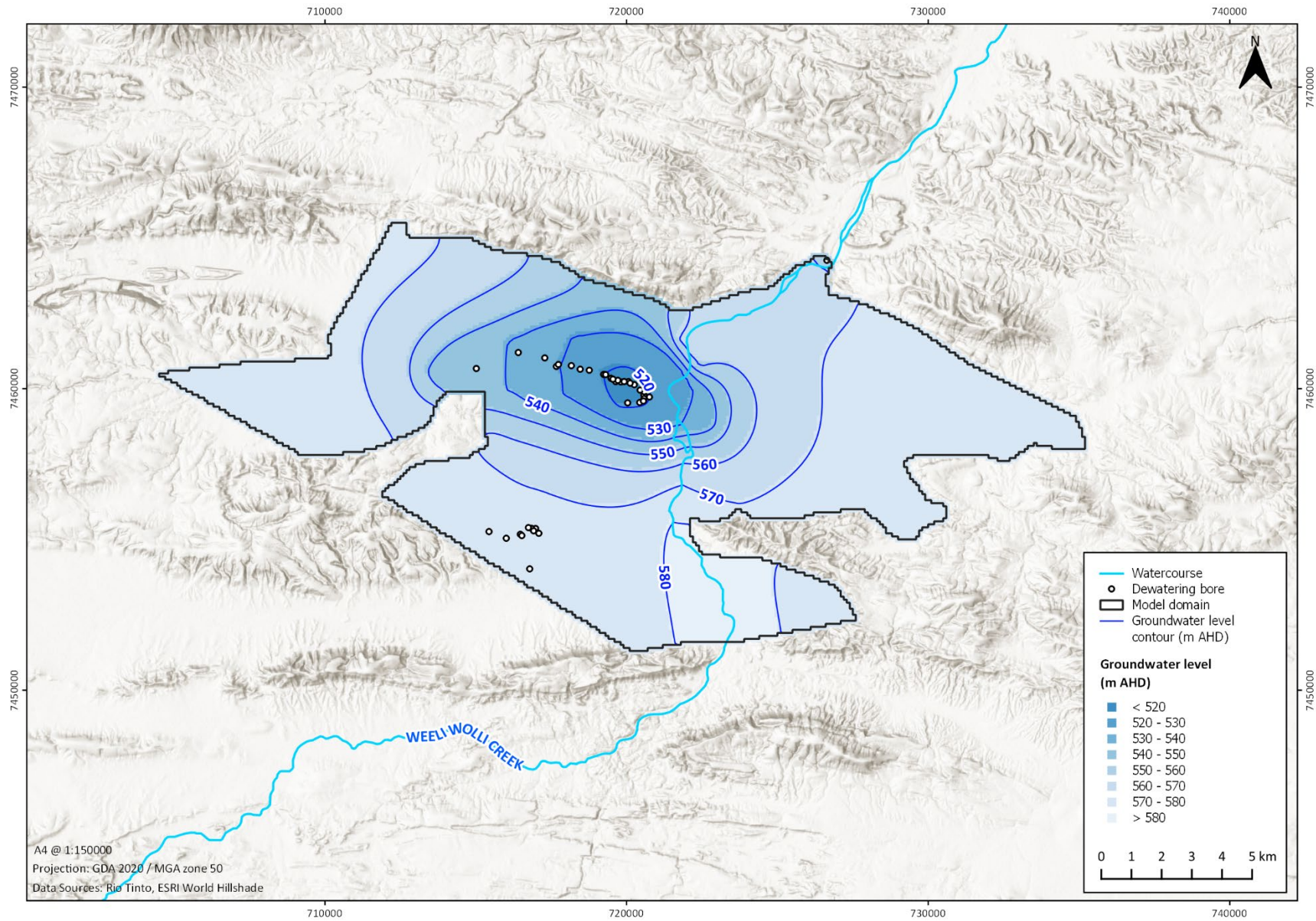
Figure 26 2011 simulated hydraulic heads for model with creek recharge (0.009 m/d)
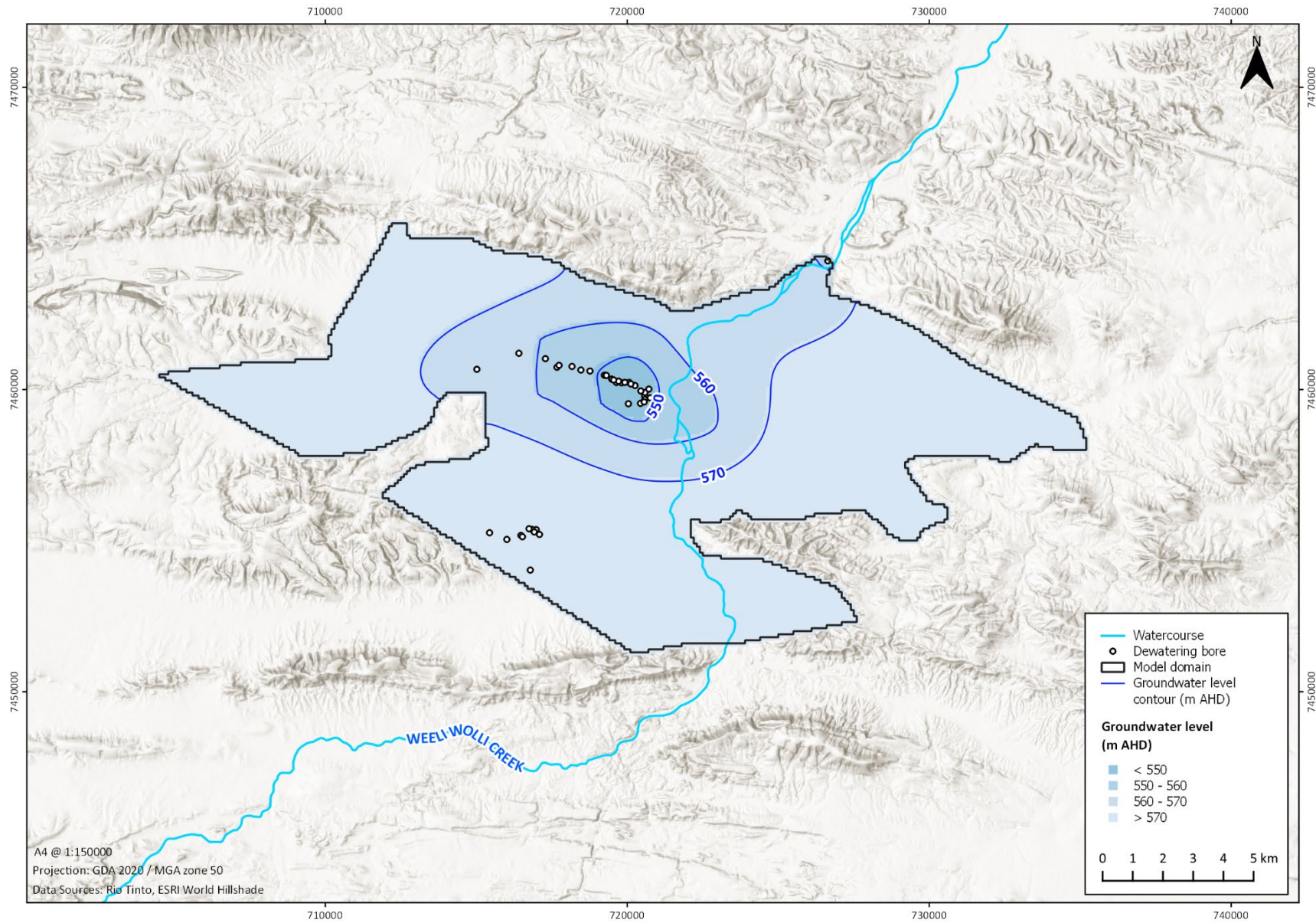
Figure 27 2008 simulated hydraulic heads for RTIO model
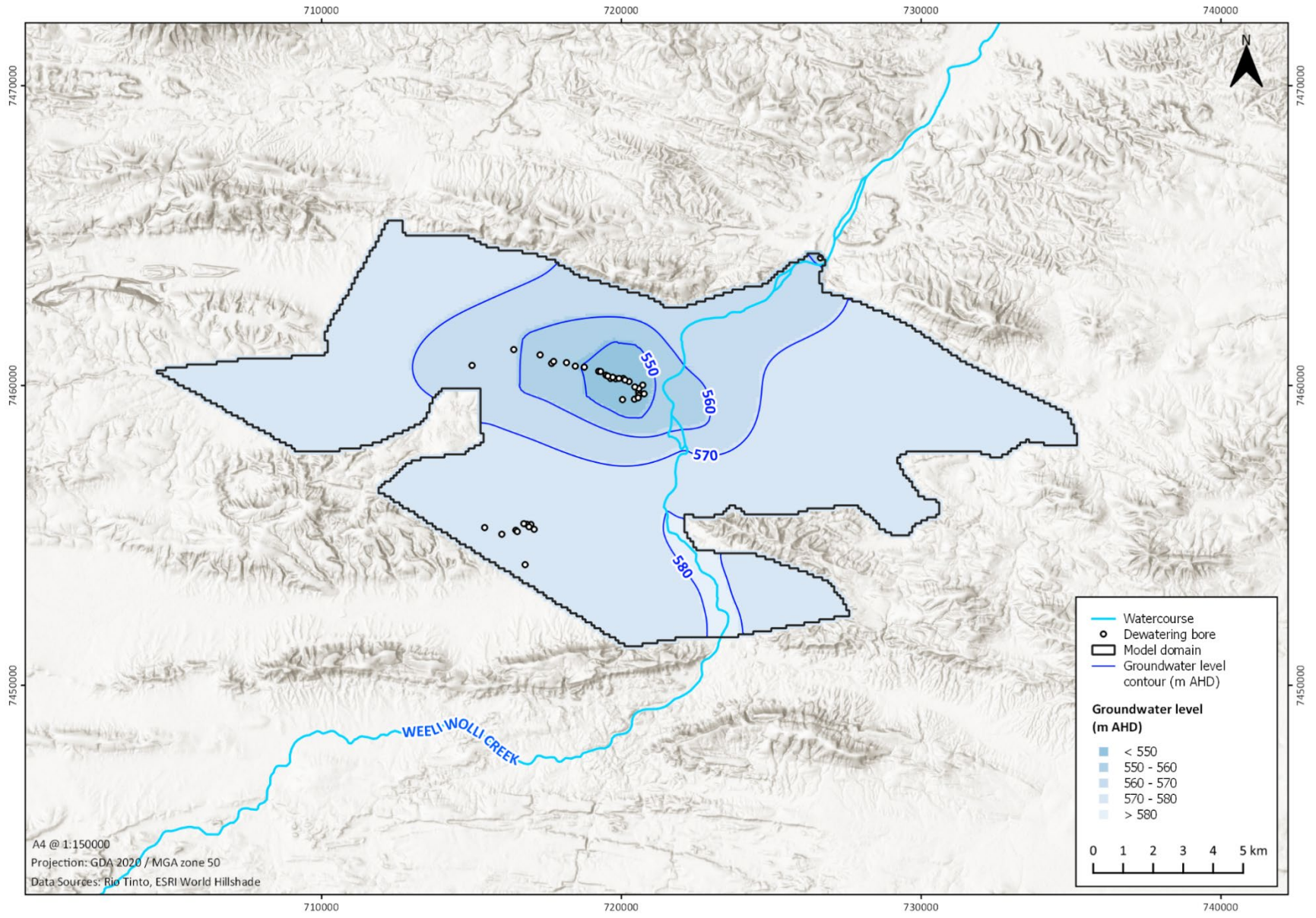
Figure 28 2008 simulated hydraulic heads for model with creek recharge (0.009 m/d)

Particle tracking

Overview

The results from the particle tracking analysis are presented in the following sections. In total, four scenarios were run across four time varying simulations (2017, 2014, 2011 and 2008) to compare the temporal changes between measured and simulated age derived CFC-12 concentrations. For the purposes of the results, the pre-existing RTIO calibrated model simulations are referred to as the "base case", while the creek recharge applied model simulations are referred to as "Scenario 1". A sensitivity analysis was also undertaken using different rates of recharge (0.006 m/d and 0.012 m/d applied to Weeli Wolli Creek) to address uncertainty in recharge parameterisation. The 0.006 m/d and 0.012 m/d simulations are "Scenario 2" and "Scenario 3", respectively. Spur irrigation recharge was deactivated in the mod-PATH3DU simulations on the premise that irrigation is not taking place prior to commencement of mining. Thus, diffuse and river recharge via Weeli Wolli Creek are the only recharge mechanisms in the particle tracking simulations. Results are presented in the form of advective transport statistics (i.e. minimum, maximum, and median particle termination ages for each simulation), a concentration comparison between observed and simulated derived values over time, the root mean square error (RMSE) between measured and simulated concentrations (in pg/kg), and visual outputs from the simulations showing particle pathlines and the age of recharged particles derived from travel times. Scatter plots with 1:1 slope lines of measured concentrations are also presented to assess fit to simulated concentrations.

The summary of particle simulations undertaken as part of this study are as follows:

- Pre-calibrated RTIO (2018) model with no creek recharge applied (**Base case**)
- Recharge estimated via WTF method with 0.009 m/d of creek recharge applied (**Scenario 1**)
- Sensitivity analysis with 0.006 m/d of creek recharge applied (**Scenario 2**)
- Sensitivity analysis with 0.012 m/d of creek recharge applied (**Scenario 3**)

Base case

The RMSE (97 pg/kg) indicates a relatively poor match between measured and simulated CFC-12 concentrations. Figure 29 shows a scatter plot and 1:1 line of measured and simulated concentrations over the simulated periods. The 2011 simulation is not presented due to the absence of measured data. It indicates that simulated concentrations plot well below the measured concentration slope line. Advective statistics are presented in Table 8 and show median particle travel times to range from 224.6 years at DW07HD1N005 to 375.3 years at DW07HD1N0002 in 2017. Minimum, maximum and median particle ages mostly increase with earlier time periods with median particle travel times ranging from 799 to 1450 years in 2008. Simulated concentrations in 2017 range from 2.5 pg/kg at DW07HD1N0002 to 12.1 pg/kg at DW06HD1N0008 and decrease linearly with earlier time periods as median ages increases (Table 9).

For the 2014 simulation, minimum particle ages range from approximately 12 to 18 years with the only exception being DW07HD1N0002 which simulates a minimum particle age of 148 years. This is expected given the top of the water table at the beginning of the simulation (500 m AHD) is over 20 m higher in comparison to the top of the well screen (477 m AHD, see Table 4), thus younger recharged water is not being captured by the bore. The same trend is seen in DW07HD1N0004 and DW07HD1N0005, albeit at an earlier period given the top of the well screens are positioned higher (524 and 511 m AHD for DW07HD1N0004 and DW07HD1N0005, respectively).

The simulations fail to produce the spike in CFC-12 concentrations observed in 2016/2017 in the sampled data. Median particle ages increase and corresponding equivalent concentrations mostly decrease linearly from 2017 to 2008 (Figure 30). This is because particle velocity is drastically reduced as drawdown decreases with earlier time periods. This consequently leads to longer travel times on account of a reduction in the hydraulic gradient. Overall, approximately 10% of particles are recharged in the appropriate timeframe for atmospheric CFC-12 (< 85 years) and as a consequence produce low simulated concentrations. The results indicate that solely applying a diffuse recharge equivalent to 5.8 mm/year across the model domain does not produce a rise in CFC-12 concentrations brought on from localised recharged processes.

Visual outputs from the 2017, 2014, 2011 and 2008 base case simulations are presented in Figure 31, Figure 32, Figure 33, Figure 34, respectively. Most particles terminate close to the edges of the model domain and take extensively long times to reach their area of recharge (> 100 years). Pathlines from the eastern-most and closest bores to Weeli Wolli Creek (DW07HD1N0002, DW06HD1N0003 and DW06HD1N0005) generally run parallel along the zone of high hydraulic conductivity underneath the creek and recharge either east of Weeli Wolli Creek towards the alluvial plain or to the north-east towards Weeli Wolli Spring. 60% of particles released from DW07HD1N0004 and DW07HD1N0005 recharge to the north-east while the remaining 40% recharge towards the south, which is predictable given the bores are located where groundwater drawdown is at its greatest. It also justifies using a circular distribution of particles instead of single point placement. Particles emitted from DW06HD1N0008 terminate towards the west across all time periods due to the orientation of the water table surface in the area.
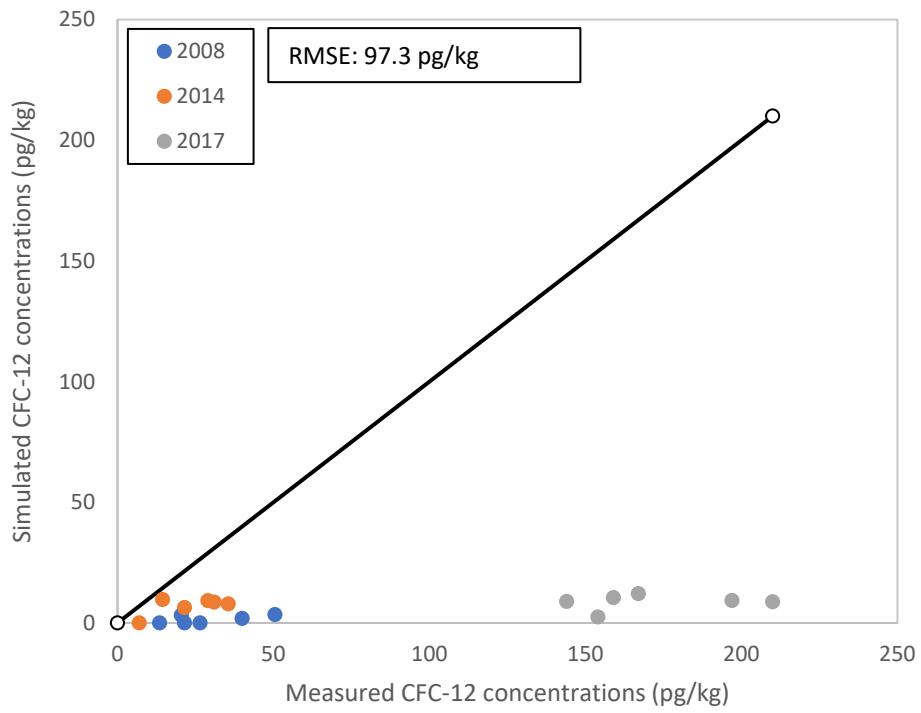
Figure 29 Scatter plot of measured vs and CFC-12 simulated concentrations over different sampling periods (base case)

Table 8 Advective statistics for base case simulations (in years)

Well	2008 (years)			2011 (years)			2014 (years)			2017 (years)		
	Min	Max	Median	Min	Max	Median	Min	Max	Median	Min	Max	Median
DW07HD1N0002	852.9	6390.6	**1449.5**	392.6	4344.9	**519.7**	147.9	2745.6	**399.2**	41.2	2055.5	**375.3**
DW07HD1N0004	278.6	5567.4	**1406.9**	16.8	3886.3	**589.6**	12.1	2693.6	**617.7**	8.4	1905.6	**344.6**
DW07HD1N0005	480.1	12065.9	**1882.0**	63.2	7270.4	**856.4**	11.8	3150.2	**455.4**	8.9	2349.2	**224.6**
DW06HD1N0003	24.7	2531.9	**799.4**	17.9	1562.4	**423.2**	12.1	1486.4	**330.0**	12.6	876.3	**259.2**
DW06HD1N0005	22.4	4269.8	**979.0**	16.2	3431.5	**670.9**	11.8	3150.2	**440.6**	16.3	1276.0	**334.3**
DW06HD1N0008	30.4	2850.9	**846.2**	25.5	3813.6	**923.6**	18.6	1823.1	**488.9**	12.5	1398.3	**358.5**

Table 9 Measured vs simulated concentration comparison for base case simulations (in pg/kg)

Well	2008 (pg/kg)		2011 (pg/kg)		2014 (pg/kg)		2017 (pg/kg)	
	Obs.	Sim.	Obs.	Sim.	Obs.	Sim.	Obs.	Sim.
DW07HD1N0002	26.5	0.0	-	0.0	7.0	0.0	154.0	2.5
DW07HD1N0004	13.5	0.0	-	8.7	14.5	9.6	197.0	9.3
DW07HD1N0005	21.5	0.0	-	0.0	29.0	9.2	144.0	8.9
DW06HD1N0003	50.5	3.4	-	5.7	35.5	7.9	159.0	10.5
DW06HD1N0005	40,0	1.9	-	4.3	21.5	6.3	210.0	8.8
DW06HD1N0008	20.5	3.2	-	3.4	31.0	8.6	167.0	12.1
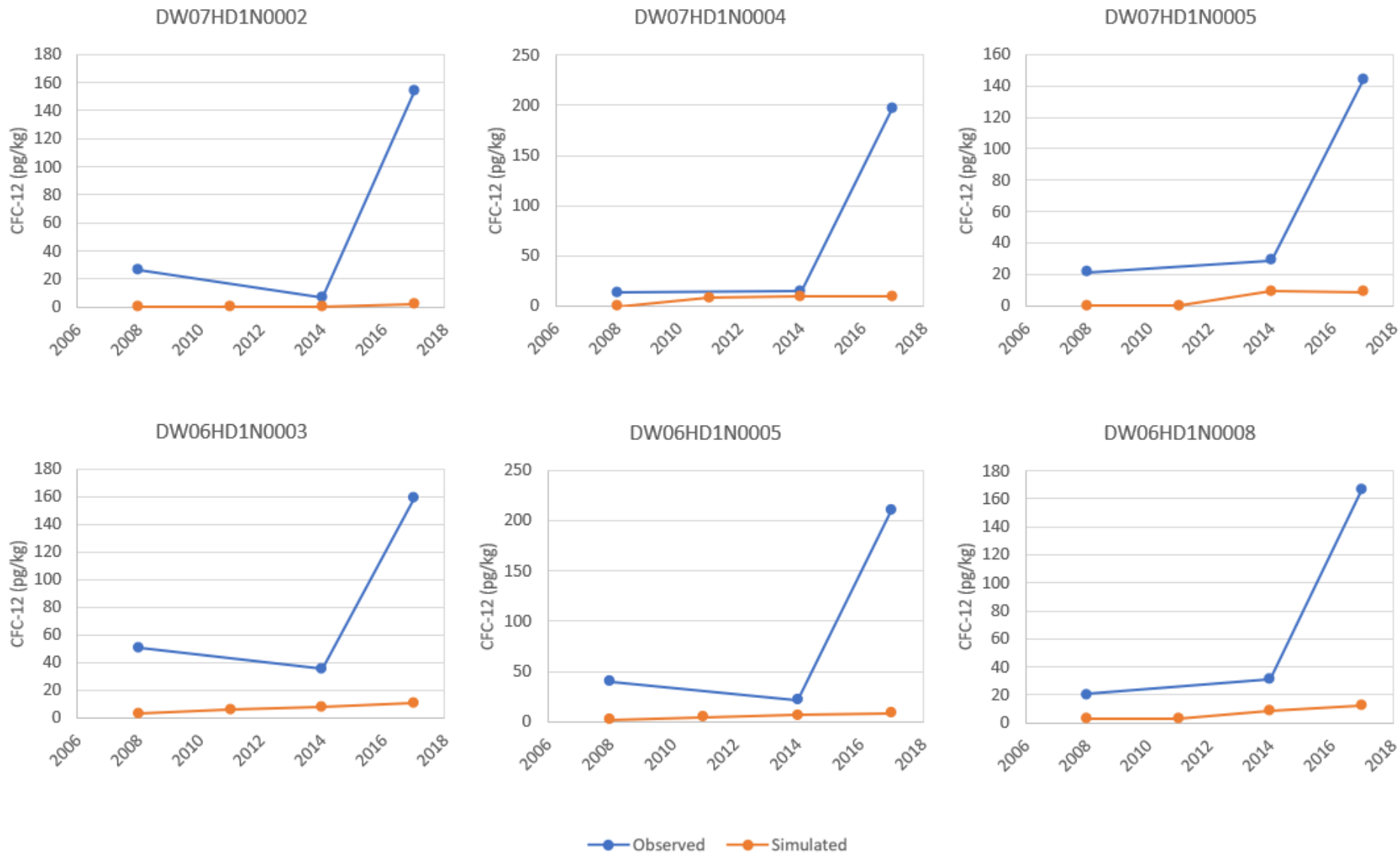
Figure 30 Observed vs simulated CFC-12 concentrations (base case)
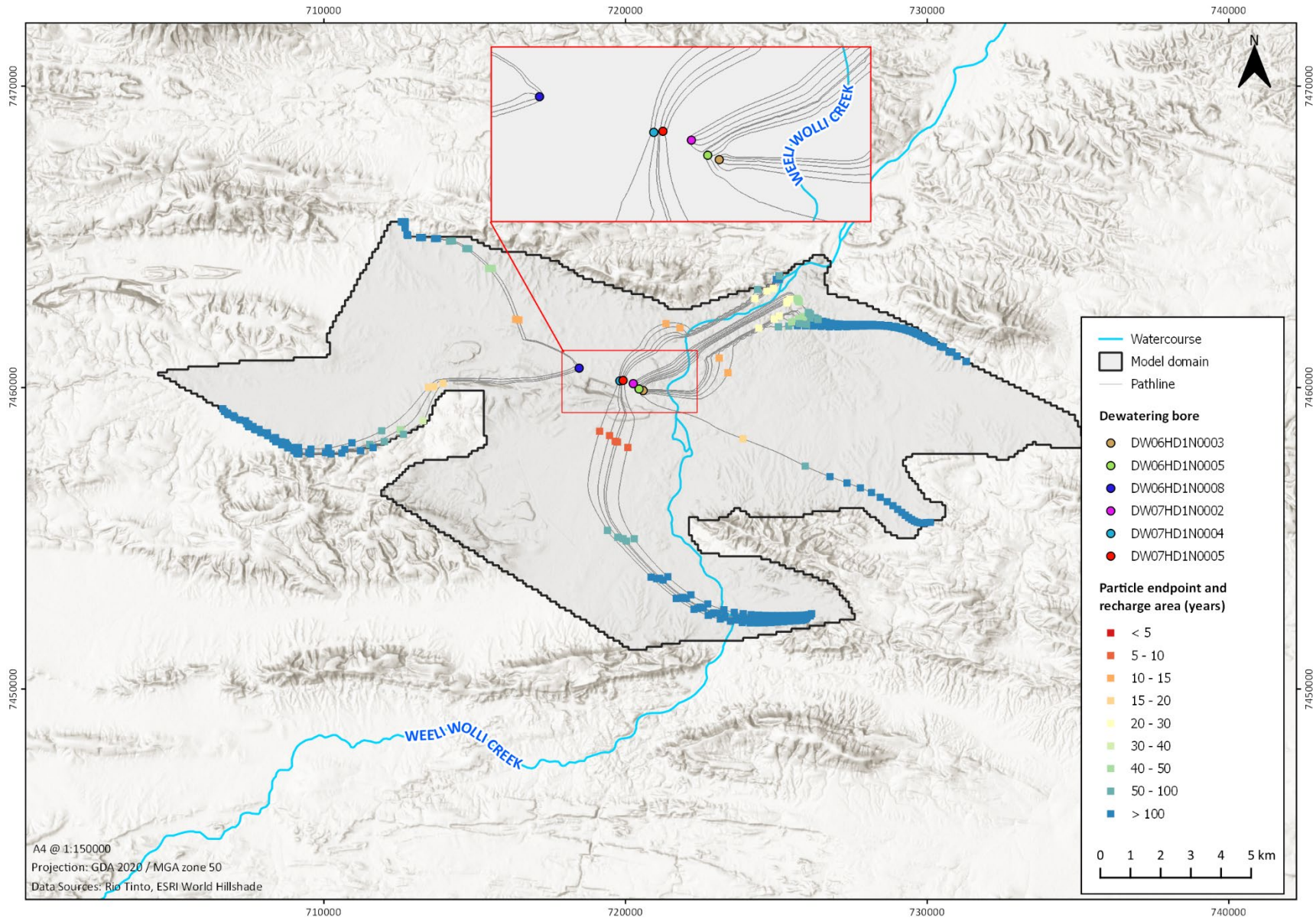
Figure 31 Particle tracking results (2017 base case)
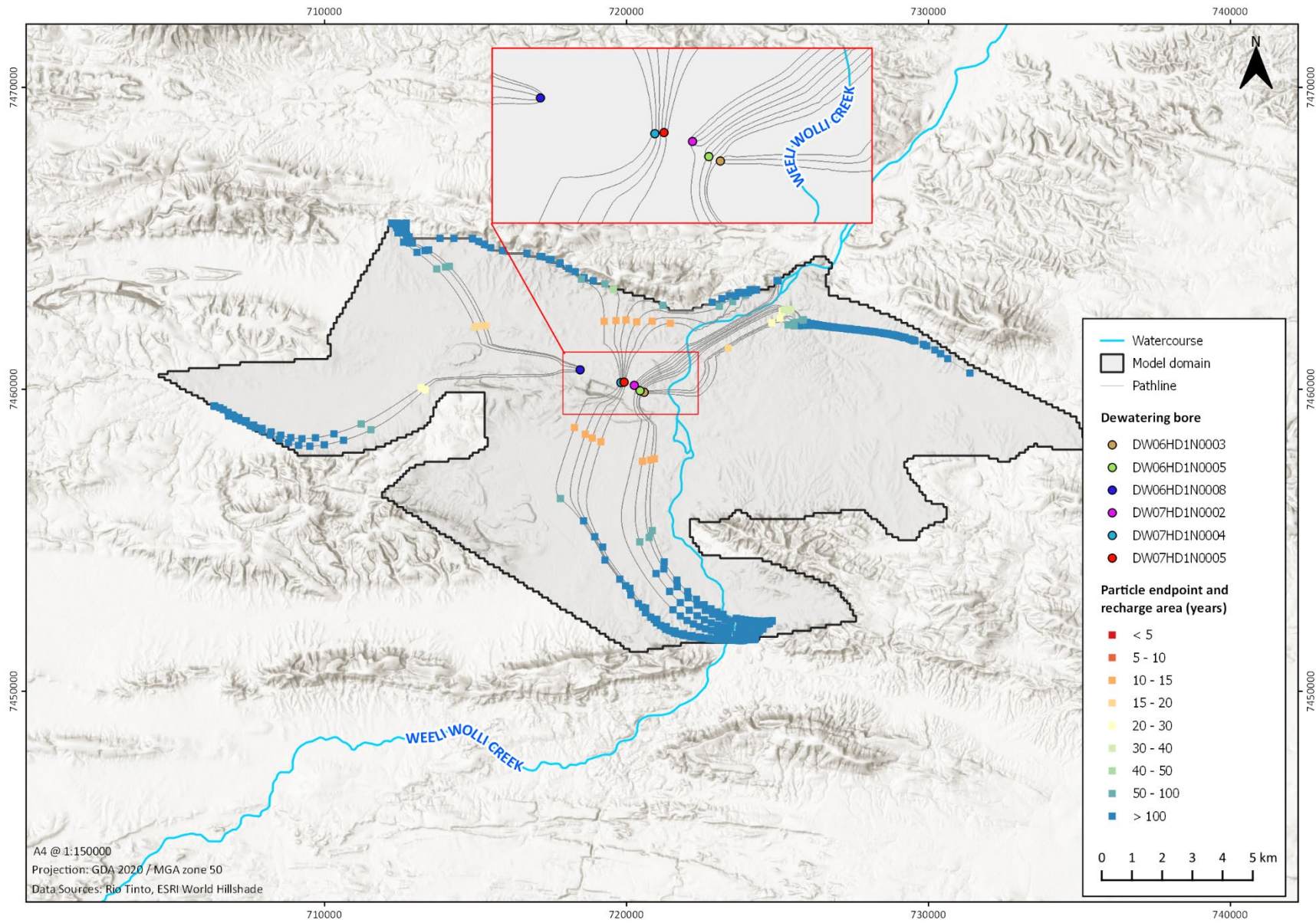
Figure 32 Particle tracking results (2014 base case)
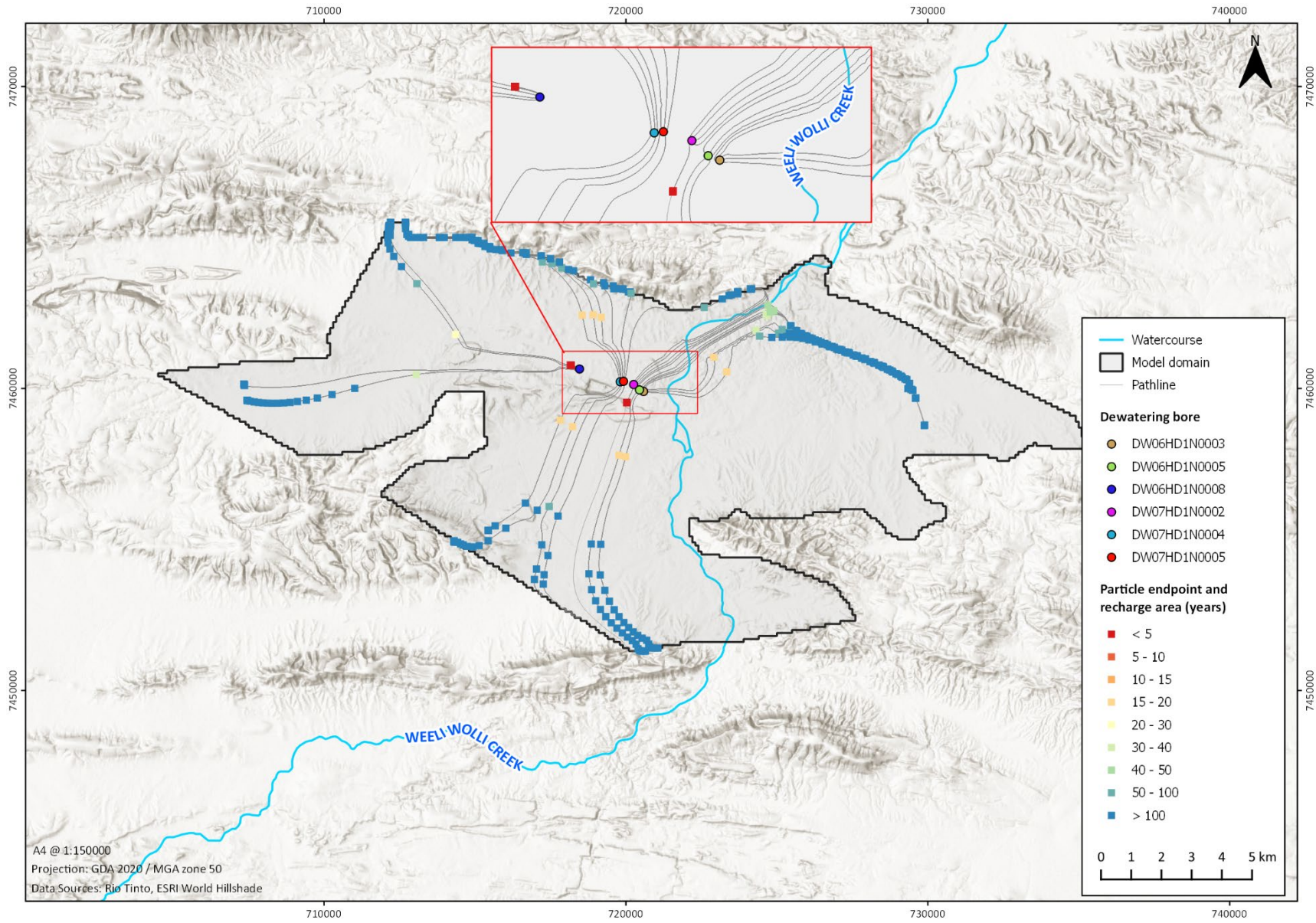
Figure 33 Particle tracking results (2011 base case)
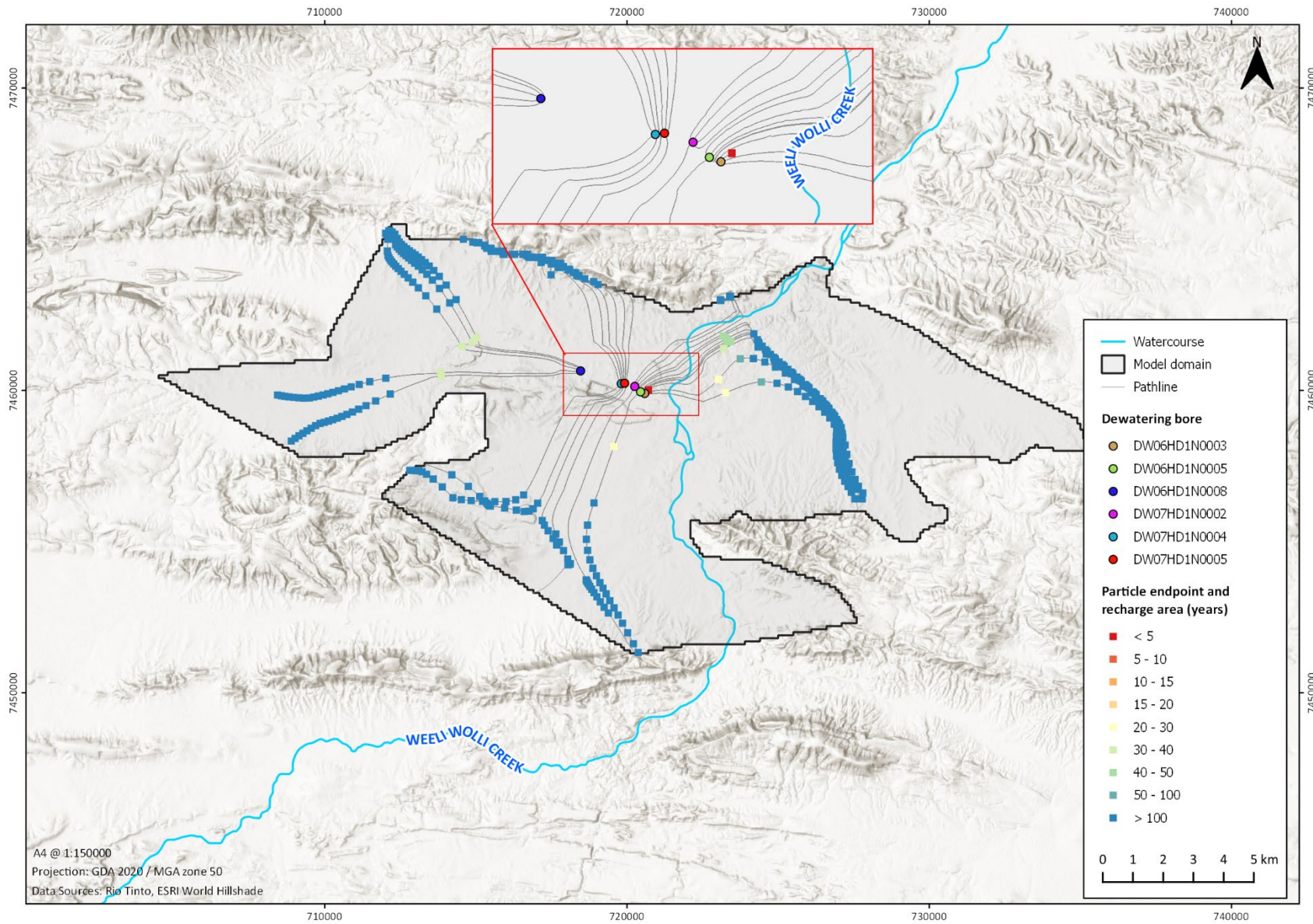
Figure 34 Particle tracking results (2008 base case)

Scenario 1

The RMSE between measured and simulated CFC-12 concentrations for the six dewatering bores (74 pg/kg) indicates the overall fit to be an improvement in comparison to the base case simulation (97 pg/kg). There is also an element of spatial variability to the results, as some areas produce a good overall match while others produce a poorer fit on account of variations in the orientation of drawdown between simulated periods. The scatter plot and 1:1 line shows a greater variability between measured and simulated concentrations (Figure 35) in comparison to the base case model. Two of the six bores immediately north of HD1N (i.e. DW07HD1N0004 and DW07HD1N0005) show a good agreement between measured and simulated CFC-12 concentrations, with a combined RMSE of 42 pg/kg. In comparison, the RMSE for the corresponding bores in the base case simulation is 114 pg/kg.

Median particle ages for all time periods are significantly less in comparison to the base case model (Table 10) due to more particles terminating along the creek. Median ages range from 21.3 years at DW07HD1N0005 to approximately 469 years at DW06HD1N0003 for the 2017 simulation. Median particle termination ages progressively get higher towards 2008 as observed in the base case simulations. Results from DW07HD1N0002 indicate that all particles are coming from the creek, whether east of HD1N or further north towards Weeli Wolli Spring. Median particle ages for the bore range from 19.1 years in the 2017 simulation to 65.4 years in the 2008 simulation. The equivalent age derived concentrations are 178.3 and 2.2 pg/kg for the two time periods, respectively (Table 11, Figure 36).

The northern-most bores (DW07HD1N0004 and DW07HD1N0005) show good agreement between measured and simulated concentrations (Table 11, Figure 36). Minimum particle ages for DW07HD1N0004 and DW07HD1N0005 are 9 and 11.6 years, respectively, which correspond to recharge dates along Weeli Wolli Creek. Simulated concentrations (102.7 pg/kg) of CFC-12 at DW07HD1N0004 are slightly lower than measured concentrations (197 pg/kg) when the 2017 simulation is considered which might suggest the creek recharge rate of 0.009 m/d is slightly underestimated, however similar declining trends are observed temporally. The simulated concentration in 2014 in DW07HD1N0004 is 9.2 pg/kg, while the measured concentration is 14.5 pg/kg. DW07HD1N0005 produces a similar trend whereby simulated concentrations decrease from 112.4 to 42.2 pg/kg between 2017 and 2014, in comparison to the corresponding time period for measured concentrations, which decrease from 144 to 29 pg/kg. From the similarity in observed and measured concentrations for the two bores over time, it can be inferred that it takes approximately 9 to 12 years for creek recharged groundwater to reach the northern border of HD1N.

The application of recharge to Weeli Wolli Creek does not affect simulated concentrations at DW06HD1N0008, where values range from 12.8 pg/kg in 2017 to 0.2 pg/kg in 2008. This does not differ greatly from outputs from the base case model, which show simulated equivalents of 12.1 and 3.2 pg/kg in 2017 and 2008, respectively. It is expected both models would produce similar results given the location of

the bore in relation to the orientation and extent of groundwater drawdown in that area of the model domain. The slightly higher CFC-12 concentrations observed in 2008 in the base case model are likely due to model sensitivities and slight differences in hydraulic gradient between the respective models.

The eastern most bores (DW06HD1N0005 and DW06HD1N0003) show a poor match between simulated and observed concentrations. In the case of DW06HD1N0005, simulated concentrations increase from 78.9 pg/kg in 2017 to 109.9 pg/kg in 2014. Similarly, DW06HD1N0003 shows a related pattern with simulated concentrations increasing from 22.2 to 53.3 pg/kg between 2017 and 2014. Both bores are located immediately east of HD1N nearby to Weeli Wolli Creek and are approximately 150 m apart. This is largely due to the changes in the water table surface and orientation of drawdown between respective time periods. In 2014, more particles are diverted towards Weeli Wolli Creek in the southern part of the domain (as opposed to the floodplain east of the creek as observed in 2017) resulting in shorter travel times and consequently higher simulated concentrations. The approximate travel time from DW06HD1N0003 to Weeli Wolli Creek ranges between 2.1 and 3.9 years (as indicated by the minimum particle ages). Realistically, an increase in CFC-12 concentrations in the bore would not be seen until sometime between 2010 and 2012.

Visual outputs from the 2017, 2014, and 2011 and 2008 Scenario 1 simulations are presented in Figure 37, Figure 38, Figure 39, Figure 40, respectively. Overall, particle pathline directions are similar to the base case simulations with the obvious difference being the influence of Weeli Wolli Creek on particle termination points and the deviation of particles in DW06HD1N0003 and DW06HD1N0005 towards the creek in the south. Typically, most of the other particles recharging along Weeli Wolli Creek in the south are not affected in the calculated concentrations given extensively long travel times (> 100 years) to reach recharge areas.
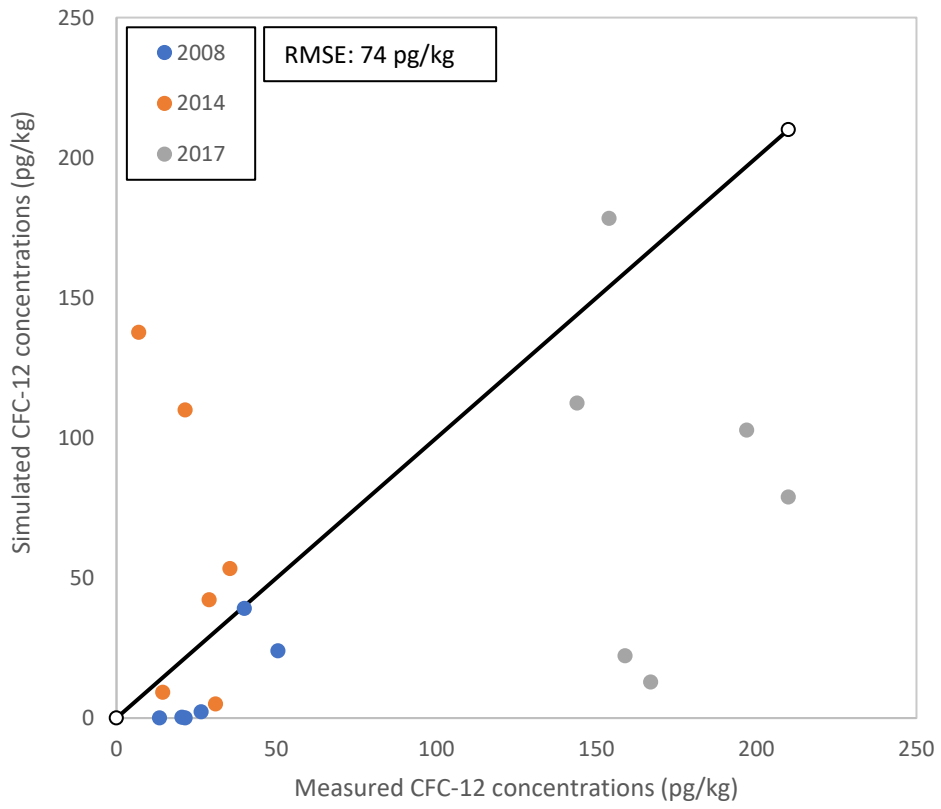
Figure 35 Scatter plot measured vs simulated CFC-12 concentrations over different sampling periods (Scenario 1)

Table 10 Advective statistics for scenario 1 (in years)

Well	2008 (years)			2011 (years)			2014 (years)			2017 (years)		
	Min	Max	Median	Min	Max	Median	Min	Max	Median	Min	Max	Median
DW07HD1N0002	47.5	5534.3	**65.4**	23.3	323.6	**33.0**	17.6	95.3	**21.4**	5.8	27	**19.1**
DW07HD1N0004	462.4	9358.3	**2194.1**	27.1	6431.2	**1448.6**	19.2	1454.1	**337.1**	11.6	331.0	**31.7**
DW07HD1N0005	713.4	11150.3	**1259.5**	59.2	1621.5	**691.9**	18.6	2432.7	**187.0**	9.0	117.0	**21.3**
DW06HD1N0003	3.9	4169.5	**1141.6**	2.6	2799.8	**165.3**	2.1	1857.2	**109.4**	2.1	1794.9	**468.9**
DW06HD1N0005	10.7	6492.8	**167.8**	8.8	191.6	**34.1**	5.4	65.0	**27.4**	2.8	3251.9	**102.7**
DW06HD1N0008	49.5	4655.4	**1360.0**	-	-	**-**	17.6	3104.0	**784.3**	18.9	2411.8	**504.1**

Table 11 Measured vs simulated concentration comparison for Scenario 1 (in pg/kg)

Well	2008 (pg/kg)		2011 (pg/kg)		2014 (pg/kg)		2017 (pg/kg)	
	Obs.	Sim.	Obs.	Sim.	Obs.	Sim.	Obs.	Sim.
DW07HD1N0002	26.5	2.2	-	72.2	7.0	137.7	154.0	178.3
DW07HD1N0004	13.5	0.0	-	5.8	14.5	9.2	197.0	102.7
DW07HD1N0005	21.5	0.0	-	0.3	29.0	42.2	144.0	112.4
DW06HD1N0003	50.5	24.0	-	32.8	35.5	53.3	159.0	22.2
DW06HD1N0005	40.0	39.1	-	70.2	21.5	109.9	210.0	78.9
DW06HD1N0008	20.5	0.2	-	-	31.0	5.0	167.0	12.8
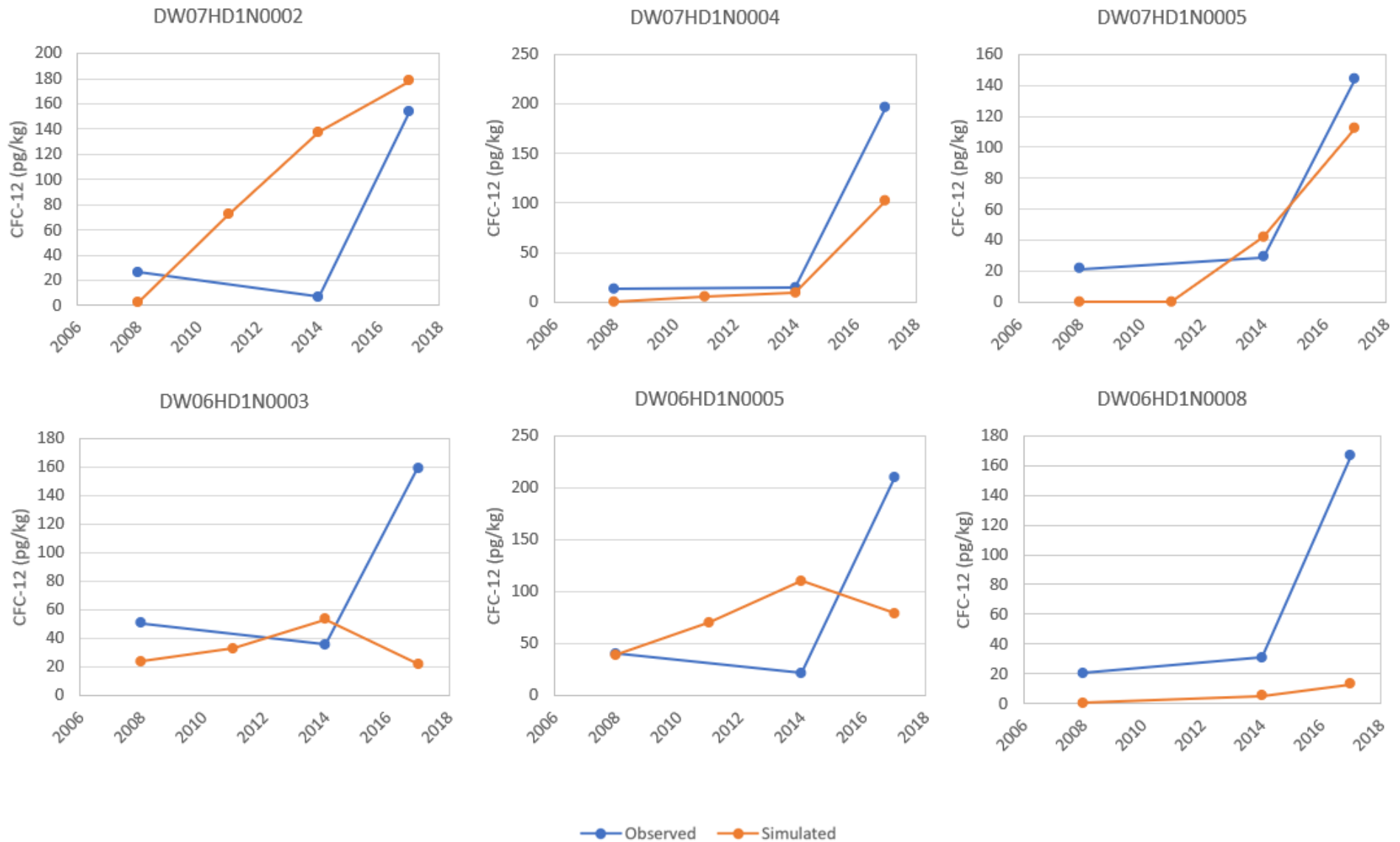
Figure 36 Observed vs simulated CFC-12 concentrations (Scenario 1)
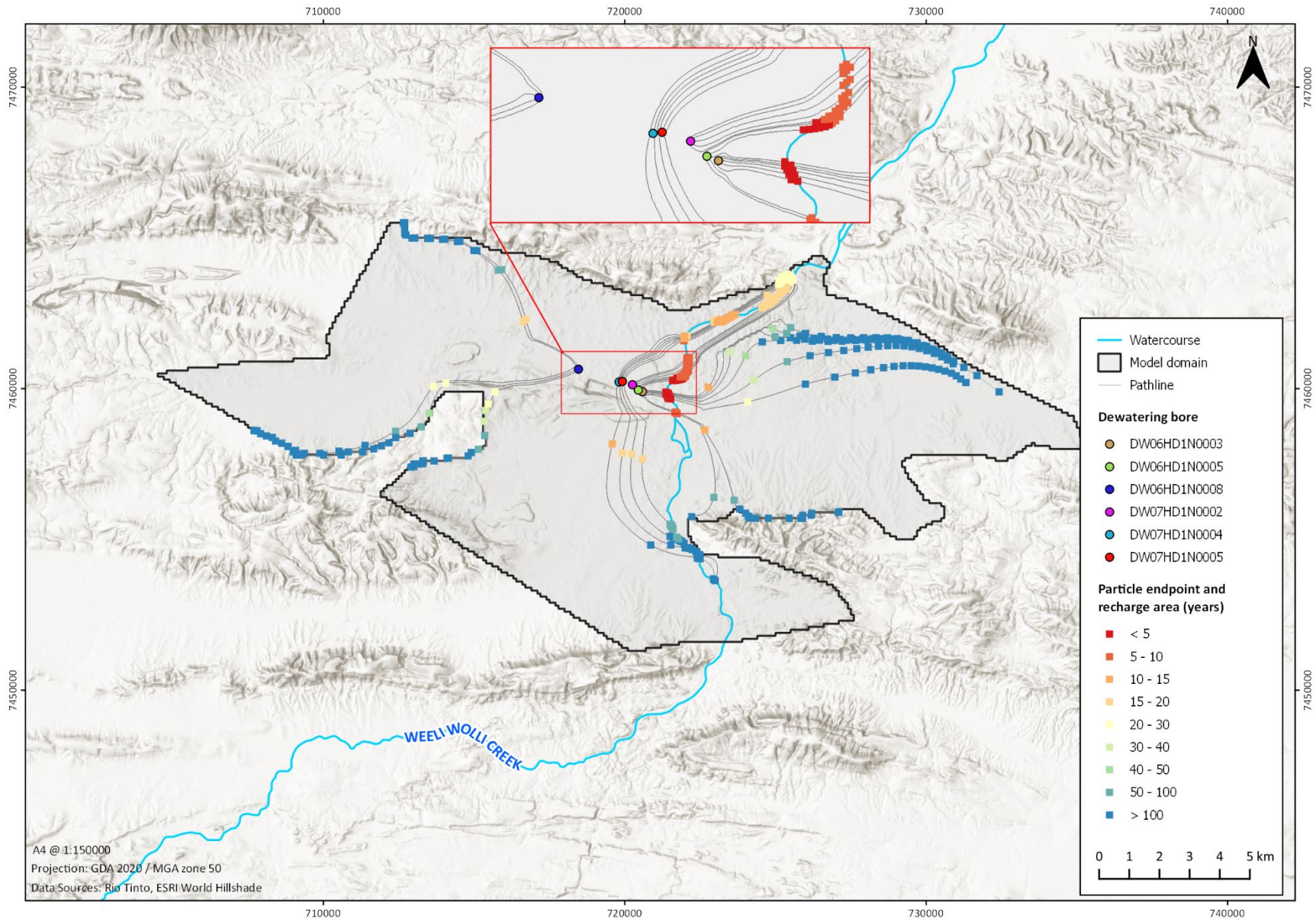
Figure 37 Particle tracking results (2017 Scenario 1)
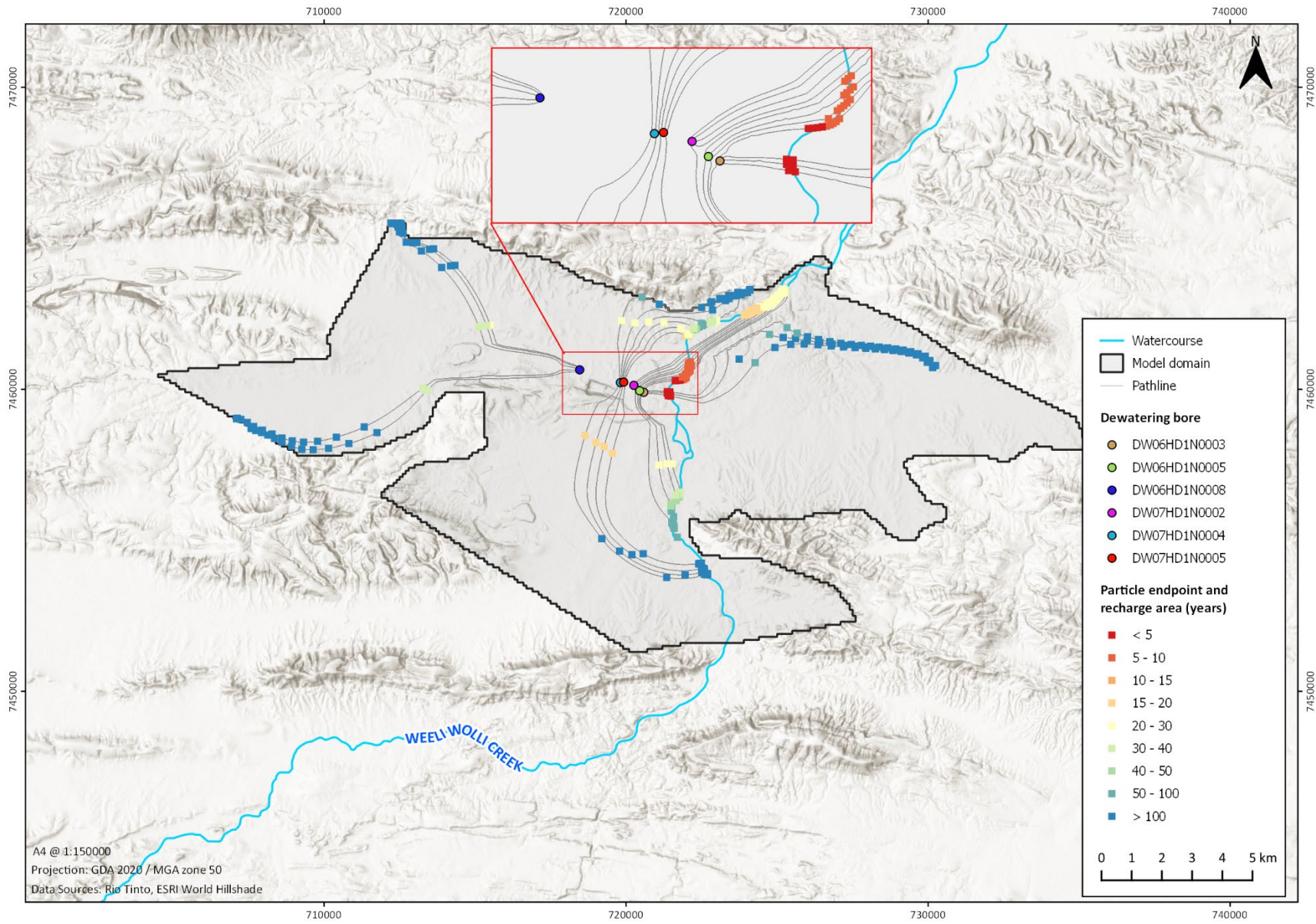
Figure 38 Particle tracking results (2014 Scenario 1)
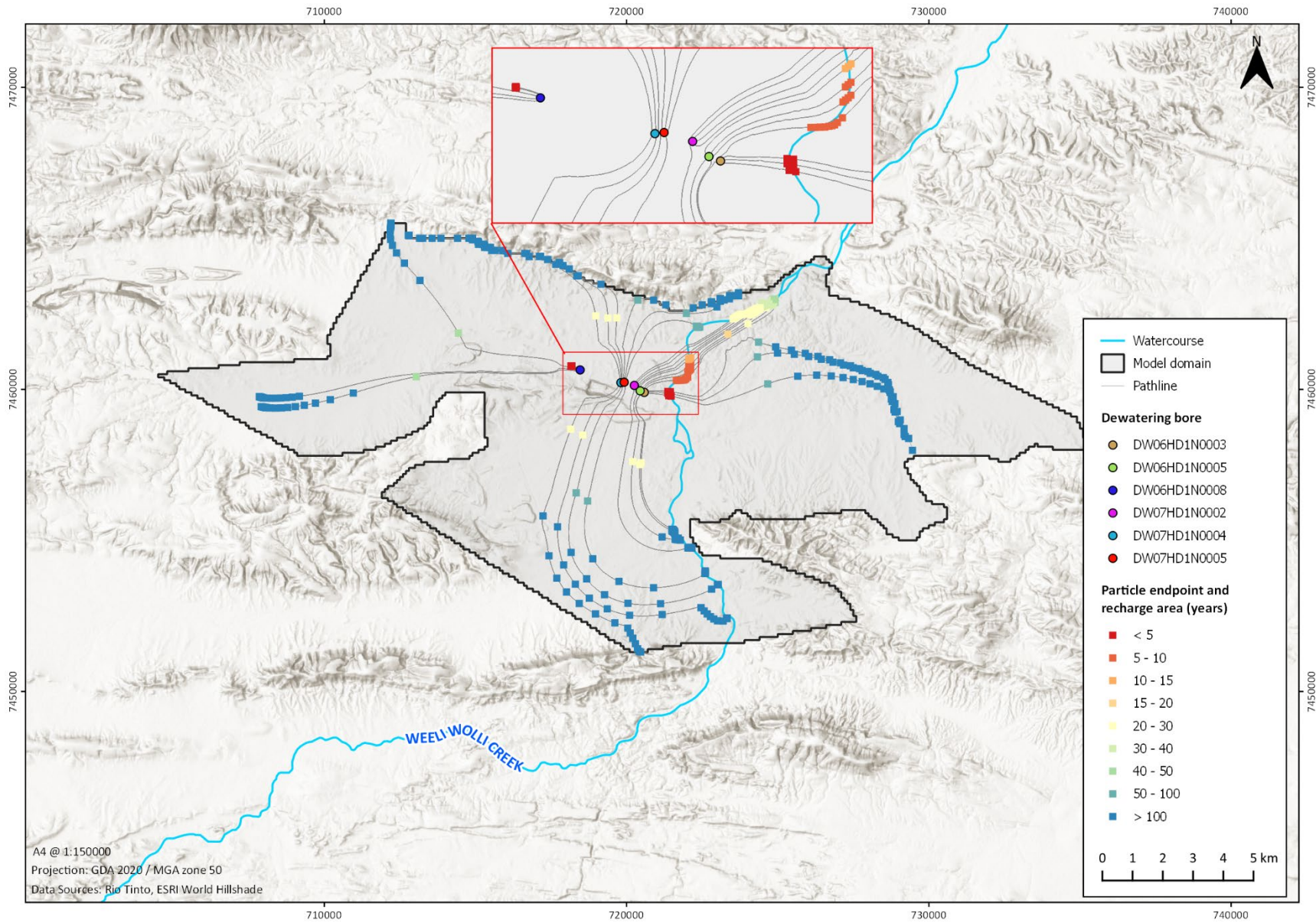
Figure 39 Particle tracking results (2011 Scenario 1)
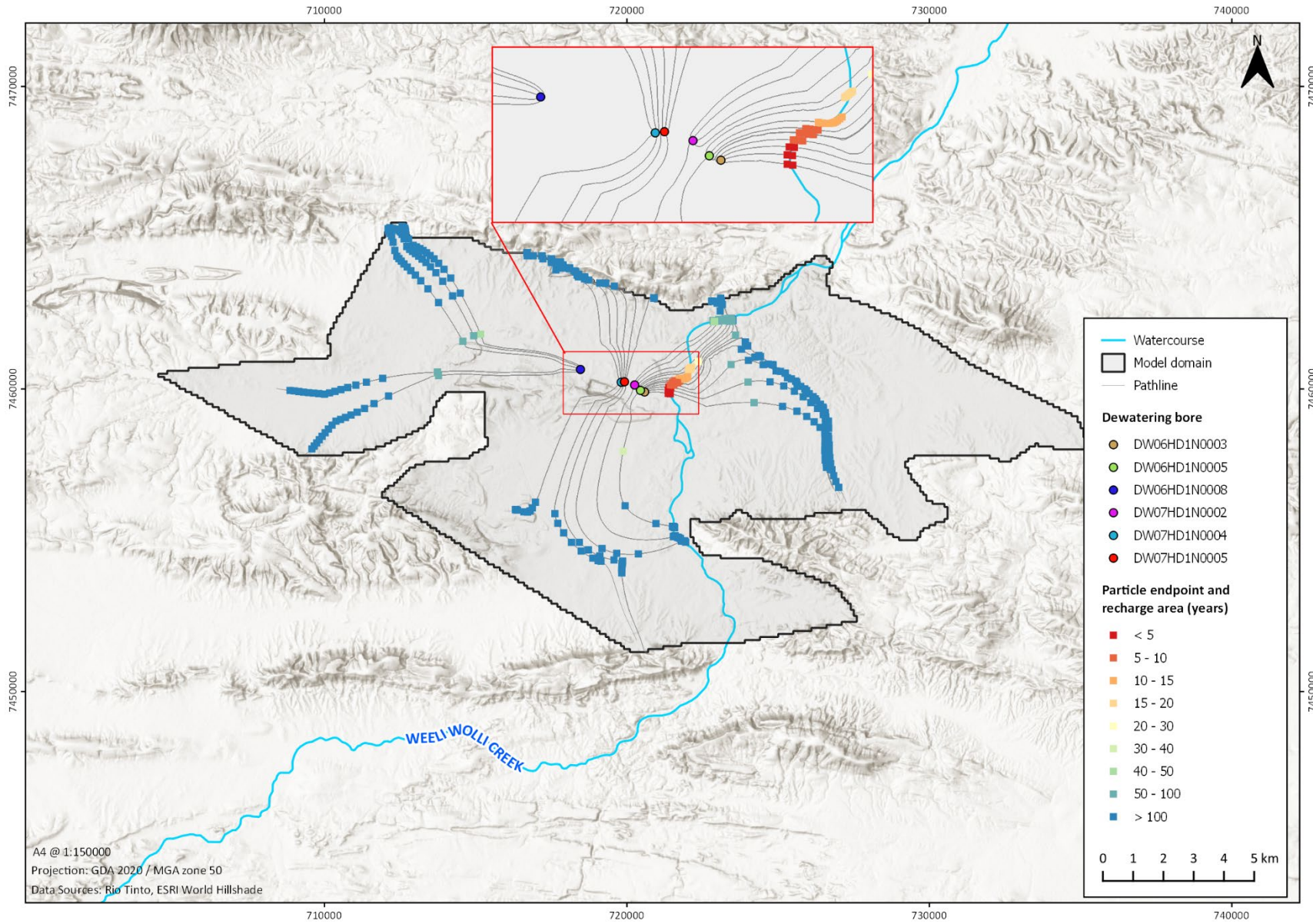
Figure 40 Particle tracking results (2008 Scenario 1)

Sensitivity analysis (Scenario 2 and 3)

Scatter plots with 1:1 lines for both Scenario 2 (0.006 m/d of creek recharge) and Scenario 3 (0.012 m/d of creek recharge) are presented in Figure 41 and Figure 42, respectively. The RMSE for scenarios 2 and 3 are 81.3 and 75.9 pg/kg, respectively. The RMSE for both scenarios are slightly lower than scenario 1 (74 pg/kg), suggesting a slightly reduced match between simulated and measured concentration. Nevertheless, the same temporal trends are observed from all the particle tracking simulations with creek recharge applied. Advective statistics and measured/simulated concentration comparisons for Scenario 2 are provided in Table 12, Table 13 and Figure 43, while the corresponding datasets for Scenario 3 are provided in Table 14, Table 15 and Figure 44.

Like scenario 1, both sensitivity tests show a good match between measured and simulated concentrations for the northern-most bores (DW07HD1N0004 and DW07HD1N0005). For scenario 2, the simulated concentrations in DW07HD1N0004 decrease from 38.9 pg/kg in 2017 to 8.9 pg/kg in 2014. The same pattern is exhibited in Scenario 3, whereby concentrations decrease from 75 to 17 pg/kg during the same time span. DW07HD1N0005 produces a similar trend whereby simulated concentrations decrease from 119.4 to 45.1 pg/kg between 2017 and 2014 when scenario 3 is concerned, in comparison to the corresponding time period for measured concentrations, which decrease from 144 to 29 pg/kg. Peak concentrations simulated in 2017 for scenario 3 are less in comparison to scenario 1 when DW07HD1N0004 is concerned, despite a higher recharge rate. This is largely due to model sensitivities between respective simulations as one extra pathline is diverted towards the south in scenario 3, producing a lower simulated concentration on account of less particles terminating along Weeli Wolli Creek.

The sensitivity analysis does not change the temporal trend seen in Scenario 1 whereby peak concentrations are reached between 2014 and 2017. Minimum particle ages for DW07HD1N0004 and DW07HD1N0005 (which correspond to Weeli Wolli Creek recharged water) span from 8.9 to 12.9 years for Scenario 2, and 9.1 to 11.3 years for Scenario 3. The slight differences in travel time are likely attributed to changes in the hydraulic gradient between respective scenarios (i.e. more groundwater mounding on account of extra recharge applied).

DW06HD1N0003 and DW06HD1N0005 exhibit the same temporal pattern, whereby peak concentrations are reached in preceding simulated time periods. For scenario 3, a peak simulated concentration is reached in 2011 (58.2 pg/kg) as opposed to 2014 which is observed in Scenarios 1 and 2. Similarly, DW07HD1N0002 has a slightly reduced peak simulated concentration in Scenario 3 in comparison to Scenario 1 as one pathline is diverted away from Weeli Wolli Creek towards the alluvial plain in the eastern part of the domain. Overall, minor sensitivities in groundwater recharge are not enough to majorly impact results as evidenced by similar temporal trends in all simulations.
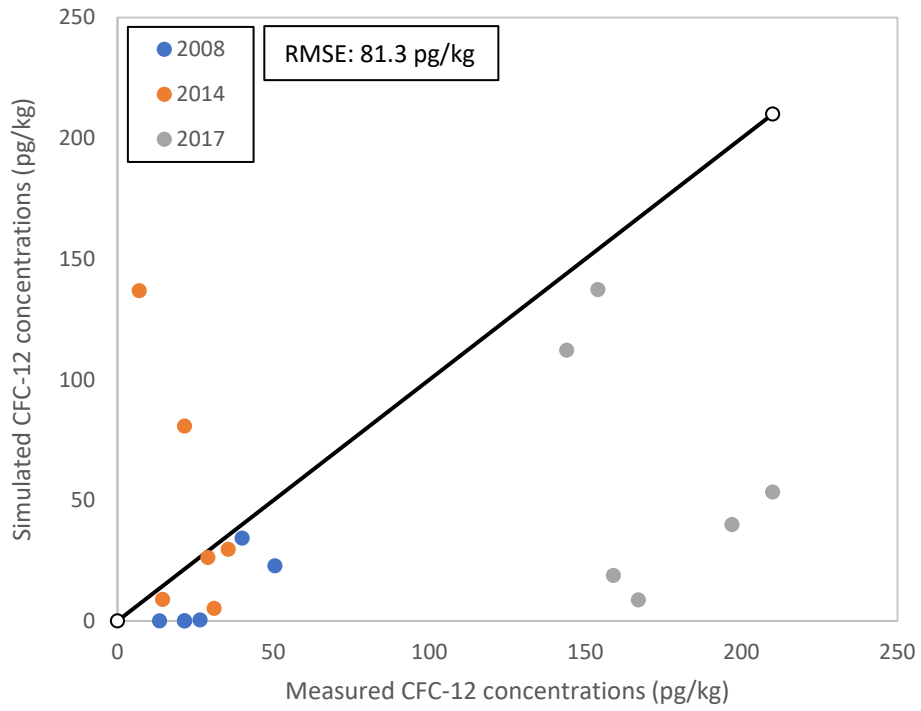
Figure 41 Scatter plot of measured vs simulated CFC-12 concentrations over different sampling periods (Scenario 2)
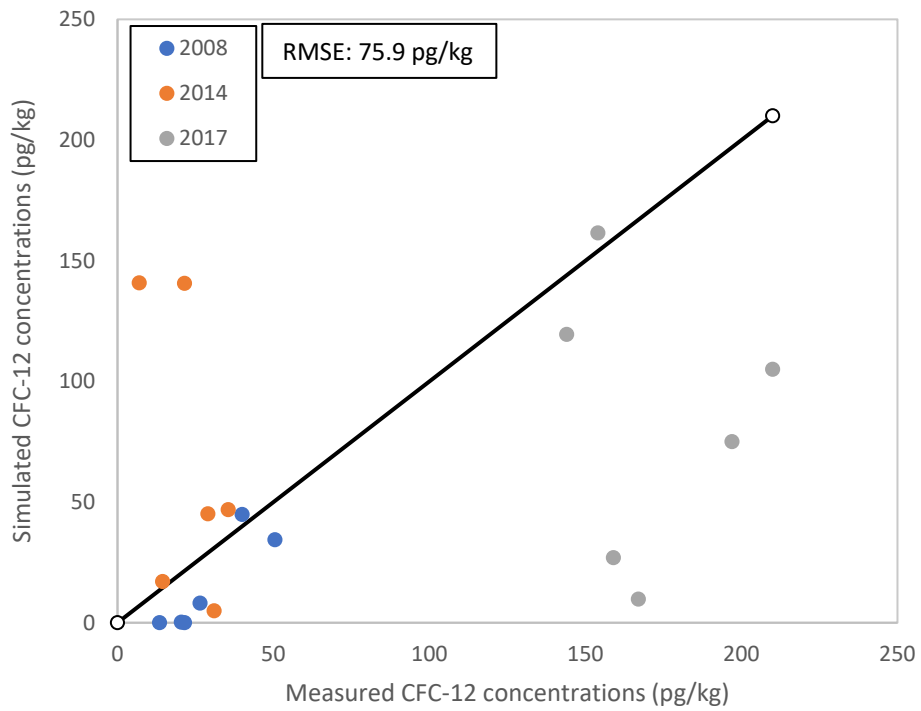
Figure 42 Scatter plot of measured vs simulated CFC-12 concentrations over different sampling periods (Scenario 3)

Table 12 Advective statistics for scenario 2 (in years)

Well	2008 (years)			2011 (years)			2014 (years)			2017 (years)		
	Min	Max	Median	Min	Max	Median	Min	Max	Median	Min	Max	Median
DW07HD1N0002	52.6	2101.5	**960.8**	23.3	580.2	**37.1**	17.4	153.9	**21.5**	6.0	348.3	**23.4**
DW07HD1N0004	427.2	9297.1	**2170.2**	26.5	6499.1	**1360.0**	18.4	4623.4	**522.0**	12.9	318.5	**197.3**
DW07HD1N0005	742.4	11548.1	**2621.7**	45.8	6617.4	**1408.7**	18.8	1255.8	**152.5**	8.9	3231.7	**21.2**
DW06HD1N0003	3.9	4160.5	**1181.2**	2.7	2776.9	**395.7**	2.1	1825.7	**256.2**	2.1	1705.3	**453.4**
DW06HD1N0005	8.8	4682.2	**181.4**	8.9	432.0	**43.1**	6.4	1341.1	**28.9**	3.9	1965.9	**342.8**
DW06HD1N0008	49.4	4610.4	**1358.3**	-	-	**-**	29.3	3007.5	**767.9**	18.3	2333.5	**383.1**

Table 13 Measured vs simulated concentration comparison for Scenario 2 (in pg/kg)

Well	2008 (pg/kg)		2011 (pg/kg)		2014 (pg/kg)		2017 (pg/kg)	
	Obs.	Sim.	Obs.	Sim.	Obs.	Sim.	Obs.	Sim.
DW07HD1N0002	26.5	0.4	-	77.6	7.0	136.8	154.0	137.3
DW07HD1N0004	13.5	0.0	-	5.9	14.5	8.9	197.0	39.9
DW07HD1N0005	21.5	0.0	-	0.7	29.0	26.2	144.0	112.1
DW06HD1N0003	50.5	22.8	-	29.7	35.5	29.7	159.0	18.8
DW06HD1N0005	40.0	34.3	-	55.0	21.5	80.7	210.0	53.4
DW06HD1N0008	20.5	0.2	-	-	31.0	5.2	167.0	8.7
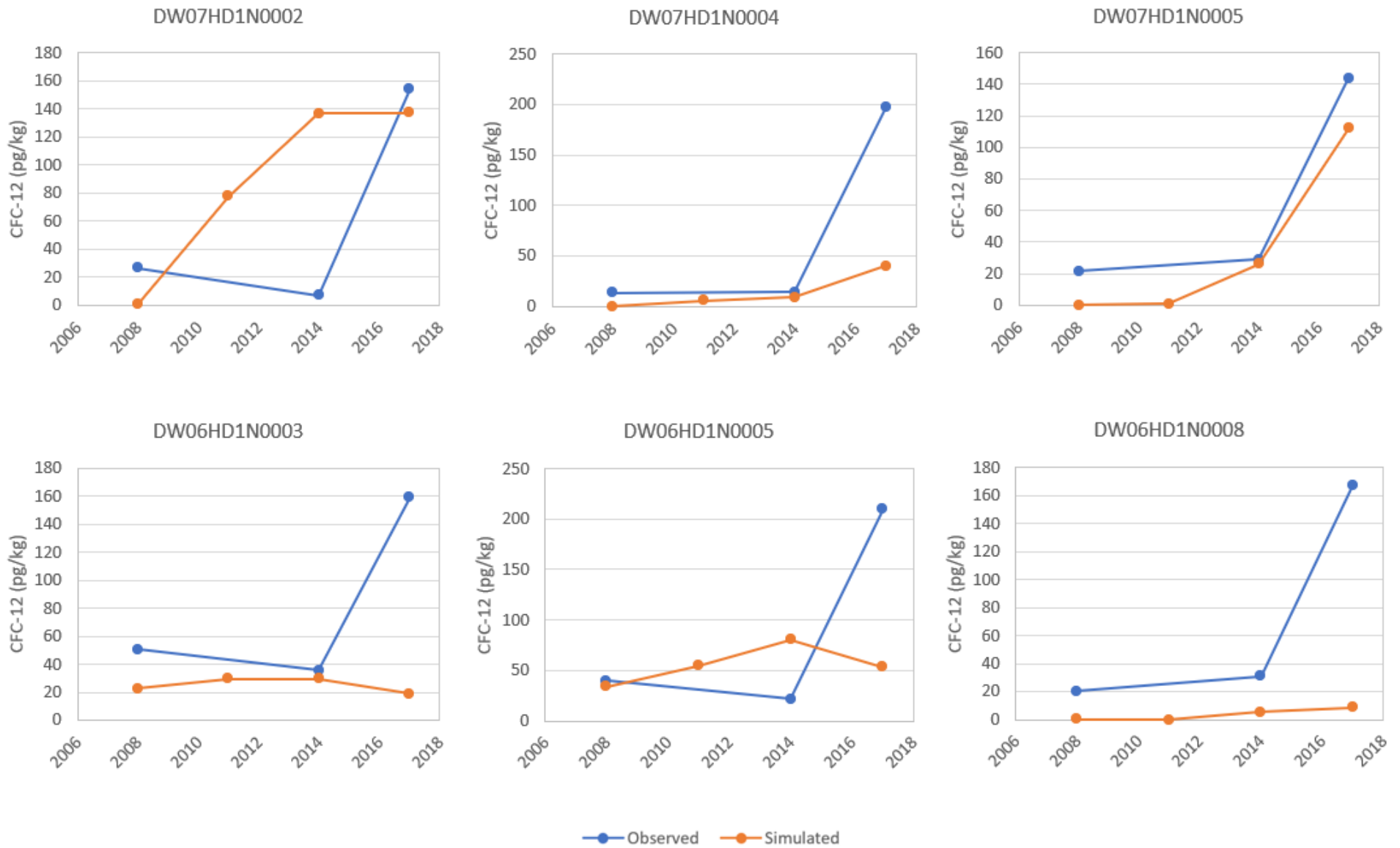
Figure 43 Observed vs simulated CFC-12 concentrations (Scenario 2)

Table 14 Advective statistics for scenario 3 (in years)

Well	2008 (years)			2011 (years)			2014 (years)			2017 (years)		
	Min	Max	Median	Min	Max	Median	Min	Max	Median	Min	Max	Median
DW07HD1N0002	28.5	2039.5	**62.3**	23.2	171.9	**29.1**	17.9	58.6	**21.4**	7.6	34.1	**25.7**
DW07HD1N0004	463.4	9632.7	**1689.0**	27.1	7968.0	**956.1**	20.2	1037.5	**249.0**	11.3	144.2	**78.8**
DW07HD1N0005	723.7	11153.6	**1044.7**	45.6	1444.8	**389.8**	16.4	1019.8	**202.9**	9.1	86.8	**22.5**
DW06HD1N0003	3.8	4169.6	**694.6**	2.6	3022.8	**130.6**	2.1	1943.7	**321.1**	2.2	1887.8	**498.5**
DW06HD1N0005	7.0	240.2	**84.4**	6.7	117.7	**32.4**	4.5	45.2	**24.9**	2.8	2163.2	**84.1**
DW06HD1N0008	49.6	4682.7	**1359.9**	-	-	**-**	30.3	3209.3	**801.3**	19.8	2355.2	**358.4**

Table 15 Measured vs simulated concentration comparison for Scenario 3 (in pg/kg)

Well	2008 (pg/kg)		2011 (pg/kg)		2014 (pg/kg)		2017 (pg/kg)	
	Obs.	Sim.	Obs.	Sim.	Obs.	Sim.	Obs.	Sim.
DW07HD1N0002	26.5	8.1	-	101.4	7.0	140.7	154.0	161.5
DW07HD1N0004	13.5	0.0	-	5.7	14.5	17.0	197.0	75.0
DW07HD1N0005	21.5	0.0	-	2.9	29.0	45.1	144.0	119.4
DW06HD1N0003	50.5	34.3	-	58.2	35.5	46.8	159.0	26.9
DW06HD1N0005	40.0	44.8	-	79.6	21.5	140.6	210.0	105.0
DW06HD1N0008	20.5	0.2	-	-	31.0	4.9	167.0	9.7
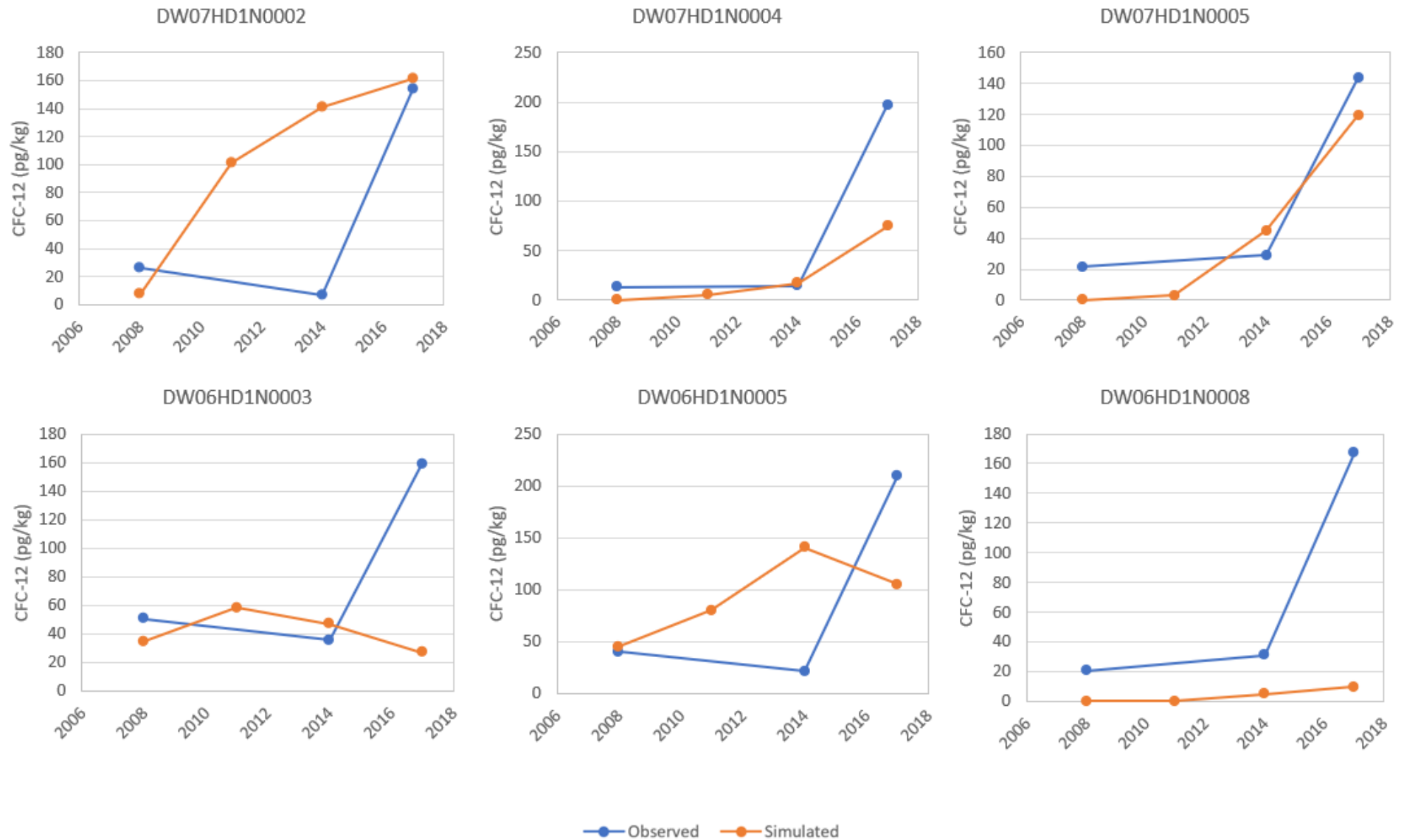
Figure 44 Observed vs simulated CFC-12 concentrations (Scenario 3)

7. DISCUSSION

Results from the study have shown that applying creek recharge into the groundwater model helps to improves calibration performance. The RMSE gathered from model simulations indicates that a recharge rate equivalent to 0.009 m/d, estimated via the WTF method (74 pg/kg) produces a closer match between simulated and measured concentrations in comparison to the pre-existing model (97 pg/kg). Similarly, the two sensitivity scenarios also produced a markedly improved calibration performance as evidenced by an RMSE of 81 and 76 pg/kg for scenario 2 and 3, respectively. The biggest drawback in the base case model is that it does not include creek recharge and is thus unable to simulate the influx of younger groundwater observed in the 2016/2017 sampling round (Figure 2). The results from the base case simulations have shown that median particle ages increase linearly, and simulated concentration equivalents of CFC-12 respectively decrease from 2017 to 2008 mostly as a function of the hydraulic gradient. Simulated concentrations do not exceed 12.1 pg/kg and only 10% of particles are recharged within appropriate timeframes for atmospheric concentrations of CFC-12. A diffuse recharge equivalent to 5.8 mm/year (as per the chloride mass balance) applied to the model domain does not effectively represent localised recharge processes brought on from creek infiltration, as conceptualised.

The results have shown to be spatially variable and that bores lying immediately north of HD1N produce a much-improved match to measured concentrations when the three scenarios with creek recharge are concerned. When only DW07HD1N0004 and DW07HD1N0005 are considered, the RMSE is 42, 66 and 52 pg/kg for scenarios 1 (0.009 m/d recharge), 2 (0.006 m/d) and 3 (0.012 m/d), respectively. In comparison, the RMSE for the respective bores for the base case simulation is 114 pg/kg. The sensitivity analysis indicates that 0.009 m/d of recharge applied to Weeli Wolli Creek produces the best fit between simulated and measured CFC-12 concentrations, validating the WTF method used to estimate creek recharge to some degree. Realistically, the 0.009 m/d of recharge applied is location specific and other areas are still likely to be greatly over or underestimated.

It is also important to recognise that the sensitivity analysis is limited to creek recharge and that other model parameters were not significantly altered in model calibration (i.e. hydraulic conductivity zonation, evapotranspiration, other recharge processes). The sensitivity analysis indicates that applying a lesser recharge equivalent to 0.006 m/d produces a poorer fit in comparison to 0.009 m/d (Scenario 1) and 0.012 m/d (Scenario 3). Recharge rates < 0.006 m/d along Weeli Wolli Creek have also been independently tested throughout the initial stages of model calibration but failed to produce significant improvements on the base case pre-existing model on account of particles bypassing the creek.

The sensitivity analysis has shown that slight variations in recharge are not enough to majorly alter results. The same temporal trends are observed in all three scenarios in that concentrations significantly increase

between 2014 and 2017 when bores DW07HD1N0004 and DW07HD1N0005 are considered. The low concentrations observed in the two bores for earlier time simulations (2008 and 2011) are due to the changes in the potentiometric surface between time varying simulations as more particles are diverted towards the northern portion of the domain. Low concentrations are also attributed to the screen depths relative to the water table surface as both bores have relatively deep screens (524 and 511 m AHD for DW07HD1N0004 and DW07HD1N0005, respectively). Thus, from this perspective the bores also provide valuable information. Namely, during earlier time periods, younger groundwater cannot be contributing to the bores given the water table height in comparison to the top of the well screens. Bores with shallower screen depths (i.e. DW06HD1N0003 and DW06HD1N0005) typically show elevated simulated concentrations even during earlier time periods, producing a poorer fit on account of creek recharge still contributing to the bores. The depth of the water table relative to the depth to the top of the well screens for bores DW06HD1N0003 and DW06HD1N0005 is such that younger groundwater is entirely screened throughout most of the mining period.

Simulated CFC-12 concentrations in DW07HD1N0002 largely exceed measured CFC-12 concentrations due to almost all particles recharging along Weeli Wolli Creek. The groundwater in the bores at HD1 is composed of a mix of younger and older water as identified by Cook et al. (2017), however the model assumes all contributing water to that bore has at one point been recharged into the system via the creek, whether directly north-east of HD1N or towards Weeli Wolli Spring. Realistically, this is not the case as prior to dewatering groundwater flowed from south-west to north-east.

The particle simulations provide some insight from an advective standpoint, particularly when travel times between the bores and Weeli Wolli Creek are considered. For Scenario 1, minimum particle ages for DW07HD1N0004 and DW07HD1N0005 are 9 and 11.6 years, respectively, which correspond to recharge dates along Weeli Wolli Creek. Given the similarity in observed and measured concentrations for the two bores over time, it can be inferred that it takes at least 9 to 12 years for creek recharged groundwater to reach the northern border of HD1N. When the eastern most and closest bores to Weeli Wolli Creek are considered, travel times between the bores and the creek are short, which is expected given the relatively short distance ($\sim$ 1 km). For Scenario 1 – 3, minimum particle ages range anywhere from 2.1 to 3.8 years for bores DW06HD1N0003 and DW06HD1N0005. These simulated travel times would suggest that there would be an increase in CFC-12 concentrations sometime between 2009 and 2011. However, temporal variations in the measured concentrations of CFC-12 in all bores are relatively consistent (Figure 2), in that concentration increases in CFC-12 are all observed in the same time frame (2016-2017). The disparity between travel times and measured concentrations could be due to several reasons:

(1) the particle velocity in the groundwater model is greatly overestimated due to a misrepresentation of model parameters (i.e. hydraulic conductivity, specific yield), in which case further calibration is required;

(2) younger groundwater is reaching the bores within a relatively short time frame but groundwater collected at the time of sampling is from a depth where aquifer permeability is lower, and;

(3) infiltration rates underneath Weeli Wolli Creek and through the unsaturated zone are slow.

Infiltration rates and vertical velocities from Weeli Wolli Creek and nearby Marillana Creek have been measured during steady flow conditions to be in the order of 1.5 - 3.5 m/d (Dogramaci et al. 2015; Cook et al. 2017). However, these rates are indicative of shallow infiltration and are likely to decrease significantly with depth. The depth to the water table east of HD1N in 2017 ranges from approximately 90 to 100 m, with a water table elevation ranging between 490 and 500 m AHD (Figure 22), which could suggest long travel times through the unsaturated zone. One of the limitations to mod-PATH3DU and other particle tracking codes in general, is that they do not simulate unsaturated zone flow processes. Thus, particle ages can be misrepresented when there is a large disparity between the ground surface and water table.

Despite usefulness of the WTF method, it does have several limitations. The method assumes rainfall to be the only recharge mechanism. All other causes leading to a rise in the water table need to be filtered out to avoid an overestimation of recharge (Crosbie, Binning and Kalma, 2005, p. 1). The method typically assumes aerially uniform recharge and rates also vary spatially as hydrographs will show different responses in groundwater levels depending on location. For example, monitoring bore BH20d (Figure 6, Figure 7) does not show the same fluctuations in groundwater levels despite its location nearby to Weeli Wolli Creek. Ideally, monitored water levels utilised in WTF calculations should be representative of the entire catchment (Healy and Cook, 2002, p. 93). Additionally, the method cannot account for a steady state of recharge. Namely, if recharge and drainage rates away from the water table are constant then water levels would not change and the WTF method would be ineffective (Healy and Cook, 2002, p. 93).

The proportion of younger or modern groundwater from the simulations (i.e. particles terminating along Weeli Wolli Creek) ranges from 10% at DW06HD1N0003 to 100% of particles at DW07HD1N0002 when the creek recharge model scenarios are concerned. Thus, it is difficult to estimate the true portion of younger groundwater within the bores from the simulations. Additionally, each bore can draw a different proportion of water from the creek, depending on proximity.

This study aimed at constraining the rates of recharge via creek infiltration. Largely, this has been achieved. However, more work would be required to calibrate the model further and improve results. Applying

recharge to other ephemeral creeks/drainage lines in the study area can help further constrain the model as spatial variability in recharge will create noticeably different age distributions. The rise in CFC-12 concentrations in DW06HD1N0008 suggests that younger groundwater also comprises a portion of the pumped water in the bore. However, the extent and orientation of the cone of depression in relation to the bore's location is such that no water can be coming from Weeli Wolli Creek in the east. This suggests that tributaries draining towards Weeli Wolli Creek north of HD1N are also contributing recharge to the groundwater system during periods of heavy rain/creek flow. Weather attributed fluctuations in groundwater levels are observed in BH19 (Figure 6, Figure 7), although not as prominently as observed at BH15, suggesting recharge from creek infiltration is occurring along ephemeral drainage lines in the alluvial plain east of Weeli Wolli Creek. The quantification of creek recharge in some of the sections of the model may prove difficult given the absence of observation data. Thus, implementing a trial-and-error approach when applying creek recharge and using spatial variations in recharge as opposed to uniform rates throughout the whole domain would best be utilised to further calibrate the model.

The simulations for the model with creek recharge applied produced significant groundwater mounding (> 20 m) underneath Weeli Wolli Creek in the southern part of the model domain and east to HD1S. This had an impact on some of the particle tracking results as pathlines were being diverted towards the creek on account of changes in the orientation of the water table surface between time periods (i.e. DW06HD1N0003 and DW06HD1N0005). Groundwater levels in BH20d (Figure 6) would suggest that creek recharge is minimal given the lack of weather induced fluctuations. This could be attributed to differences in the lithological composition of the creek bed, a reduced vertical hydraulic conductivity or that more water is being lost to evapotranspiration processes in the area. Further investigation would be required to parameterise the southern part of the study area and some of the other lesser-known parts of the aquifer. Future groundwater sampling of dewatering bores located in the vicinity of HD1S could indicate as to whether Weeli Wolli Creek or any other drainage lines/ephemeral creeks are contributing to groundwater recharge in that part of the aquifer.

In addition to recharge parameterisation, hydraulic conductivity has an impact on age distributions. Minor adjustments were necessarily made to some of the hydraulic characteristics in the base case model, however further work would be required to improve calibration results. It is likely the hydraulic conductivity of large parts of the model domain is underestimated. The response in groundwater drawdown at BH13 (Figure 6) is also evidence that hydraulic conductivity may be higher in the western part of the study area. Conversely, age distributions from DW06HD1N0003 and DW06HD1N0005 have shown that hydraulic conductivity east of HD1N may be lower if measured and simulated concentrations are to be compared over time. The model assumes homogeneous and isotropic conditions for each respective zone of hydraulic conductivity (i.e. horizontal and vertical hydraulic conductivity is the same). Typically, vertical hydraulic conductivity is much lower and would effect particle travel times as such. Spatial heterogeneity in

hydraulic conductivity also influences particle pathlines, as evidenced in the north-east part of the domain between the transition of low hydraulic conductivity and high hydraulic conductivity underneath Weeli Wolli Creek (180 m/d), whereby some particle pathlines were behaving erratically. Reducing the abrupt transition between zones and applying finer grid discretisation will improve particle tracking performance.

8. CONCLUSION

Atmospheric tracer concentrations are an effective means to calibrate and improve groundwater model performance and constrain model parameters when combined with particle analysis, as shown in this study. The simple application of recharge along a creek conceptualised to be contributing to groundwater recharge produced similar trends between simulated and observed values for selected regions in the model.

In this study, a reverse particle tracking approach was utilised by placing 100 uniformly placed particles along the screen lengths of six dewatering bores and tracking to their points of origin (i.e. recharge areas). When the pre-calibrated model is considered, only 10% of particles were recharged within appropriate timeframes for atmospheric concentrations of CFC-12, producing low simulated concentrations in comparison to measured concentrations. The diffuse recharge equivalent to 5.8 mm/year (as per the chloride mass balance) applied to the model domain did not effectively represent localised recharge processes brought on from creek infiltration, as conceptualised.

When applying uniform recharge rates equivalent to 0.006, 0.009, and 0.012 m/d along the creek line, two of the six bores (i.e. DW07HD1N0004 and DW07HD1N0005) showed a good agreement between measured and simulated CFC-12 concentrations, while others showed a poorer fit on account of variations in the orientation of drawdown between simulated periods. A sensitivity analysis was also undertaken using different rates of recharge to address uncertainty in recharge parameterisation. The RMSE indicated that a recharge rate equivalent to 0.009 m/d, estimated via the WTF method (74 pg/kg) produced a closer match between simulated and measured concentrations in comparison to 0.006 m/d (81 pg/kg) or 0.012 m/d (0.006 pg/kg).

The study also showed that applying a uniform recharge rate along a selected creek alone is not enough to achieve a finalised calibration. Using a spatial variability of recharge and applying it other sections of the model domain can improve model performance and particle simulated ages for selected bores, as can variations in the hydraulic conductivity.

REFERENCES

Ackerman, DJ, Rousseau, JP, Rattray, GW & Fisher JC 2004, 'Steady-State and Transient Models of Groundwater Flow and Advective Transport, Eastern Snake River Plain Aquifer, Idaho National Laboratory and Vicinity, Idaho', U.S. Geological Survey Scientific Investigations Report 2010-5123, pp. 1 – 134

Bedekar, V., Morway, E.D., Langevin, C.D., and Tonkin, M., 2016, MT3D-USGS version 1: A U.S. Geological Survey release of MT3DMS updated with new and expanded transport capabilities for use with MODFLOW: U.S. Geological Survey Techniques and Methods 6-A53, 69 p.,

Bethke, C & Johnson T 2007, 'Groundwater age and groundwater age dating. Annual Review of Earth and Planetary Sciences, vol. 36 (1), pp. 121 – 152.

Bureau of Meteorology (2021) 'Climate statistics for Australian locations' Available at http://www.bom.gov.au/climate/averages/tables/cw_007151.shtml

Chesnaux, R, Allen, DM & Simpson MWM 2011, 'Comparing isotopic groundwater age measurements with simulated groundwater ages: example of the Abbotsford-Sumas Aquifer (USA and Canada) and application', *Water and Environment Journal*, vol. 26, pp. 30 – 37.

Clark, B.R, Landon, M.K, Kauffman L.J & Hornberger, G.Z 2007, 'Simulations of Groundwater Flow, Transport, Age, and Particle Tracking near York, Nebraska, for a Study of Transport of Anthropogenic and Natural Contaminants (TANC) to Public-Supply Wells', U.S Geological Survey Scientific Investigations Report 2007-5068, pp. 1 – 47.

Cook, PG & Bohlke, JK 2000, 'Determining timescales for groundwater flow and solute transport. In: Cook, PG, Herzceg, AL (eds) Environmental tracers in subsurface hydrology. Kluwer, Boston, pp. 1 – 30.

Cook PG & Dogramaci S 2019, 'Estimating Recharge from Recirculated Groundwater with Dissolved Gases: An End-Members Mixing Analysis, *Water Resources Research*, 55, pp. 5468 – 5486.

Cook, P, Dogramaci, S, McCallum, J & Hedley, J 2017, 'Groundwater age, mixing and flow rates in the vicinity of large open pit mines, Pilbara region, northwestern Australia', *Hydrogeol J*, vol. 25, pp. 39 – 53.

Crandall, CA, Kauffman LJ, Katz BG, Metz, PA, McBride WS & Berndt MP 2008, 'Simulations of Groundwater Flow and Particle Analysis in the Area Contributing Recharge to a Public-Supply Well near Tampa, Florida, 2002-05', U.S. Geological Survey Scientific Investigations Report 2008-5231, pp. 1 – 53

Crosbie, RS, Binning, P & Kalma JD 2005, 'A time series approach to inferring groundwater recharge using the water table fluctuation method', *Water Resources Research*, vol. 41, pp. 1 – 9.

Department of Water Environmental Regulation, *Evaluating the environmental condition of Weeli Wolli Creek – February 2018*, Environmental Protection Authority, Western Australia

Dogramaci, S, Firmani, G, Hedley, P, Skrzypek, G & Grierson, PF 2015, 'Evaluating recharge to an ephemeral dryland stream using a hydraulic model and water, chloride and isotope mass balance', *Journal of Hydrology*, vol. 521, pp. 520 – 532.

Doyle, JM, Gleeson, T, Manning AH & Ulrich Mayer K 2015, 'Using noble gas tracers to constrain groundwater flow model with recharge elevations: A novel approach for mountainous terrain', *Water Resources Research*, 51, p. 8094.

Frind, EO, Molson, JW and Rudolph, DL 2006, 'Well vulnerability: a quantitative approach for source water protection', *Ground Water*, vol. 44, no. 5, pp. 732 – 742.

Golder Associates Pty Ltd, 2019, 'Hope Downs 1 Closure Modelling – Updated Scenarios', September 2019, Report, 19123590-7403-002-R-Rev0.

Gusyev, M.A, Towes, M, Morgenstern, U, Stewart, M, White, P, Daughney, C and Hadfield, J 2013, 'Calibration of a transient transport model to tritium data in streams and simulation of groundwater ages in the western Lake Taupo catchment, New Zealand', *Hydrology and Earth System Sciences*, vol. 17, p. 1217.

Hanson, RT, Kauffmann, LK, Hill, MC, Dickinson, JE & Mehl, SW 2013, 'Advective Transport Observations with MODPATHS-OBS-Documentation of the MODPATH Observation Process', U.S. Geological Survey Techniques and Methods 6-A42.

Healy, RW & Cook PG 2002, 'Using groundwater levels to estimate recharge', *Hydrogeology Journal*, vol 10, pp. 91 – 109.

Heath, RC 1983, 'Basic ground-water hydrology', U.S. Geological Survey Water-Supply Paper 2220, pp. 1 – 86.

Hinkle, SR & Snyder, DT 1997, 'Comparison of Chlorofluorocarbon-Age Dating with Particle-Tracking Results of a Regional Ground-Water Flow Model of the Portland Basin, Oregon and Washington', U.S. Geological Survey Water-Supply Paper 2483, pp. 1 – 47.

Izbicki, JA, Stamos, CL, Nishikawa, T & Martin, P 2004, 'Comparison of groundwater flow model particle-tracking results and isotopic data in the Mojave River groundwater basin, southern California, USA', *Journal of Hydrology*, vol. 292, pp. 30 – 47.

Johnson, SL & Wright, AH 2001, 'Central Pilbara Groundwater Study', Water and Rivers Commission, *Hydrogeological Record Series*, Report HG 8, p. 4.

Kuniansky, EL, Falhquist, L & Ardis, A 2001, 'Travel Times Along Selected Flow Paths of the Edwards Aquifer, Central Texas', U.S. Geological Survey Water Resources Investigations Report 01-4011, pp. 69 – 77.

Kunstmann, H and Kastens, M 2006, 'Determination of stochastic well head protection zones by direct propagation of uncertainties of particle tracks', *Journal of Hydrology*, vol. 323, no. 1 – 4, pp. 214 – 229.

Lindgren, RJ, Houston, NA, Musgrove, M, Fahlquist, LS & Kauffmanm LF 2011, 'Simulations of Groundwater Flow and Particle-Tracking Analysis in the Zone of Contribution to a Public-Supply Well in San Antonio, Texas', U.S. Geological Survey Scientific Investigations Report 2011-5149, pp. 1 – 93.

Morris, DA & Johnson AI 1967, 'Summary of hydrologic and physical properties of rock and soil materials as analyzed by the Hydrologic Laboratory of the U.S. Geological Survey, U.S. Geological Survey Water-Supply Paper 1839-D, pp. 1 – 42.

Muffles, C, Wang, X, Tonkin, M & Neville C 2014, 'User's Guide for mod-PATH3DU: A groundwater path and travel-time simulator', S.S. Papadopulos & Associates, Inc., Bethesda, MD.

Nimmo, JR, Horowitz, C & Mitchell, L 2011, 'Discrete-Storm Water-Table Fluctuation Method to Estimate Episode Recharge', *Groundwater*, p. 3.

Panday, S, Langevin, CD, Niswonger, RG, Ibaraki, M & Hughes JD 2013, 'MODFLOW-USG version 1: An unstructured grid version of MODFLOW for simulating groundwater flow and tightly coupled processes using a control volume finite difference formulation: U.S Geological Survey Techniques and Methods 6 A45.

Pollock, DW 1994, 'User's guide for MODPATH/MODPATH-PLOT, version 3: A particle-tracking post processing package for MODFLOW, the U.S. Geological Survey finite-difference groundwater flow model: U.S. Geological Survey Open-File Report 94-464.

Pollock, DW 2012, 'User's guide for MODPATH version 6 A particle-tracking model for MODFLOW: U.S. Geological Survey Techniques and Methods, 6 – A41, p. 58.

RTIO, 2018, 'Hope Downs 1 Closure Modelling Report', December 2018, RTIO-PDE-0164879.

RTIO, 2018a, 'Hope Downs 1: Updated hydrogeological conceptualisation model', May 2018, Internal Report, IODMS: RTIO-PDE-0160125.

Sanford, W 2011, 'Calibration of models using groundwater age', *Hydrogeology Journal*, vol. 19, pp. 13 – 16.

Siracusa, G, La Rosa, AD, Musumeci, L & Maiolino G 2007, 'Modelling of contaminant migration in unsaturated soils', WIT Transactions on Ecology and the Environment, vol. 102, pp. 455 – 465.

Starn, JJ, Bagtzoglou AC & Robbins GA 2010, 'Using Atmospheric Tracers to Reduce Uncertainty in Groundwater Recharge Areas', ground-water, vol. 48, pp. 858 – 868.

Starn, JJ, Green, CT, Hinkle, SR, Bagtzoglou AC & Stolp, BJ 2014, 'Simulating water-quality trends in public-supply wells in transient flow systems, *Groundwater*, vol. 52, pp. 53 – 62.

Tiedeman, CR, Hill, MC, D'Agnese FA & Faunt CC 2003, 'Methods for using groundwater model predictions to guide hydrogeologic data collection, with application to the Death Valley regional groundwater flow system', *Water Resources Research*, vol. 39, pp. 1 – 17.

Thiros, NE, Gardner WP & Kuhlman, KL 2021, 'Utilizing Environmental Tracers to Reduce Groundwater Flow and Transport Model Parameter Uncertainties', Water Resources Research, vol. 57,

Wilske, C, Suckow A, Mallast, U, Meier, C, Merchel, S, Merkel, B, Pavetich, S, Rodiger, T, Rugel, G, Sachse, A, Weise, SM & Siebert C 2019', A multi-environmental tracer study to determine groundwater residence times and recharge in a structurally complex multi-aquifer system', Hydrology and Earth System Sciences, pp. 1 -30.

Zuber, A, Rozanski, K, Kania, J & Purtschert 2011, 'On some methodological problems in the use of environmental tracers to estimate hydrogeologic parameters and to calibrate flow and transport models', *Hydrogeology Journal*, vol. 19, pp. 53 – 69.

APPENDICES

Appendix A – Atmospheric equilibrium CFC-12 concentrations

Date	CFC-12 (pg/kg)	Date	CFC-12 (pg/kg)	Date	CFC-12 (pg/kg)	Date	CFC-12 (pg/kg)
1/07/1932	0.00	1/01/1945	0.31	1/07/1957	6.70	1/01/1970	33.75
1/01/1933	0.00	1/07/1945	0.42	1/01/1958	6.70	1/07/1970	38.28
1/07/1933	0.00	1/01/1946	0.42	1/07/1958	7.76	1/01/1971	38.28
1/01/1934	0.00	1/07/1946	0.55	1/01/1959	7.76	1/07/1971	43.22
1/07/1934	0.01	1/01/1947	0.55	1/07/1959	8.86	1/01/1972	43.22
1/01/1935	0.01	1/07/1947	0.79	1/01/1960	8.86	1/07/1972	48.51
1/07/1935	0.01	1/01/1948	0.79	1/07/1960	10.10	1/01/1973	48.51
1/01/1936	0.01	1/07/1948	1.15	1/01/1961	10.10	1/07/1973	54.26
1/07/1936	0.01	1/01/1949	1.15	1/07/1961	11.58	1/01/1974	54.26
1/01/1937	0.01	1/07/1949	1.57	1/01/1962	11.58	1/07/1974	60.62
1/07/1937	0.02	1/01/1950	1.57	1/07/1962	13.23	1/01/1975	60.62
1/01/1938	0.02	1/07/1950	2.02	1/01/1963	13.23	1/07/1975	67.47
1/07/1938	0.04	1/01/1951	2.02	1/07/1963	15.12	1/01/1976	67.47
1/01/1939	0.04	1/07/1951	2.51	1/01/1964	15.12	1/07/1976	74.05
1/07/1939	0.06	1/01/1952	2.51	1/07/1964	17.34	1/01/1977	74.05
1/01/1940	0.06	1/07/1952	3.06	1/01/1965	17.34	1/07/1977	80.35
1/07/1940	0.09	1/01/1953	3.06	1/07/1965	19.91	1/01/1978	80.35
1/01/1941	0.09	1/07/1953	3.62	1/01/1966	19.91	1/07/1978	86.28
1/07/1941	0.12	1/01/1954	3.62	1/07/1966	22.82	1/01/1979	88.16
1/01/1942	0.12	1/07/1954	4.25	1/01/1967	22.82	1/07/1979	92.19
1/07/1942	0.18	1/01/1955	4.25	1/07/1967	26.04	1/01/1980	94.87
1/01/1943	0.18	1/07/1955	4.96	1/01/1968	26.04	1/07/1980	97.21
1/07/1943	0.24	1/01/1956	4.96	1/07/1968	29.68	1/01/1981	101.26
1/01/1944	0.24	1/07/1956	5.77	1/01/1969	29.68	1/07/1981	
1/07/1944	0.31	1/01/1957	5.77	1/07/1969	33.75	1/01/1982	106.16

Date	CFC-12 (pg/kg)	Date	CFC-12 (pg/kg)	Date	CFC-12 (pg/kg)
1/07/1982	110.27	1/01/1995	176.25	1/07/2007	183.55
1/01/1983	113.31	1/07/1995	177.18	1/01/2008	183.41
1/07/1983	116.16	1/01/1996	178.21	1/07/2008	183.00
1/01/1984	118.14	1/07/1996	179.14	1/01/2009	182.77
1/07/1984	120.48	1/01/1997	180.10	1/07/2009	182.50
1/01/1985	123.98	1/07/1997	180.74	1/01/2010	182.23
1/07/1985	127.74	1/01/1998	181.58	1/07/2010	181.95
1/01/1986	130.72	1/07/1998	181.78	1/01/2011	181.68
1/07/1986	133.93	1/01/1999	182.66	1/07/2011	181.41
1/01/1987	136.96	1/07/1999	183.01	1/01/2012	181.14
1/07/1987	138.90	1/01/2000	183.39	1/07/2012	180.87
1/01/1988	143.22	1/07/2000	183.57	1/01/2013	180.59
1/07/1988	146.53	1/01/2001	184.07	1/07/2013	180.32
1/01/1989	150.97	1/07/2001	184.08	1/01/2014	180.05
1/07/1989	153.61	1/01/2002	184.58	1/07/2014	179.76
1/01/1990	157.08	1/07/2002	184.49	1/01/2015	179.47
1/07/1990	159.96	1/01/2003	184.76	1/07/2015	179.18
1/01/1991	162.68	1/07/2003	184.73	1/07/2016	178.60
1/07/1991	164.51	1/01/2004	184.92	1/07/2017	178.02
1/01/1992	167.26	1/07/2004	184.77		
1/07/1992	169.26	1/01/2005	184.72		
1/01/1993	171.37	1/07/2005	184.43		
1/07/1993	171.56	1/01/2006	184.46		
1/01/1994	173.65	1/07/2006	184.13		
1/07/1994	174.96	1/01/2007	184.00		

Appendix B – Water Table Fluctuation (WTF) method calculations for BH15

Stress period	Monitoring interval		Δt	Δh	Recharge (m) ($S_y = \Delta h/\Delta t$)	Total recharge for stress period (m)
1	1/01/2007	1/02/2007	31	0.1	0.0008	0.0016
	1/02/2007	1/03/2007	28	0.1	0.0008	
	1/03/2007	1/04/2007	31	0	0.0000	
2	1/04/2007	1/05/2007	30	0.5	0.0040	0.0056
	1/05/2007	1/06/2007	31	0	0.0000	
	1/06/2007	1/07/2007	30	0.2	0.0016	
3	1/07/2007	1/08/2007	31	0	0.0000	0.0024
	1/08/2007	1/09/2007	31	0	0.0000	
	1/09/2007	1/10/2007	30	0.3	0.0024	
4	1/10/2007	1/11/2007	31	0.6	0.0050	0.0133
	1/11/2007	1/12/2007	30	0	0.0000	
	1/12/2007	1/01/2008	31	1	0.0083	
5	1/01/2008	1/02/2008	31	0	0.0000	0.0081
	1/02/2008	1/03/2008	29	1	0.0081	
	1/03/2008	1/04/2008	31	0	0.0000	
6	1/04/2008	1/05/2008	30	0.5	0.0040	0.0053
	1/05/2008	1/06/2008	31	0.05	0.0004	
	1/06/2008	1/07/2008	30	0.1	0.0008	
7	1/07/2008	1/08/2008	31	0.1	0.0008	0.0024
	1/08/2008	1/09/2008	31	0	0.0000	
	1/09/2008	1/10/2008	30	0.2	0.0016	
8	1/10/2008	1/11/2008	31	0	0.0000	0.0041
	1/11/2008	1/12/2008	30	0.2	0.0016	
	1/12/2008	1/01/2009	31	0.3	0.0025	
9	1/01/2009	1/02/2009	31	0.5	0.0040	0.0048
	1/02/2009	1/03/2009	28	0.1	0.0008	
	1/03/2009	1/04/2009	31	0	0.0000	
10	1/04/2009	1/05/2009	30	0.9	0.0073	0.0081
	1/05/2009	1/06/2009	31	0	0.0000	
	1/06/2009	1/07/2009	30	0.1	0.0008	
11	1/07/2009	1/08/2009	31	0.05	0.0004	0.0053
	1/08/2009	1/09/2009	31	0	0.0000	
	1/09/2009	1/10/2009	30	0.6	0.0048	
12	1/10/2009	1/11/2009	31	0.4	0.0033	0.005
	1/11/2009	1/12/2009	30	0	0.0000	
	1/12/2009	1/01/2010	31	0.2	0.0017	
13	1/01/2010	1/02/2010	31	0	0.0000	0
	1/02/2010	1/03/2010	28	0	0.0000	
	1/03/2010	1/04/2010	31	0	0.0000	
14	1/04/2010	1/05/2010	30	0	0.0000	0.0025
	1/05/2010	1/06/2010	31	0.3	0.0025	
	1/06/2010	1/07/2010	30	0	0.0000	

15	1/07/2010	1/08/2010	31	0	0.0000	0.0008
	1/08/2010	1/09/2010	31	0.1	0.0008	
	1/09/2010	1/10/2010	30	0	0.0000	
16	1/10/2010	1/11/2010	31	0.1	0.0008	0.0033
	1/11/2010	1/12/2010	30	0.1	0.0008	
	1/12/2010	1/01/2011	31	0.2	0.0017	
17	1/01/2011	1/02/2011	31	0.1	0.0008	0.03
	1/02/2011	1/03/2011	28	1.4	0.0113	
	1/03/2011	1/04/2011	31	2	0.0179	
18	1/04/2011	1/05/2011	30	0	0.0000	0.0041
	1/05/2011	1/06/2011	31	0.2	0.0017	
	1/06/2011	1/07/2011	30	0.3	0.0024	
19	1/07/2011	1/08/2011	31	0.3	0.0025	0.0041
	1/08/2011	1/09/2011	31	0.1	0.0008	
	1/09/2011	1/10/2011	30	0.1	0.0008	
20	1/10/2011	1/11/2011	31	0.1	0.0008	0.0074
	1/11/2011	1/12/2011	30	0.2	0.0016	
	1/12/2011	1/01/2012	31	0.6	0.0050	
21	1/01/2012	1/02/2012	31	0	0.0000	0.029
	1/02/2012	1/03/2012	29	3.6	0.0290	
	1/03/2012	1/04/2012	31	0	0.0000	
22	1/04/2012	1/05/2012	30	1	0.0081	0.0122
	1/05/2012	1/06/2012	31	0.5	0.0042	
	1/06/2012	23/07/2012	52	0	0.0000	
23	23/07/2012	21/08/2012	29	0.2	0.0010	0.0035
	21/08/2012	27/09/2012	37	0.3	0.0026	
24	27/09/2012	1/10/2012	4	0	0.0000	0.0063
	1/10/2012	1/11/2012	31	0.1	0.0063	
	1/11/2012	1/12/2012	30	0	0.0000	
	1/12/2012	1/01/2013	31	0	0.0000	
25	1/01/2013	1/02/2013	31	0.7	0.0056	0.0065
	1/02/2013	1/03/2013	28	0	0.0000	
	1/03/2013	1/04/2013	31	0.1	0.0009	
26	1/04/2013	1/05/2013	30	0.2	0.0016	0.0081
	1/05/2013	1/06/2013	31	0.3	0.0025	
	1/06/2013	1/07/2013	30	0.5	0.0040	
27	1/07/2013	28/08/2013	58	0.7	0.0058	0.0074
	28/08/2013	28/09/2013	31	0	0.0000	
	28/09/2013	1/10/2013	3	0.2	0.0016	
28	1/10/2013	1/11/2013	31	0.1	0.0083	0.019
	1/11/2013	1/12/2013	30	0.65	0.0052	
	1/12/2013	1/01/2014	31	0.65	0.0054	
29	1/01/2014	1/02/2014	31	1.7	0.0137	0.0359
	1/02/2014	1/03/2014	28	2.75	0.0222	
	1/03/2014	1/04/2014	31	0	0.0000	
30	1/04/2014	1/05/2014	30	0	0.0000	0.0074
	1/05/2014	1/06/2014	31	0.5	0.0042	

	1/06/2014	1/07/2014	30	0.4	0.0032	
31	1/07/2014	29/08/2014	59	0	0.0000	0.0013
	29/08/2014	30/09/2014	32	0.3	0.0013	
32	30/09/2014	28/10/2014	28	0.3	0.0023	0.0042
	28/10/2014	24/11/2014	27	0.1	0.0009	
	24/11/2014	27/12/2014	33	0.1	0.0009	
33	27/12/2014	24/01/2015	28	0.2	0.0015	0.0104
	24/01/2015	27/02/2015	34	1	0.0089	
	27/02/2015	31/03/2015	32	0	0.0000	
34	31/03/2015	2/05/2015	32	2.5	0.0195	0.031
	2/05/2015	19/06/2015	48	0	0.0000	
	19/06/2015	11/07/2015	22	2.2	0.0115	
35	11/07/2015	18/08/2015	38	0	0.0000	0.002
	18/08/2015	29/09/2015	42	0.3	0.0020	
36	29/09/2015	26/10/2015	27	0.2	0.0012	0.003
	26/10/2015	23/11/2015	28	0.1	0.0009	
	23/11/2015	9/01/2016	47	0.1	0.0009	
37	9/01/2016	1/02/2016	23	0	0.0000	0.0174
	1/02/2016	1/03/2016	29	1.6	0.0174	
	1/03/2016	1/04/2016	31	0	0.0000	
38	1/04/2016	1/05/2016	30	0.3	0.0024	0.0041
	1/05/2016	1/06/2016	31	0.2	0.0017	
	1/06/2016	1/07/2016	30	0	0.0000	
39	1/07/2016	1/08/2016	31	0.2	0.0017	0.0041
	1/08/2016	1/09/2016	31	0.2	0.0016	
	1/09/2016	1/10/2016	30	0.1	0.0008	
40	1/10/2016	1/11/2016	31	0.1	0.0008	0.0033
	1/11/2016	1/12/2016	30	0.1	0.0008	
	1/12/2016	1/01/2017	31	0.2	0.0017	
41	1/01/2017	1/02/2017	31	0.2	0.0016	0.0169
	1/02/2017	1/03/2017	28	1.9	0.0153	
42	1/03/2017	1/04/2017	31	0	0.0000	0.021
	1/04/2017	5/06/2017	65	2.6	0.0210	
	5/06/2017	3/07/2017	28	0	0.0000	
43	3/07/2017	28/09/2017	87	2	0.0179	0.0179
44	28/09/2017	24/12/2017	87	0	0.000575	0.0006
						0.0088 (Mean)

Appendix C – Water balance output rates (base case RTIO model)

From	To	Days	In: Well	IN: Storage	IN: Recharge	Total IN	OUT: Storage	OUT: Wells	OUT: Drains	OUT: ET	Total OUT
1/01/2007	1/04/2007	90	1.1	44287.8	3209.6	47498.5	-8278.9	-34182.4	-3707.9	-1329.8	-47499.0
1/04/2007	1/07/2007	181	1.4	50595.0	8669.6	59266.0	-4499.5	-48897.3	-3866.0	-2003.4	-59266.1
1/07/2007	1/10/2007	273	1.4	51742.9	11841.6	63585.9	-4817.3	-52646.4	-4042.5	-2080.0	-63586.3
1/10/2007	1/01/2008	365	1.3	57395.5	12153.6	69550.4	-3446.7	-59611.2	-4233.8	-2258.8	-69550.6
1/01/2008	1/04/2008	456	1.0	63661.1	12985.6	76647.8	-2763.6	-66966.7	-4417.1	-2500.5	-76648.0
1/04/2008	1/07/2008	547	0.8	58858.0	16001.6	74860.4	-4417.6	-63833.0	-4996.2	-1614.0	-74860.7
1/07/2008	1/10/2008	639	1.2	85632.2	19537.6	105171.0	-4578.1	-92296.9	-5039.2	-3256.7	-105171.0
1/10/2008	1/01/2009	731	1.2	88628.3	15377.6	104007.1	-1151.8	-94482.3	-5122.6	-3250.7	-104007.4
1/01/2009	1/04/2009	821	1.1	95506.5	10957.6	106465.2	-529.1	-97876.1	-5029.4	-3030.8	-106465.4
1/04/2009	1/07/2009	912	0.9	84788.6	19017.6	103807.1	-2133.9	-93194.5	-5203.3	-3275.6	-103807.3
1/07/2009	1/10/2009	1004	0.8	75362.1	36229.6	111592.4	-14073.2	-87721.8	-5958.2	-3840.0	-111593.2
1/10/2009	1/01/2010	1096	0.8	77637.1	28013.6	105651.5	-4521.1	-90964.7	-6309.3	-3856.6	-105651.6
1/01/2010	1/04/2010	1186	0.8	79865.2	25361.6	105227.7	-1712.0	-93064.7	-6473.6	-3977.6	-105227.9
1/04/2010	1/07/2010	1277	0.9	80189.8	29521.6	109712.2	-3394.0	-95137.7	-6725.2	-4455.6	-109712.5
1/07/2010	1/10/2010	1369	0.9	83544.7	26609.6	110155.2	-888.3	-98000.6	-6791.6	-4475.0	-110155.5
1/10/2010	1/01/2011	1461	0.9	85032.3	25049.6	110082.8	-419.0	-98528.7	-6778.6	-4356.8	-110083.1
1/01/2011	1/04/2011	1551	0.8	81415.7	23853.6	105270.1	-372.7	-93996.9	-6716.2	-4184.9	-105270.7
1/04/2011	1/07/2011	1642	0.8	79640.2	21305.6	100946.5	-337.3	-90145.1	-6564.2	-3900.2	-100946.9
1/07/2011	1/10/2011	1734	0.6	74726.1	20421.6	95148.3	-309.6	-84610.2	-6388.7	-3840.0	-95148.6
1/10/2011	1/01/2012	1826	0.6	80828.0	26245.6	107074.2	-445.2	-96306.6	-6446.8	-3876.1	-107074.7
1/01/2012	1/04/2012	1917	0.7	72867.6	25517.6	98385.9	-267.1	-87825.2	-6434.3	-3859.5	-98386.1
1/04/2012	1/07/2012	2008	0.9	88495.8	33213.6	121710.4	-3238.2	-107591.3	-6680.7	-4200.2	-121710.4
1/07/2012	1/10/2012	2100	0.9	87065.1	33889.6	120955.6	-2513.6	-107085.6	-6889.1	-4467.7	-120956.0
1/10/2012	1/01/2013	2192	0.8	83960.8	32433.6	116395.2	-902.3	-103964.7	-6987.8	-4540.7	-116395.5
1/01/2013	1/04/2013	2282	0.8	80485.5	33473.6	113959.9	-913.5	-101199.9	-7084.2	-4762.5	-113960.0
1/04/2013	1/07/2013	2373	0.8	83294.8	33629.6	116925.2	-567.5	-104310.8	-7143.3	-4903.9	-116925.5
1/07/2013	1/10/2013	2465	0.7	81958.0	35137.6	117096.3	-833.1	-103835.8	-7226.1	-5201.5	-117096.6

1/10/2013	1/01/2014	2557	0.7	84269.5	37113.6	121383.8	-1305.3	-107031.7	-7327.0	-5720.3	-121384.3
1/01/2014	1/04/2014	2647	0.6	85146.4	31341.6	116488.6	-162.5	-104195.6	-7201.5	-4929.0	-116488.6
1/04/2014	1/07/2014	2738	0.9	92172.4	34513.6	126686.9	-188.6	-114148.3	-7233.1	-5117.3	-126687.3
1/07/2014	1/10/2014	2830	0.7	91706.7	27493.6	119200.9	-141.8	-107757.7	-6983.2	-4318.6	-119201.3
1/10/2014	1/01/2015	2922	0.7	93100.3	30301.6	123402.6	-134.2	-112097.5	-6908.6	-4262.6	-123402.9
1/01/2015	1/04/2015	3012	0.8	94373.1	29833.6	124207.5	-127.3	-113124.5	-6807.3	-4148.7	-124207.8
1/04/2015	1/07/2015	3103	0.6	96396.6	26505.6	122902.9	-120.7	-112216.6	-6602.2	-3963.6	-122903.1
1/07/2015	1/10/2015	3195	0.6	93856.7	23177.6	117034.8	-114.5	-106918.8	-6294.3	-3707.2	-117034.7
1/10/2015	1/01/2016	3287	0.5	93042.7	20681.6	113724.8	-108.8	-104498.7	-5917.5	-3200.0	-113724.9
1/01/2016	1/04/2016	3378	0.7	96022.5	21669.6	117692.8	-103.3	-108918.4	-5649.8	-3021.3	-117692.9
1/04/2016	1/07/2016	3469	0.5	92832.9	21253.6	114087.0	-98.1	-105900.6	-5420.3	-2668.0	-114087.0
1/07/2016	1/10/2016	3561	0.7	95115.1	26193.6	121309.4	-93.1	-113188.2	-5384.1	-2644.0	-121309.4
1/10/2016	1/01/2017	3653	0.6	94546.3	22969.6	117516.4	-88.3	-109814.3	-5224.7	-2389.2	-117516.4
1/01/2017	1/04/2017	3743	0.6	93358.2	22761.6	116120.4	-83.8	-108795.3	-5082.2	-2159.0	-116120.4
1/04/2017	1/07/2017	3834	0.5	83956.5	27597.6	111554.5	-113.0	-104143.6	-5105.8	-2192.2	-111554.6
1/07/2017	1/10/2017	3926	0.5	86831.6	23333.6	110165.7	-75.2	-103268.6	-4966.1	-1855.9	-110165.8
1/10/2017	1/01/2018	4018	0.4	102793.8	3209.6	106003.9	-71.2	-100244.9	-4221.5	-1466.3	-106003.9

Appendix D – Water balance output rates (Scenario 1, model with creek recharge applied)

From	To	Days	In: Well	IN: Storage	IN: Recharge	Total IN	OUT: Storage	OUT: Wells	OUT: Drains	OUT: ET	Total OUT
1/01/2007	1/04/2007	90	1.2	34374.5	21047.1	55422.8	-11425.2	-34182.4	-7591.1	-2224.0	-55422.7
1/04/2007	1/07/2007	181	1.5	44123.0	24323.1	68447.5	-9247.5	-48897.3	-8033.5	-2269.7	-68447.9
1/07/2007	1/10/2007	273	1.4	45451.5	26226.3	71679.3	-8122.6	-52646.4	-8441.6	-2468.9	-71679.5
1/10/2007	1/01/2008	365	1.4	51007.0	26413.5	77421.9	-6540.8	-59611.2	-8677.6	-2592.2	-77421.8
1/01/2008	1/04/2008	456	1.1	57223.9	26912.7	84137.7	-5679.0	-66966.7	-8819.0	-2673.3	-84138.0
1/04/2008	1/07/2008	547	0.8	52129.0	28722.3	80852.1	-5992.1	-63833.0	-9419.6	-1607.4	-80852.2
1/07/2008	1/10/2008	639	1.3	78969.3	30843.9	109814.5	-5191.8	-92297.0	-9298.6	-3027.5	-109814.8
1/10/2008	1/01/2009	731	1.3	82696.8	28347.9	111046.0	-4493.4	-94482.3	-9174.5	-2896.2	-111046.4
1/01/2009	1/04/2009	821	1.1	87795.5	25695.9	113492.5	-4234.6	-97876.2	-8842.0	-2540.2	-113493.1
1/04/2009	1/07/2009	912	0.9	78173.1	30531.9	108706.0	-4044.3	-93194.5	-8898.0	-2569.4	-108706.2
1/07/2009	1/10/2009	1004	0.8	67794.8	40856.5	108652.1	-8129.8	-87721.8	-9639.2	-3161.5	-108652.3
1/10/2009	1/01/2010	1096	0.8	71639.2	35929.5	107569.6	-3794.5	-90964.8	-9695.5	-3115.0	-107569.7
1/01/2010	1/04/2010	1186	0.8	74873.0	34338.3	109212.2	-3598.4	-93064.7	-9546.8	-3002.4	-109212.4
1/04/2010	1/07/2010	1277	0.9	74385.1	36834.3	111220.3	-3471.2	-95137.7	-9591.1	-3020.4	-111220.5
1/07/2010	1/10/2010	1369	0.9	78505.3	35087.1	113593.3	-3337.2	-98000.6	-9432.9	-2822.9	-113593.6
1/10/2010	1/01/2011	1461	0.9	79403.8	34151.1	113555.8	-3213.7	-98528.7	-9203.6	-2610.1	-113556.1
1/01/2011	1/04/2011	1551	0.8	75033.9	33433.5	108468.2	-3097.2	-93996.9	-8936.0	-2438.4	-108468.5
1/04/2011	1/07/2011	1642	0.7	72056.5	31904.7	103961.9	-2983.4	-90145.1	-8562.5	-2270.7	-103961.7
1/07/2011	1/10/2011	1734	0.5	66062.1	31374.3	97437.0	-2872.6	-84610.3	-8194.5	-1759.5	-97436.9
1/10/2011	1/01/2012	1826	0.6	74010.1	34868.7	108879.5	-2765.8	-96306.6	-8129.8	-1677.7	-108879.9
1/01/2012	1/04/2012	1917	0.6	65668.4	34431.9	100101.0	-2662.7	-87825.3	-7991.2	-1621.7	-100100.9
1/04/2012	1/07/2012	2008	0.9	81354.2	39049.5	120404.7	-3000.8	-107591.4	-8157.1	-1655.6	-120405.0
1/07/2012	1/10/2012	2100	0.9	80182.8	39455.1	119638.9	-2616.6	-107085.6	-8255.1	-1682.0	-119639.3
1/10/2012	1/01/2013	2192	0.8	77610.4	38581.5	116192.7	-2346.5	-103964.8	-8216.1	-1665.8	-116193.1
1/01/2013	1/04/2013	2282	0.8	74089.8	39205.5	113296.1	-2245.2	-101199.9	-8190.4	-1661.2	-113296.7
1/04/2013	1/07/2013	2373	0.8	76947.5	39299.1	116247.4	-2146.9	-104310.8	-8138.7	-1651.4	-116247.8
1/07/2013	1/10/2013	2465	0.7	75460.0	40203.9	115664.6	-2052.5	-103835.8	-8127.1	-1649.6	-115665.0

1/10/2013	1/01/2014	2557	0.7	77458.6	41389.5	118848.9	-1992.2	-107031.7	-8167.6	-1657.7	-118849.3
1/01/2014	1/04/2014	2647	0.6	77680.4	37926.3	115607.3	-1880.8	-104195.7	-7921.9	-1609.0	-115607.5
1/04/2014	1/07/2014	2738	0.9	85557.7	39829.5	125388.0	-1802.5	-114148.3	-7837.8	-1600.0	-125388.6
1/07/2014	1/10/2014	2830	0.7	82844.3	35617.5	118462.5	-1728.2	-107757.7	-7421.1	-1555.7	-118462.7
1/10/2014	1/01/2015	2922	0.7	85167.4	37302.3	122470.4	-1658.4	-112097.5	-7205.5	-1509.3	-122470.8
1/01/2015	1/04/2015	3012	0.8	86149.3	37021.5	123171.6	-1594.3	-113124.5	-6992.9	-1460.3	-123172.0
1/04/2015	1/07/2015	3103	0.6	86761.8	35024.7	121787.2	-1532.9	-112216.5	-6658.2	-1379.8	-121787.3
1/07/2015	1/10/2015	3195	0.5	82783.8	33027.9	115812.3	-1473.9	-106918.8	-6267.0	-1152.7	-115812.4
1/10/2015	1/01/2016	3287	0.5	81144.4	31530.3	112675.2	-1417.8	-104498.7	-5883.6	-875.1	-112675.3
1/01/2016	1/04/2016	3378	0.7	84497.2	32123.1	116621.0	-1365.1	-108918.5	-5583.7	-753.8	-116621.1
1/04/2016	1/07/2016	3469	0.5	81217.9	31873.5	113092.0	-1314.8	-105900.6	-5328.0	-548.7	-113092.1
1/07/2016	1/10/2016	3561	0.7	85380.9	34837.5	120219.1	-1266.0	-113188.1	-5252.2	-512.9	-120219.2
1/10/2016	1/01/2017	3653	0.6	83555.6	32903.1	116459.3	-1219.5	-109814.3	-5076.7	-348.9	-116459.4
1/01/2017	1/04/2017	3743	0.5	82320.6	32778.3	115099.5	-1176.0	-108795.4	-4896.2	-232.0	-115099.6
1/04/2017	1/07/2017	3834	0.4	74705.8	35679.9	110386.1	-1133.7	-104143.7	-4866.7	-242.2	-110386.3
1/07/2017	1/10/2017	3926	0.4	76045.7	33121.5	109167.7	-1092.6	-103268.7	-4699.3	-107.1	-109167.8
1/10/2017	1/01/2018	4018	0.4	84107.0	21047.1	105154.5	-1053.1	-100245.0	-3856.5	0.0	-105154.6